1991

Novel methods of separation and detection for columns of capillary dimension

William D. Pfeffer
Iowa State University

Order Number 9126236

Novel methods of separation and detection for columns of capillary dimension

Pfeffer, William David, Ph.D.

Iowa State University, 1991

U·M·I
300 N. Zeeb Rd.
Ann Arbor, MI 48106

Novel methods of separation and detection for columns of capillary dimension

by

William D. Pfeffer

A Dissertation Submitted to the

Graduate Faculty in Partial Fulfillment of the

Requirements for the Degree of

DOCTOR OF PHILOSOPHY

Department: Chemistry
Major: Analytical Chemistry

Approved:

Signature was redacted for privacy.

In Charge of Major Work

Signature was redacted for privacy.

For the Major Department

Signature was redacted for privacy.

For the Graduate College

Iowa State University
Ames, Iowa

1991

TABLE OF CONTENTS

GENERAL INTRODUCTION

The popularity of a scientific technique can be related to its performance with respect to similar techniques, the number of scientific articles devoted to the subject and the amount of commercial support it receives. Knowing this, it is of no surprise that of the separation techniques available, liquid chromatography (LC) is one of the most used. This acceptance is well rooted in its ability to separate a vast array of substances important to nearly every field of science, its high degree of sensitivity, and its relative ease of quantitation.

The work in this thesis is devoted to the area of microcolumn liquid chromatography. The term microcolumn, which will be defined further along, generally refers to LC columns whose internal diameters are 1 mm or less. The i.d. of a conventional column is understood to be 4.3 mm. The research presented can be grouped into two subjects. The first concerns specifically detection in microcolumn LC (Sections I-III). The second subject concerns itself with separation principles in microcolumns using chromatographic techniques (Sections IV-V). Although separated by name, separation and detection are highly dependent on each other since each can benefit by advances made in the other.

Microcolumn Separations

Microcolumn development

Just as capillary gas chromatography emerged from its forerunner, packed column gas chromatography, so too has much of microcolumn liquid chromatography. The concept of chromatography in open tubes was addressed as early as 1958 by Golay (1). The idea of actually performing liquid chromatography in open tubes was addressed by Giddings (2) in 1964 and Golay (3) in 1973. The first reported use of a small-bore column for LC was by Hovarth et al. (4) in 1967. In their work, they used a 1-mm x 193-cm ion exchange column. The reduced bore was more for convenience of coiling the column than for exploitation of any benefits it may have had.

In 1976, Scott and Kucera (5) regenerated interest in microbore columns by reporting a theoretical plate number (N) of 250,000 which they obtained from a 1-mm x 10-m column (6,7). Tsuda and Novotny (8,9) and Hirata et al. (10) propelled this interest further by using narrow packed capillaries (i.d. $< 500\ \mu m$) to perform LC. In addition, they also reported that solute dispersion in unpacked capillaries of approximately 50 μm i.d. could be described by the Golay equation (8). This led to the development of open-tubular capillary (OTC) liquid chromatography, but it wasn't until Knox and Gilbert (11) explored OTCLC and developed practical operating parameters that the potential of OTCLC was understood.

From these early experiments, two motivations for using microcolumns developed. The first was that reducing the diameter of the column a few-fold allowed for lower flow rates to be used. This reduced the solvent consumption. The second motivation was that by drastically reducing the diameter, e.g. an OTC column with an i.d. of a few μm, one would not only reduce solvent consumption but also achieve unprecedented levels of chromatographic efficiency along with increased sensitivity for certain type of LC detectors. The result of these motivations was the emergence of three types of microbore columns: slurry-packed capillaries, packed capillaries and open-tubular capillary columns.

Classification and characterization of microbore columns

A quantitative comparison for each of the three types of microbore columns can be made by employing a factor know as separation impedance, I, which was first introduced by Bristow and Knox (12).

$$I = \frac{t\Delta p}{N^2 \eta} = h^2 \phi \qquad (1)$$

Here, t is the elution time of a non-retained solute, Δp is the pressure gradient along the column, N is the number of theoretical plates, η is the viscosity of the eluent, ϕ is the column resistance factor, and h is the reduced plate height. For packed columns, $h = H/d_p$ with H being the plate height and d_p being the particle diameter. For OTC columns, $h = H/d_c$ with d_c being the column i.d.

Many comparisons between columns of unlike geometry have been made with consideration to only plate number or plate height. However, large plate numbers can be achieved at the expense of long analysis times; therefore, such comparisons can be unrealistic. Separation impedance considers all LC operating parameters, including ϕ, which accounts for the resistance the eluent experiences as it flows through a particular column. The smaller the value for I, the better the performance of the column. Knox (13), using values of minimum reduced plate height, h_{min}, calculated the minimum separation impedances, I_{min}, for the three types of microcolumns. These values are shown in Table 1. The values for ϕ are commonly used to classify columns (13,14).

Table 1. Comparison of I_{min}, h_{min}, ν_{opt} and ϕ for microcolumns (14)

Column	I_{min}	h_{min}	ν_{opt}	ϕ
Slurry-packed Capillary	2000	2	2-5	500-1000
Packed Capillary	600	2	5	150
Open-tubular Capillary	20	0.8	5	32

In Table 1, the optimum reduced eluent velocity, ν_{opt}, which will be discussed later, is the velocity at which h_{min} is achieved (13).

Slurry-packed microcolumns have ϕ between 500 and 1000. As the name indicates, the stationary phase, prior to packing, is made up in a balanced density

slurry which is then packed rapidly into the column using high pressure (15). These columns are similar to conventional columns except for the internal diameter, which can be between 50 μm and 1 mm. It was initially held that plate height for these columns was a function of d_p. However, Karlsson and Novotny (16) have recently shown that plate height decreases as a function of d_c in slurry-packed capillaries.

Packed capillary columns exhibit ϕ = 150. These columns are prepared by packing large bore glass or fused silica capillaries with stationary phase particles. The capillary is then heated and drawn to its final i.d. of roughly 40-80 μm (9,10). Theoretical studies show that column performance is a function of both particle size and column i.d. (17). For a packed column, the low value of ϕ, as compared to that of slurry-packed columns, results from its d_c/d_p ratio (d_c/d_p = 2-3) being smaller than that for slurry-packed columns (d_c/d_p = 50-200). This means that for all other chromatographic parameters in eq (1) being equal for the two types of columns, a packed capillary can achieve the same efficiency as a slurry-packed column using a smaller pressure gradient.

The result of ϕ = 32 for OTC columns is of direct consequence of the Poiseuille equation. These columns typically have their internal diameters between 5-10 μm, with the optimum i.d. being between 1-3 μm (18). The stationary phases for these columns are usually liquids that are coated or bonded onto the treated surface of a glass capillary (19,20), or cross-linked polymer films in fused silica capillaries (21,22). OTC columns represent the simplest column

geometry available, but because of the extremely small dimensions, attaching ancillary devices such as a detector and an injector to these columns can be difficult.

Of the microcolumns discussed, OTC columns are unique in that they can produce extremely efficient separations in a reasonable period of time. To understand this, consider the following comparison between an OTC column and a slurry-packed column. Since t for a non-retained compound is proportional to I, we see from eq (1) and Table 1 that for identical Δp, η, and N, an OTC column could perform the separation 100 times faster than a slurry-packed column. Alternatively, with t, Δp and η identical, an OTC column could produce 10 times as many plates as the slurry-packed column (11,13).

The example above, although illustrative, is unrealistic when one considers the dimensions of the columns involved (23). To understand this, consider the expressions for particle diameter and column internal diameter

$$d_p = \left(\frac{Nh\nu\phi\eta D_m}{\Delta p} \right)^{1/2} \tag{2}$$

$$d_c = \left(\frac{Nh\nu\phi\eta D_m}{\Delta p} \right)^{1/2} \tag{3}$$

where D_m is the diffusion coefficient, and ν is the reduced velocity. Reduced velocity is related to the linear velocity, u, through $\nu = ud_p/D_m$ for packed

columns and $\nu = ud_c/D_m$ for OTC columns. For the optimum values listed in Table 1, values for d_p and d_c reduce to their optimum forms (11)

$$d_{p_{opt}} = \left(\frac{4000N\eta D_m}{\Delta p}\right)^{1/2} \tag{4}$$

$$d_{c_{opt}} = \left(\frac{128N\eta D_m}{\Delta p}\right)^{1/2} \tag{5}$$

Therefore, for typical chromatographic conditions of $\eta = 1 \times 10^{-3}$ N s m^{-2}, $D_m = 1 \times 10^{-9}$ m^2 s^{-1}, $\Delta p = 7 \times 10^6$ N $m^{-2} \approx 1000$ psi, to achieve 15,000 theoretical plates, $d_{p_{opt}}$ must be 3 μm for a slurry-packed column. For an OTC column to achieve the same value of N under the same conditions, it would need an i.d. of 0.54 μm and a column length of 8.6 mm. Such an OTC column is unattainable today.

From the discussion above, it would appear that slurry-packed columns are more practical than OTC columns due to technological limitations. However, using OTC columns available today, one finds that an OTC column can meet or exceed the performance of a slurry-packed column for the condition of a set peak elution volume. To demonstrate this, plate theory and factors affecting band broadening in OTCs must be discussed.

Plate theory and dispersion in open-tubular capillary columns

Plate height theory for OTCs in LC is similar to that for capillary gas chromatography in that it is derived from the Golay equation (24).

$$H = \frac{2D_m}{u} + \frac{(1 + 6k + 11k^2)d_c^2 u}{96(1 + k)^2 D_m} + \frac{2}{3}\frac{kd_f^2 u}{3(1 + k)^2 D_s} \qquad (6)$$

Here, k, d_f, and D_s represent the capacity coefficient of the solute, the film thickness of the stationary phase, and the diffusion coefficient of the solute in the stationary phase. Because $d_f < d_c$ and $D_s < D_m$ for a typical OTC column, the last portion of eq (6) can be neglected (13). Using the reduced parameters discussed earlier, eq (6) becomes

$$h = \frac{2}{\nu} + C_m \nu \qquad (7)$$

where C_m represents the contribution to mass transfer in the mobile phase. Observe from eq (6) that in order to achieve low values of H, strict attention must be paid to column i.d. as well as the capacity coefficient of the solute. This is not the case for the capillary form of zone electrophoresis, which is largely independent of column diameter and mass transfer effects.

Other factors beside mass transfer contribute to the volume of a peak for both conventional and microcolumn LC. However, they are of more concern for

microcolumns because of the small column volumes.

Dispersion in LC is of two forms: volumetric and temporal. Volumetric dispersion involves the dilution of the peak via such devices as injectors and detectors. The second form of dispersion, temporal, involves the lag time associated with instruments responsible for detecting and recording the eluting peak, thereby increasing the recorded peak width (25).

Total column variance in OTCLC is the sum of the various variances which contribute. This can be expressed as

$$\sigma^2_{tot} = \sigma^2_{col} + \sigma^2_{inj} + \sigma^2_{con} + \sigma^2_{\mathrm{det}} + \sigma^2_{tem} \tag{8}$$

where the variance subscripts tot, col, inj, con, det, and tem stand for total, column, injector, connector, detector, and temporal, respectively.

The key to a successful separation is to keep all extra column variances as a small fraction of the actual column variance, σ^2_{col}, which is given by

$$\sigma^2_{col} = (\pi r_c^2 \epsilon_t)^2 HL \tag{9}$$

where ϵ_t is the total porosity of the column (ϵ_t = 0.85 for slurry-packed columns, and 1 for OTC columns) and r_c is the radius of the column (25).

To understand this, consider an injector where the injection volume, V_{inj}, is described by

$$V_{inj}^2 = (\theta K \pi r^2 \epsilon_t)^2 HL = K^2 \sigma_{inj}^2 \quad (10)$$

Here, θ^2 represents the fractional increase in the volumetric variance on a non-retained peak and K^2 is a constant descriptive of the injection profile ($K^2 = 12$ for an ideal plug injection) (26). Therefore, assuming near ideal conditions ($K^2 = 12$, $H \approx d_c$), and that a 5% ($\theta^2 = 0.05$) increase in volumetric variance can be tolerated, a peak eluting from a 1-m x 10-μm OTC column would need to have had an injection volume of 0.2 nL. Commercially available injectors capable of such a volume are not yet available. However, injection methods such as split injection (27), microsyringe injection (28), stopped flow injection (29) and gravity or hydrodynamic injection (30) have been used to deliver sub-nanoliter volumes successfully. Berry and Lawson (31) have reviewed an array of sub-microliter injection techniques available for liquid chromatography.

The next ancillary device an eluting peak encounters is the connector between the flow cell and column. For a tubular connector, the variance, σ_{con}^2, can be described as

$$\sigma_{con}^2 = \frac{\pi^2 r_c^6 L u}{24 D_m} \quad (11)$$

which is simply the result of substituting $d_c^2 u/96 D_m$ (approximate plate height for

a non-retained compound) for H in eq (10). It is noted from eq (11) that by keeping the radius of the connecting tubing small, the variance associated with the connector can be minimized. In cases where on-column detection, which will be discussed later, is employed, σ_{con}^2 can be essentially eliminated from eq (9).

The ideal detector volume can be calculated in much the same way that V_{inj} was calculated. A requirement imposed upon detectors is that the volume should be such that early eluting peaks will be resolved. Knox and Gilbert (11) suggest a detector volume, V_{det}, be 1/2 the column volumetric standard deviation, as shown below:

$$4V_{det}^2 \leq (\pi r_c^2 \epsilon_t)^2 HL \tag{12}$$

The actual dispersion of a cylindrical flow cell, such as commonly used for optical detectors, is described by the following (25):

$$\sigma_{det}^2 = \frac{V_{det}^2}{12} = \frac{(\pi r_c^2 d_c)^2}{12} \tag{13}$$

For the column in the example above, an optical detector such as an on-column laser fluorometric detector would give V_{det} = 0.8 pL. Such a volume is well below the conditions imposed by eq (12). This will be discussed further in considering the importance of laser based fluorometric detectors for microcolumn

LC.

Even if volumetric requirements for the connector, injector and detector are met, peak broadening can occur from slow response of the detector and recording electronics. The electronic circuits of such devices respond in an exponential manner to the incoming signal as a result of RC components (e.g., filters). The speed with which a circuit responds to a signal is dictated by the RC time constant, t_{RC}. Since the fastest eluting peak will be that of a non-retained component, t_{RC} should be tailored after its elution time (25,26). Therefore, for an acceptable fractional increase in apparent volumetric variance, the value of t_{RC} will be described by

$$t_{RC}^2 = \frac{\theta^2 HL}{u^2} \tag{14}$$

For a known value of t_{RC}, the apparent volumetric variance can be calculated using

$$\sigma_{tem}^2 = (\pi r_c^2 \epsilon_t \mu) t_{RC}^2 \tag{15}$$

From this, we see that a 10-m x 10-μm i.d. OTC column operating under typical chromatographic conditions ($H \approx d_c$, u = 0.3 cm/sec) would require $t_{RC} \approx 230$ milliseconds in order for $\theta^2 = 0.05$. Faster flow rates or more efficient columns

will require smaller t_{RC}. This can be achieved by reducing the size of the RC filter or by interfacing the detector directly to a computer. In the latter case, various software methods can be used to remove noise from the chromatogram without significantly broadening the peak.

To return to the reason why the above discussion was presented, if care is taken to keep extra column effects to a minimum ($\theta^2 \approx 0.05$), an upper limit to σ_{tot} can be established, which is approximately σ_{col}. Equation (9) is useful for determining σ_{col} for a non-retained peak, but for a retained component, mass transfer broadening must be considered. Knox and Gilbert (11) realized this and suggest that since OTC columns will be operated at flow rates above optimum for practical use, $h = C_m\nu$ when $\nu \geq 20$. Also, when $k = 2$, C_m is approximately equal to 0.08 (11). By replacing h with $C_m\nu$ in eq (3) and eliminating d_c between eq (3) and eq (9), a new expression for h is obtained.

$$h = \left(\frac{16\sigma_{col}^2 \Delta p^3 C_m^3}{\pi^2 \phi^3 \eta^3 D_m^3} \right)^{1/8} N^{-1/2} \qquad (16)$$

Equation (16) is useful in that it allows h to be eliminated in the expressions for t, d_c and L.

$$t = \left(\frac{16\phi\eta\sigma_{col}^2 C_m^3}{\pi^2 \Delta p D_m^3} \right)^{1/4} N \qquad (17)$$

$$d_c = \left(\frac{16\phi\eta\sigma_{col}^2 D_m}{\pi^2 \Delta p C_m} \right)^{1/8} \qquad (18)$$

$$L = \left(\frac{16\sigma_{col}^2 C_m \Delta p}{\pi^2 \phi\eta D_m} \right)^{1/4} N^{1/2} \qquad (19)$$

The significance of eqns (17-18) is that by choosing an OTC column i.d., a value for σ_{col} is imposed. This value of σ_{col}, in turn, dictates the column length and analysis time for an OTC column separation yielding a plate number, N. Using t as a gauge then, the performance of an OTC column, whose length is allowed to vary, can be compared to that of a slurry-packed column for a separation yielding N plates with identical Δp, η and D_m.

To visualize such a comparison, Figure 1 shows the elution time for a 10 μm i.d. OTC column and a slurry-packed column. Optimum conditions of $h_{min} = 2$ and $\phi = 500$ (Table 1) are assumed for the slurry-packed column. From Figure 1, it becomes clear that the OTC column will perform better than the slurry-packed column for N > 30,000. This difference in analysis time becomes more significant for large N values, e.q., t differs by a factor of nearly 5 for N = 100,000. Herein

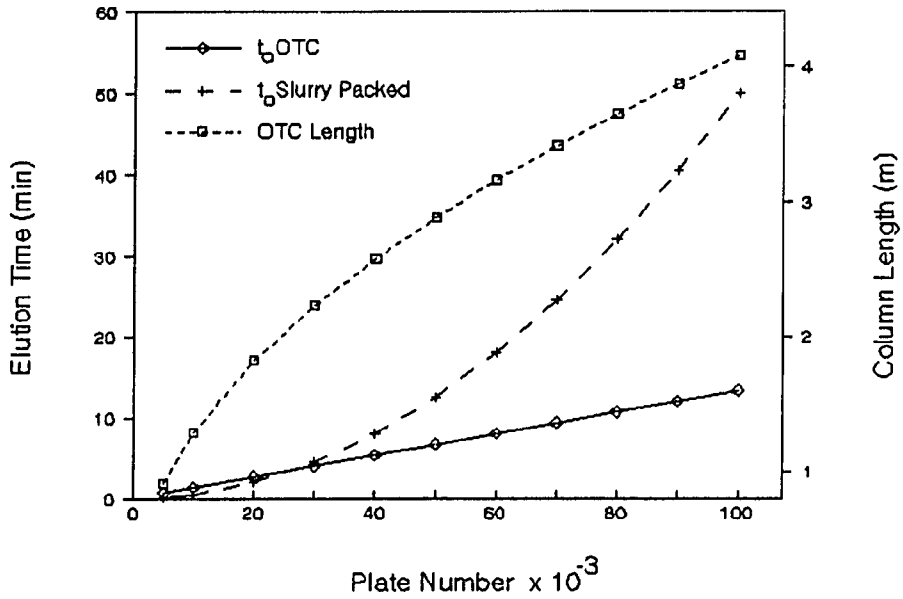

Figure 1. Comparison of elution times for an OTC column of variable length and a slurry-packed column having ϕ =500 and h_{min} = 2. Chromatography parameters are as follows: $\Delta p = 7 \times 10^6$ N $m^{-2} \approx$ 1000 psi; $\eta = 10^{-3}$ N s m^{-2} ; $D_m = 1 \times 10^{-9}$ m^2 s^{-1}; $d_c = 1 \times 10^{-5}$ m; $\sigma_{col} = 1 \times 10^{-12}$ m^3.

lies the attraction of OTC columns over the other microbore columns - highly efficient separations in reasonable times.

Mass sensitivity advantage for microcolumns

In addition to reduced solvent consumption and increased separation efficiency, reduction of the column i.d. can translate into increased mass sensitivity when concentration sensitive detectors are used. To understand this, consider that for an injected mass, m, the maximum concentration, C_{max}, at the detector is given by (25)

$$C_{\max} = \frac{m}{(2\pi^3)^{1/2} r_c^2 L^{1/2} \epsilon_t H^{1/2} (1 + k)} \tag{20}$$

The enhanced mass sensitivity for microcolumns results from the mass being eluted in a small peak volume. To envision this, consider the comparison of C_{max} between a conventional column and microcolumn for the same injected mass.

$$\frac{C_{\max_{mic}}}{C_{\max_{con}}} = \frac{\left(r_c^2 \epsilon_t L^{1/2} H^{1/2} (l + k)\right)_{con}}{\left(r_c^2 \epsilon_t L^{1/2} H^{1/2} (1 + k)\right)_{mic}} \tag{21}$$

Assuming ϵ_t, L, H, and k to be identical for the sake of simplicity, eq (21) reveals that mass sensitivity is enhanced for the microcolumn by a factor of r^2_{con}/r^2_{mic}.

In the case of an OTC column with an i.d of 10 μm, this ratio is in excess of 100,000.

Summary

The above discussions have revealed how the use of microcolumns can lead to increased separation efficiencies with reasonable analysis times as well as increased detector mass sensitivity. In particular, these gains can be profound for OTC columns. This is why the majority of the work presented in this thesis is devoted to the use of OTC columns. In addition to these advantages, microcolumns are also noted for the following: ease of interfacing with certain types of detectors, as in the case of mass spectrometry; reduced cost for exotic or expensive solvents and stationary phases; reduced sample size; ease of column thermostating, and improved efficiency in multicolumn analyses.

Electroosmosis for Chromatography in Open-Tubular Capillaries

Hydrodynamic Flow

Hydrodynamic flow in an open tube results from a pressure differential between the inlet and outlet. The resulting flow profile can be visualized by imagining that the fluid is made up of concentric layers. The layer closest to the wall clings to it and therefore, has zero velocity. This layer exerts drag on the adjacent layer, and so on so that each section has a different velocity with the

Figure 2. Profiles for hydrostatic (a) and electroosmotic (b) flow. In (a), $p_1 > p_2$. In the case of (b), direction of the flow is indicated with respect to applied potential field.

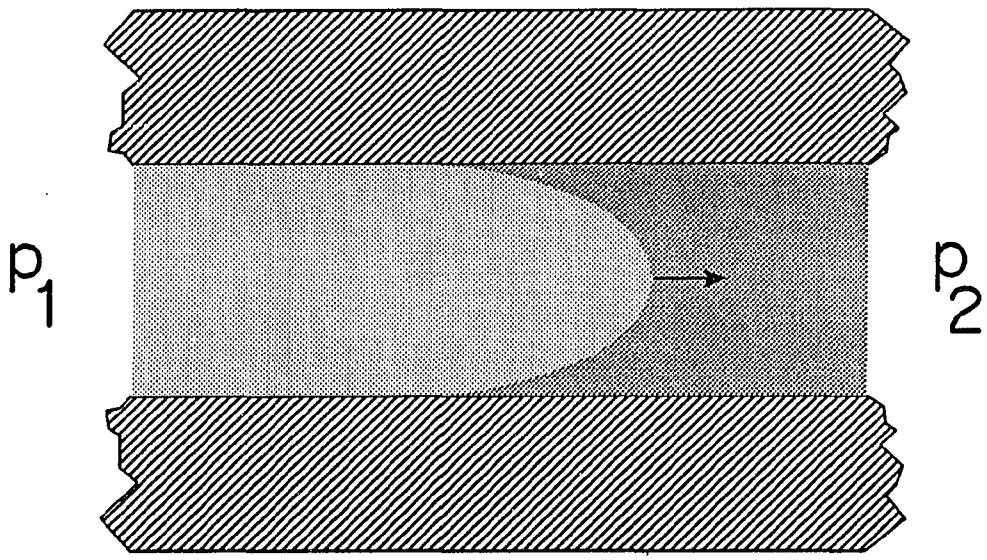

Hydrodynamic Flow

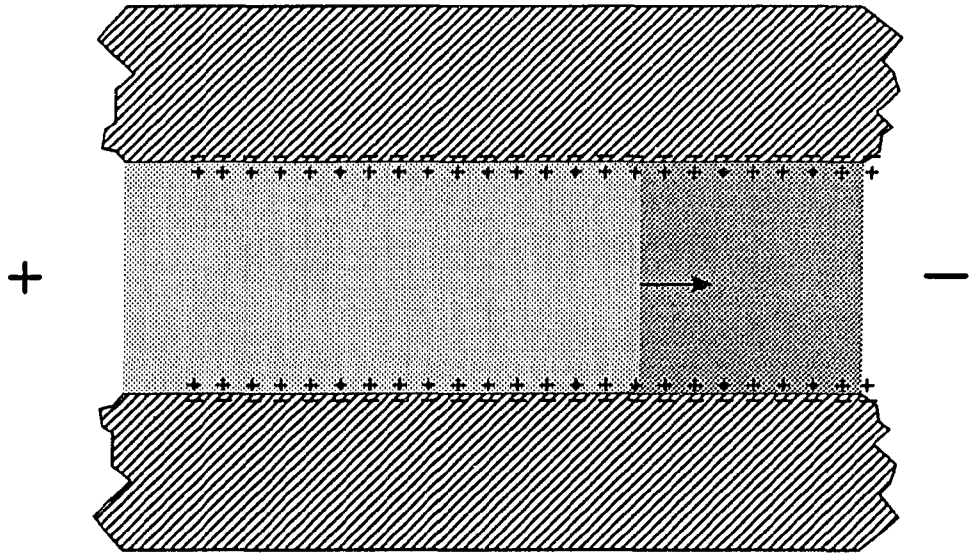

Electroosmotic Flow

center having maximum velocity. This is known as laminar flow and has a parabolic profile, as shown in Figure 2. The volumetric flow rate, f, of such a system is given by the Poiseuille equation

$$f = \frac{\pi r_c^4 \Delta p}{8\eta L} \tag{22}$$

In chromatography, this flow rate is conveniently controlled by changing Δp.

Electroosmotic Flow

Liquid can also be propelled through a tube by electroosmosis. Electroosmotic flow results when a potential, E, is placed across the ends of a liquid filled tube. The origin of this flow is often explained using the Stern-Gouy-Chapman model of the electrical double layer at a charged, solid-liquid interface (32). In the case of a water-filled fused silica or glass capillary, the exposed silanol groups which are ionized account for the negative charge. Immobilized counter charges to this are cations in the adjacent layer often called the Stern compact layer. The diffuse Gouy layer results from ions in the compact region diffusing out through thermal agitation. Solvent, in this case water, just outside the Stern layer is bound via hydration of the immobilized ions. A plane of shear develops between this bound solvent layer and the free solvent. The application of an electric field across the axis of the column exerts a force on the counter ions

in both parts of the double layer. Since only the cations of the diffuse region are free to move, they migrate toward the negative electrode, and because they are hydrated, bulk flow of the solution results. The profile of the resulting flow is nearly flat as depicted in Figure 2.

This model is shown in Figure 3 (32,33). Here, ψ_o represents the potential of the interface between the liquid and capillary wall. Traveling from the wall to the bulk solution, ψ decreases. The potential decreases linearly in the compact region and exponentially in the diffuse region. The potential at the compact-diffuse interface is called ψ_d. The double layer thickness, δ, is the distance from ψ_d to the point where $\psi = 1/e\ \psi_d$ (32). The potential at the plane of shear, ζ, is called the zeta potential and is described by

$$\zeta = \frac{4\pi\eta\mu_{eo}}{\varepsilon} \tag{23}$$

where μ_{eo} is the coefficient for electroosmotic flow, and ε is the dielectric constant of the solvent (32,33-36). The linear velocity, υ, is related to ζ through the following (34,37-39):

$$\upsilon = \frac{\varepsilon E\zeta}{4\pi\eta} \tag{24}$$

Thus, the electroosmotic flow can be conveniently controlled by varying E.

Electroosmosis has been used in conjunction with liquid chromatography in

both packed and OTC columns (30,33-35,40-48). The significant difference and motivation for using electroosmosis for the propulsion arises from the contribution to mass transfer in the mobile phase.

As discussed earlier, the contribution to mass transfer term, C_m, in pressure driven chromatography in an open tube has the form

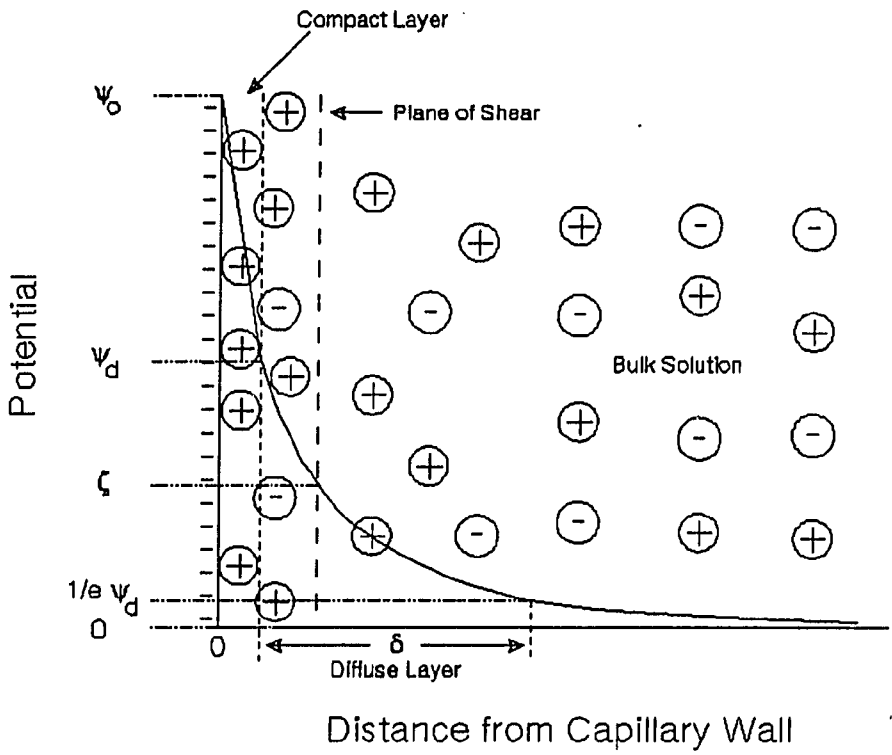

Figure 3. Potentials and relative ion positions in the double layer.

$$C_m = \frac{1 + 6k + 11k^2}{96(1 + k)^2} \tag{25}$$

However, due to the complex velocity profile, the C_m term for electroosmotically driven chromatography in open tubes is more complicated, as discussed by Martin and Guiochon (49). To formulate an equation for C_m, they used a partially flat, partially parabolic velocity profile. Their result was an intricate expression, so to simplify matters, they developed an approximation for C_m (49). Later work by Martin et al. (50), led to a more refined approximation for C_m which is shown below.

$$C_m = \frac{4 + (4n + 16)k + (n^2 + 10n + 20)k^2}{16(n + 2)(n + 4)(1 + k)^2} \tag{26}$$

Here, n is known as an approximating exponent. In the case of n = 2, eq (26) reduces to eq (25). In order for eq (26) to be useful, an expression for the estimation of n is needed. One such expression is

$$n = \kappa a - \frac{3}{2} + \frac{3}{8}\frac{1}{\kappa a}\left(1 + \frac{1}{\kappa a} + \cdots\right) \tag{27}$$

where κa is called the electrokinetic radius of the system and is simply the product of the reciprocal of the double layer thickness, δ, and the radius of the column, a

(50).

The conclusion Martin et al. (49,50) reached from their studies is that electroosmotic flow will give less peak broadening when compared to the exact same system under pressurized flow, for any value of k, due to the nearly flat velocity profile of electroosmotic flow.

This has been experimentally confirmed by Pretorius et al. (34) who used 1-mm i.d. tubes and by Tsuda et al. (41) who used 30 μm i.d. OTC columns. However, in the case of Tsuda et al., the work was performed in capillaries whose internal diameters were much larger than optimum for OTCLC; hence, the full potential of using electroosmotic flow over hydrodynamic flow was not demonstrated.

Sections IV and V of this thesis address the use of electroosmosis for LC. In Section IV, electroosmosis is used to drive a separation of several neutral, isomeric compounds. The OTCLC based upon this flow makes it possible to separate these analytes with greater than baseline resolution in all cases and an efficiency of 230,000 theoretical plates.

Section V of this thesis examines the electroosmotically driven electrochromatography separation of anions having similar electrophoretic mobility by ion pairing. The term electrochromatography, in this case, refers to the fact that separation by both partitioning differences and electrophoretic mobility differences is possible.

Laser Properties Relevant to Fluorescence Detection

The use of lasers as light sources for detection in LC is of popular interest and the subject of many reviews (51-57). To understand this interest, the properties of the laser must be discussed to reveal its unique nature.

Collimation

The most commonly used lasers in conjunction with LC detectors are those having a Gaussian beam profile, such as the argon ion and HeCd lasers. The emitted radiation from such a laser has a beam radius, w, of

$$w = w_O\left[1 + \left(\frac{\lambda z}{\pi w_O^2}\right)^2\right]^{1/2} = w_O\left[1 + \left(\frac{z}{z_R}\right)^2\right]^{1/2} \qquad (28)$$

where w_O is the radius of the beam waist inside the laser resonator, z is the distance from this beam waist, λ is the wavelength, and z_R is the Rayleigh range. In the general sense, z_R represents the useful range of collimation (52).

When such a collimated beam is focused, an extremely small spot size can be achieved. An approximation for spot size radius, w_{O2}, is given by

$$w_{o_2} = \frac{f\lambda}{\pi w_{o_1}} \tag{29}$$

where w_{o_1} is diameter of the beam prior to the focusing lens and f is the focal length of the lens. The useful path length, b, of such a focused beam can be obtained by replacing w_o with w_{o_2} in z_R.

$$b = \frac{\pi w_{o_2}^2}{\lambda} \tag{30}$$

Short focal length lenses can give diffraction limited spots of a few μm, which is useful in exciting fluorescence in OTCs. Larger focal length lenses can be used to produce a fine column of light for larger flow cells or for focusing into a fiber optic.

Monochromaticity

Most lasers are monochromatic, or can be made so with optical modifications. The importance of monochromaticity becomes apparent when one considers the Rayleigh and Raman scattering of the cell walls and eluent of an LC system. Rayleigh and Raman band widths are, at a minimum, comparable to the band width of the excitation source. Therefore, the use of a laser, as compared to a continuum source for which a 10 nm bandwidth (typical value) has been selected,

allows for more spectral distance between the Rayleigh band and Raman bands for detection of fluorescence (52,56,57).

Power

Many continuum light sources provide a total output power that matches or exceeds the output power of many lasers used with LC detectors. However, because of its monochromaticity, the laser can use its total power to excite fluorescence. In comparison, continuum sources must have a narrow band (~10 nm) selected. This drastically reduces the power available for fluorescence excitation. Further, the total laser power can be effectively coupled into the flow cell because of its low divergence.

The maximum output power of the laser is rarely used for exciting fluorescence in microbore LC since even low powers can result in extremely large power densities. This is because of the extremely small spot sizes that can be achieved. In cases where the high power of a laser is exploited, interesting optical events may occur such as two-photon excited fluorescence, which will be discussed later.

Temporal Resolution

Lasers that operate in the pulsed mode deliver intense pulses of light less than a nanosecond in length. This can be exploited for stray light rejection in fluorescence detection. Since fluorescence lifetimes are on the order of

nanoseconds and Rayleigh and Raman scattering processes are coincident with the source, a sub-nanosecond pulse will allow fluorescence to be collected in the absence of Rayleigh or Raman scatter if detection is gated shortly after the pulse.

Polarization

Most lasers produce radiation that is linearly-polarized. In comparison, continuum light sources are randomly polarized, and half the intensity is lost in the production of plane-polarized light. Since Rayleigh (58) and certain Raman lines (59) are polarized when the incident source is polarized, the use of a laser in conjunction with polarization optics on the detector or collecting the fluorescence in the same plane as the polarization vector, allows for effective rejection of Rayleigh and Raman scattered components (57).

The polarized nature of a laser also makes it useful for polarization- based detection schemes such as circular dichroism (60). Circular dichroism can be detected fluorometrically and such a scheme has been adapted for LC (61) in conventional columns and for zone electrophoresis in capillaries (62).

Fluorescence Detection in Microcolumns

A complete review of the physical and chemical principles associated with fluorescence is given in texts devoted to the subject (63,64). Briefly, fluorescence results from the absorption and subsequent emission of a photon. The emitted

fluorescence intensity, I_F, of a fluorophore excited by radiation of intensity, I_O, is described by

$$I_F = 2.303 I_O \phi_F k \epsilon b C \qquad (31)$$

where ϕ_F is the quantum efficiency, k is the collection efficiency, ϵ is the molar absorptivity, b is the cell path length and C the molar concentration.

The attractiveness of fluorescence detection in microcolumn LC can be explained by eq (31). The reduction of cell volume for microcolumns, which was discussed earlier, will result in a decreased path length. This decrease will result in a decrease in fluorescence intensity; however, this decrease can be adequately compensated for by a proportionate increase in I_O. In addition, since low divergence, monochromatic, high power laser radiation can be effectively coupled into microcolumn flow cells, a laser is an excellent choice for excitation of fluorescence in slurry-packed and packed microcolumns, and practically a necessity in OTC columns.

The fluorescence detector is very selective since only a small percentage of those molecules capable of absorbing radiation can yield analytically useful fluorescence. Depending on one's viewpoint, this can be an advantage or a disadvantage. The advantage to fluorescence detection is that since few species fluoresce, background fluorescence from contaminated eluent is unlikely. This results in essentially a zero background which allows for highly sensitive

measurements to be made. Further, complex chromatograms resulting from more general detection schemes, such as absorption, can be simplified by using fluorescence detection.

Two-Photon Excited Fluorescence

The selectivity of fluorescence can be taken a step further by employing two-photon excited fluorescence. The increased selectivity of this process is a result of the different selection rules for one-photon and two-photon absorption. As shown in Figure 4, one-photon absorption results between electronic states of different symmetry. For the absorption of two photons, such a transition is forbidden, but the transition between states of similar symmetry is allowed (65). Further, in order for emission to occur from a two-photon excited state, a third state of different symmetry must be present. Emission can occur through internal conversion to this third state followed by fluorescence from this state to the ground state (66). In this way, one-photon spectroscopy and two-photon spectroscopy are complementary techniques in much the same way Raman spectroscopy is complementary to infrared spectroscopy (65).

There exist many unique factors associated with two-photon excited fluorescence. From Figure 4, it can be seen that the excitation wavelength is longer than that of the resulting emission. This means visible lasers can be used to excite transitions in the ultraviolet. Further, because of the large shift in wavelength, rejection of stray light is simplified.

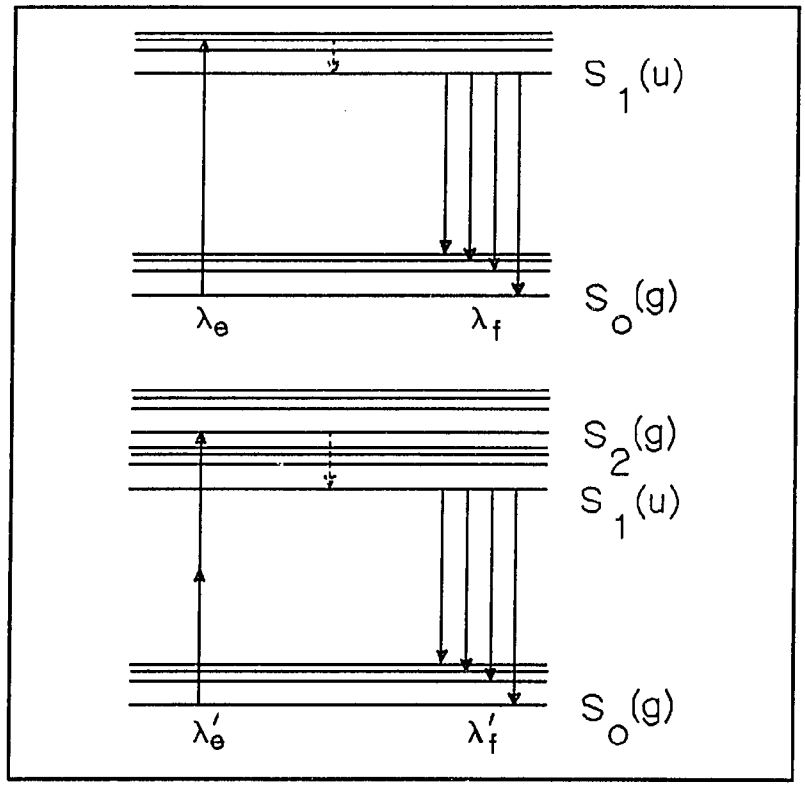

Figure 4. Diagram for one-photon (top) and two-photon (bottom) excited fluorescence. In the top figure, the upper electronic state, S_1, is reached by absorption of a photon of wavelength, λ_e. Vibrational relaxation brings the molecule to the lowest vibrational state of S_1, where it subsequently emits a photon of wavelength, λ_f, to reach S_0. In this example, $\lambda_e < \lambda_f$. In the bottom figure, simultaneous absorption of two photons of wavelength, λ_e', accesses the upper electronic state, S_2. From here, the molecule internally converts to reach the third electronic state, S_1, where it then emits a photon of wavelength, λ_f'. For the two-photon example, $\lambda_e' > \lambda_f'$.

Since two-photon excitation is a much more restrictive process, chromatograms complicated by coelution can be simplified by monitoring two-photon excited fluorescence (67), or better, it can be used as one in a series of detectors, e.q., absorbance, fluorescence, two-photon fluorescence, to provide a fingerprint for a complex sample (68).

In addition, two-photon absorption can be used to effectively excite fluorescence where the excitation of one-photon fluorescence is interfered with by the presence of other chromophores or solvents having absorption bands that coincide with that of the analyte (69).

Section I of this thesis describes a two-photon excited fluorescence detector for microcolumn LC. The power dependence of the two-photon process is examined and the efficiency of different lasers used for two-photon excitation is discussed. Also, the performance of the detector, with respect to a test mixture, is evaluated.

Derivatization

Since fluorescence is a selective process, its use is limited. However, non-fluorescent species can be detected using a fluorometric detector by either first derivatizing them with a suitable fluorescent tag or by to an indirect fluorescence scheme.

By derivatization, one can roughly tailor the absorption profile of the resulting molecule to the excitation wavelength. This is useful since the most popular lasers used for fluorescence detection in LC have only a limited number

of wavelengths available. Low limits of detection (fg) have been achieved for non-fluorescing biologically important molecules in microcolumn LC through the use of derivatizing agents (70-73). Lingeman et al. (74) has outlined a large number of fluorescent derivatization schemes used in association with LC analysis.

Although derivatization offers a method of detecting non-fluorescent species, it is tedious in terms of sample preparation. Indirect fluorometric detection offers an alternative to this.

Indirect Fluorometric Detection

In a direct detection scheme, the detector responds to a physical or chemical property of the solute. However, in an indirect detection scheme, rather than optimizing the detector for a non-responding solute, it is optimized for an eluent component, often called the probe. The probe is intentionally added to the eluent to give a background signal, and once it is equilibrated with the column, this background is essentially constant. After a solute has been introduced into the column, its elution will disrupt this equilibrium. Examples of this are simple volume displacement (refractive index detector), charge displacement (75), or perturbation of the dynamic partitioning properties of the probe (76). In any case, this disrupted equilibrium can lead to a change in the background signal which results in the solute being detected indirectly.

Various modes of LC have been coupled with indirect detection. These include ion-exchange (75), ion-pair (77), and reversed phase chromatography (78).

Indirect detection in its various forms has been reviewed (79-82) and models for detector response have been conceived (76,77,82-84).

Examples of indirect detection systems for LC include indirect polarimetry (85,86) indirect electrochemistry (87), and indirect fluorometry (88,89). Indirect photometric detection has been successfully coupled to slurry-packed microbore columns (90-94). However, such systems can not tolerate low probe concentration or further reduction in detector volume, as in the case of OTC columns, since this will result in a severe loss in sensitivity (88,95,96).

Sections II and III of this thesis are devoted to indirect fluorometric detection in OTC columns. Here, indirect fluorometric detector performance is compared with indirect photometric detector performance for cases where path length and probe concentration are reduced. Again, eq (31) shows that for indirect fluorometric detection, any loss of sensitivity due to reduced path length or probe concentration can be compensated by increasing I_0. Since indirect detection schemes are usually less sensitive than their direct detection counterparts, the union of indirect fluorometric detection with OTC columns increases mass sensitivity due to the small peak volumes associated with the capillaries.

Flow Cells

Fluorescence is usually considered a zero background technique. In reality, fluorescence detection is limited by Rayleigh scatter from cell walls as well as Rayleigh and Raman scatter from the eluent. In addition, luminescence from impurities in the solvent as well as from cell walls can add to the background. Therefore, at this level of detection, increasing I_0 will not improve the limit of detection since the background level increases concomitantly. The use of lasers complicates matters further since they are inherently noisy, with common intensity stabilities of 0.5-1%. To improve detection, several steps may be taken. First, laser intensity can be stabilized to 0.1% or better through the use of a commercially available intensity stabilizer. Second, scatter and luminescence from the eluent and cell wall may be minimized by using spectral filters and the polarization techniques discussed earlier. Further reduction can be achieved through the use of spatial filters and use of a flow cell that minimizes the interaction with the incident radiation.

In principle, the flow cell can consist of any transparent medium which directs the flow of the eluent through the area of illumination. In actuality, the nature of the medium, arrangement of light source, flow cell, and detector, and the area of illumination all affect the performance of a flow cell. A variety of flow cells exist for fluorescence detection in LC, but only a few offer a performance that maintains the efficiency of a microcolumn separation while minimizing contributions to the background. The following gives a brief description of the on-

column flow cell, the fused-silica flow cell, the sheath flow cell and the fiber optic-capillary tube based flow cell.

The first flow cell design and the most popular for OTCs and narrow packed capillaries is the on-column flow cell. This was first described by Yang (97) for UV absorbance detection and later by Guthrie and Jorgenson (98) for fluorescence detection. It consists of an end portion of a capillary stripped of its protective coating. This serves as the point of incidence and facilitates propagation of light. The presence of a stationary phase is dependent upon the system being used. In cases where the stationary phase does not interfere with excitation or emission of fluorescence, true "on-column" detection can be achieved. As described by Guthrie and Jorgenson (98), detection in the presence of a stationary phase will give narrower peaks as compared detection post stationary phase. The reason is that the length of any column between detector and stationary phase simply acts as connection tubing. In addition, Takeuchi and Yeung have shown that detection in the presence of stationary phase can lead to increased fluorescence quantum yields (99). Finally, this design has the advantage of being simple as compared to physically attaching a flow cell to the column, which can be extremely difficult for columns having an i.d. of only a few μm. Also, since there are no connections, there will be no connector band broadening (25).

The fused-silica flow cell is only slightly more elaborate than the on-column flow cell. In this case, an open tube of fused silica is attached to the outlet of the

column. The use of fused silica is prompted by its low fluorescence when exposed to ultraviolet and visible radiation. The illuminated region is kept as close as possible to the column output to reduce band broadening. The drawbacks to using the fused-silica flow cells are the misalignment problems associated with the connection and the walls becoming fragile with prolonged exposure to radiation of high intensity (51).

The sheath flow cell, originally described for LC by Hersberger et al. (100), involves surrounding the effluent exiting the column with a concentric steam of liquid of the same composition as the eluent. With the condition that the flow be laminar, no noticeable diffusion will occur for some distance. The reason for the sheath is to reduce the scatter and fluorescence due to the cell windows (100). Although not used for LC effluents, Dovichi et al. (101) report a concentration detection limit of 8.9×10^{-14} M and a mass detection limit of 18 attograms for Rhodamine 6G using such a flow cell.

Of the three cells discussed, alignment for the sheath flow cell with respect to incident radiation is most difficult. Because small changes in sheath flow can lead to changes in column flow, misalignment becomes a problem. Also, poorly cut ends of OTC columns can lead to turbulence (102). Van Vliet and Poppe (102) have studied these designs in connection with OTCs of 25 and 10 μm i.d. Their conclusions were that for the 25 μm i.d. column, similar performance could be obtained from all three designs, but for the 10 μm i.d. column, the coupled flow cells gave slightly poorer efficiency. This was thought to be due to

connection problems discussed earlier.

The fiber optic-capillary tube based flow cell involves a fused silica flow cell which has an optical fiber inserted into the end of it, such as the design described by Sepaniak and Yeung (103). Fluorescence is collected via the fiber optic, which allows close placement of the optic to the excitation region. This allows for good fluorescence collection efficiency. Since a critical cone of collection exists for the fiber optic, good rejection of scatter and fluorescence from the cell wall is achieved (103). Because fiber optics are available with diameters of a few μm, it is possible to use this type of detection cell in narrow capillaries (70).

SECTION I. LASER TWO-PHOTON EXCITED FLUORESCENCE DETECTOR FOR MICROBORE CHROMATOGRAPHY

Introduction

The fluorometric detector in liquid chromatography (LC) has the special feature of high selectivity compared to the absorption detector and the refractive index detector. With the addition of a laser as the excitation source, impressive results have been reported (1-4). In particular, the laser allowed better stray light reduction (due to better beam quality), and better focusing into small volumes (due to better spatial coherence). Coupling with microbore LC, where detector volumes less that 1 μL are required, is then relatively straightforward, and mass detectability is enhanced.

To further increase selectivity in fluorometry, one can use a two-photon excitation scheme (5). The simultaneous absorption of two photons of light is guided by different selection rules than normal absorption, so that different electronic states are excited. This provides a separate dimension for selectivity. The process is dependent on the individual polarization conditions of the photons, so polarization selection is possible. The process is enhanced by electronic states matching the energy states matching the energy of one of the photons (6) to provide a unique type of wavelength dependence. Finally, fluorescence from two-photon states back to the ground state is actually forbidden by selection rules (1).

There needs to be a third electronic state present, making this a more restrictive process than normal fluorescence. The additional selectivity has already been demonstrated in LC effluents (5).

The key to successful application of two-photon excited fluorescence is sensitivity. The two-photon event is much less probable than the one-photon event in general. The probability however increases with photon density. The relationship between the absorbed power and the incident optical power is expressed as

$$\Delta P = P^2 CLA^{-1}\delta \qquad (1)$$

where ΔP and P are the absorbed power and the incident power respectively, L is the path length, C is the concentration, A is the cross-sectional area of the optical beam, and δ is the two-photon absorption strength. Values typical for δ are $\leq 10^{-48}$ cm^4 s $photon^{-1}$ $molecule^{-1}$. This is why lasers are essential to providing useful signals. Also, fluorescence rather than absorption is monitored to provide better detection. Unlike conventional fluorometry, where detectability is limited by stray light and Raman/Rayleigh scattering in the solvent, background in two-photon excited fluorometry is almost always negligible. This is because excitation is by visible photons and observation is via UV photons. Even simple filters can reject background contributions. Furthermore, eq (1) shows that the signal increases quadratically with incident power while any background signal will

increase linearly with incident power. This favors lasers with high peak powers even though cw lasers provide adequate sensitivity (5). Naturally, another important consideration is the average power of the laser, since a low duty cycle implies poor efficiency in producing fluorescence photons. For a laser with average power P(W), pulse duration t (s) and a repetition rate of f (s^{-1}), one can derive the peak power per pulse as P/ft. The two-photon signal is then proportional to the square of this quantity. Over a 1 s period, the total number of two photon events will be proportional to

$$\Delta P \propto \left(\frac{P}{ft}\right)^2 ft \tag{2}$$

$$\Delta P \alpha \frac{P^2}{ft} \tag{3}$$

Eq (3) is an indication of the efficiency in generating a signal if the fluorescence yield, path length, beam size, and concentration are identical. In Table 1 we list the efficiencies of several commercial laser systems relative to a cw laser used in ref (5). In interpreting Table 1, one must also consider other factors, such as beam quality (which allows focusing to small volumes), excessive power density (which leads to dielectric breakdown and other nonlinear processes), and intensity stability (which contributes to baseline fluctuations).

In this work, we describe a two-photon excitation scheme for fluorometric

detection based on a copper vapor laser (LTPEF). The cell geometry allows the use of microbore columns. Substantial improvements in both concentration detectability and mass detectability are achieved.

Experimental

HPLC system

The LC system was assembled from the following components. Pump: Metering pump, ISCO, Lincoln, NE, μLC-500. Column: Alltech, Deerfield, Il, 5-μm microsphere C_{18} packing, 25 cm long, 1 mm i.d. Injector: Rheodyne, Berkeley, CA Model 7410 with 1.0-μL injection loop. Eluent: 90/10 acetonitrile/H_20. Solvent: The solvent for all samples was the same as the eluent. Compounds: 2-(4-biphenyl)-5-phenyl-1,2,3-oxidiazole, PBD (Eastman Kodak, Rochester, NY) and 2,5-diphenyl-1,3,4-oxidiazole, PPD (Pfaltz and Bauer, Waterbury, CT) were used.

All separations were performed under normal room temperatures at a flow rate of 30 μL/min, and a pump pressure of 580 psi.

LTPEF detector

The laser radiation of a copper vapor laser (Plasma Kinetics, Pleasanton, CA, Model 151 with unstable resonator cavity) leaves the aperture and passes through one Corning 3-71 sharp cut-off filter and one Corning 4-96 wide band-pass filter

mounted directly on the laser head. The purpose of the Corning 3-71 filter is to eliminate secondary laser radiation. The Corning 4-96 filter is used to block out the orange fluorescence created by the Corning 3-71. No attempt was made to separate the 510/578 nm lines from the laser. The radiation is then focused into the flow cell by a 8.5-cm focal length, 5-cm diameter lens. The flow cell consists of a 1-mm i.d. quartz rod is attached to the outlet (bottom) of the column. A quartz rod is attached to the inside of the tube to limit the actual cell volume to approximately 0.8 μL (see Figure 1). The purpose of the direct column attachment and quartz rod is to lessen the effect of band spreading associated with HPLC detectors. The fluorescence leaving the flow cell passes through three UV band-pass filters: one Corning 7-54, one Corning 7-59, and one 7-51. The fluorescence then enters a photomultiplier tube (Amperex, Hicksville, L.I., N.Y., model 56-DVP) operated at 1360 V.

Signal Processing.

The signal from the photomultiplier tube was processed by a picoammeter (High Speed Picoammeter, Keithley Instruments Inc., Cleveland, Ohio, model 417). The instrument was set at 1×10^{-10} A to measure fluorescence. The signal was adjusted with the damp control until a reasonably smooth baseline was obtained. This corresponds to a time constant of about 3 s. Chromatographs were obtained by sending the processed signal to a stripchart recorder (Fisher Recordall, Houston Instruments, Austin, Texas, Series 5000).

Figure 1. 0.8-μL flow cell for two-photon excited fluorescence. CS, microbore column outlet tube; FLB, focused region of copper vapor laser; QT, quartz tube (1 mm i.d.); QR, quartz rod (0.8 mm o.d.).

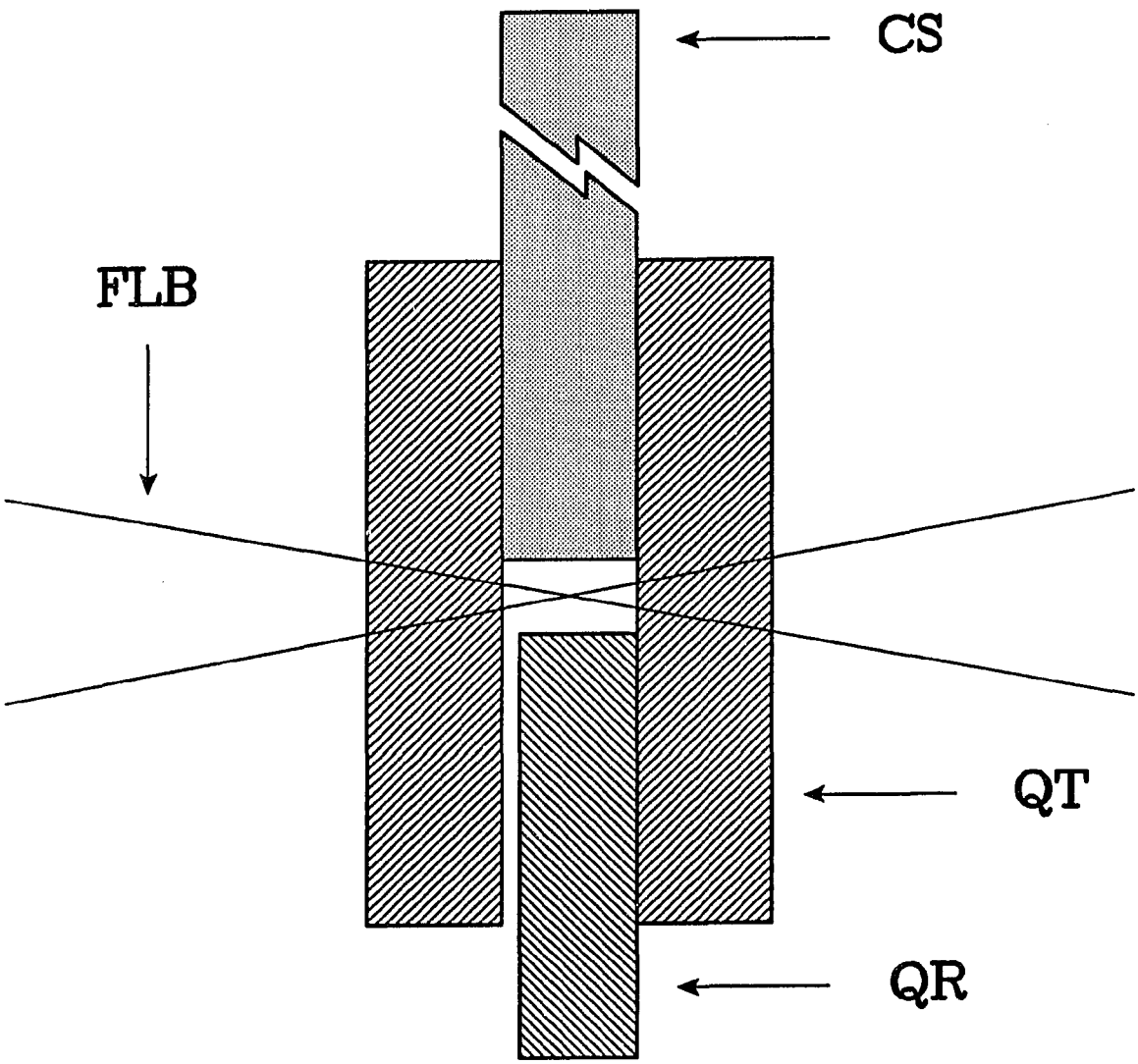
CS
FLB
QT
QR

Detector optimization

The base of the flow cell was mounted in a x,y,z translational stage which in turn was mounted to an optical bench. By viewing the focused laser radiation, the active region of the flow cell was aligned so that the radiation was focused inside the cell. The system was then fastened securely so no tension was placed on the microbore column. The entire system was then cloaked with a thick black fabric to eliminate background radiation.

Results and Discussion

An inspection of Table 1 shows that three laser systems stand out as having substantially higher conversion efficiencies than the others. A Q-switched Nd:YAG laser system (Quantel, Santa Clara, CA, Model VG480) was tested with a steady flow of PBD solution (7). Because of the poor mode structure, the beam waist at the focused region is quite large, and the two-photon efficiency in Table I was not achieved. Furthermore, the existence of hot spots in the laser beam caused damage to the capillary tube after even brief exposures. The slow repetition rate of the YAG laser and the pulse-to-pulse intensity fluctuations ($\pm 5\%$) introduced additional fluctuations in the baseline. Improvements in detectability over cw laser excitation (5) is estimated to be only about a factor of 10. On comparison of the copper vapor laser and the excimer-pumped dye laser, detectabilities are comparable but the former is easier to operate (no alignment or

Table I. Relative efficiencies of various laser systems for two-photon excitation

Type	Average Power (W)	t (s)	f (s^{-1})	Peak Power (W)	Efficiency
Ar ion	1	1	1	1	1
Cu vapor	3	3×10^{-8}	5000	2×10^{4}	6×10^{4}
mode-locked Ar ion	0.6	1.2×10^{-10}	7.6×10^{7}	66	39
mode-locked YAG, doubled	1	7×10^{-11}	7.6×10^{7}	190	190
mode-locked dye	0.06	8×10^{-13}	7.6×10^{7}	990	59
cavity-dumped dye[a]	0.045	1.5×10^{-12}	3.8×10^{6}	7.9×10^{3}	360
Q-switched YAG, doubled	1	1×10^{-8}	10	1×10^{7}	1×10^{7}
excimer-pumped dye	1	1×10^{-8}	500	2×10^{5}	2×10^{5}

[a]Pumped by a mode-locked YAG laser.

degradation of dye or gas) and has better mode structure if an unstable resonator cavity is used. So, the copper vapor laser is used for subsequent studies.

A chromatogram of the test mixture is shown in Figure 2. The injected quantities are 45 pg PPD and 3.0 pg PBD. The peaks are well separated and the manufacturer's specification for the column of 100,000 plates/m is achieved, showing negligible extra-column band-broadening. We find, however, that if the quartz rod in Figure 1 is removed, substantial band-broadening occurs, presumably

Figure 2. Two-photon excited fluorescence chromatogram of test mixture: [PPD] = 2×10^{-7} M; [PBD] = 1×10^{-8} M; injection loop, 1 μL; flow rate, 30 μL/min; eluent, 90/10 acetonitrile/water; column, 5-μm C_{18}, 1 mm i.d., 25 cm long.

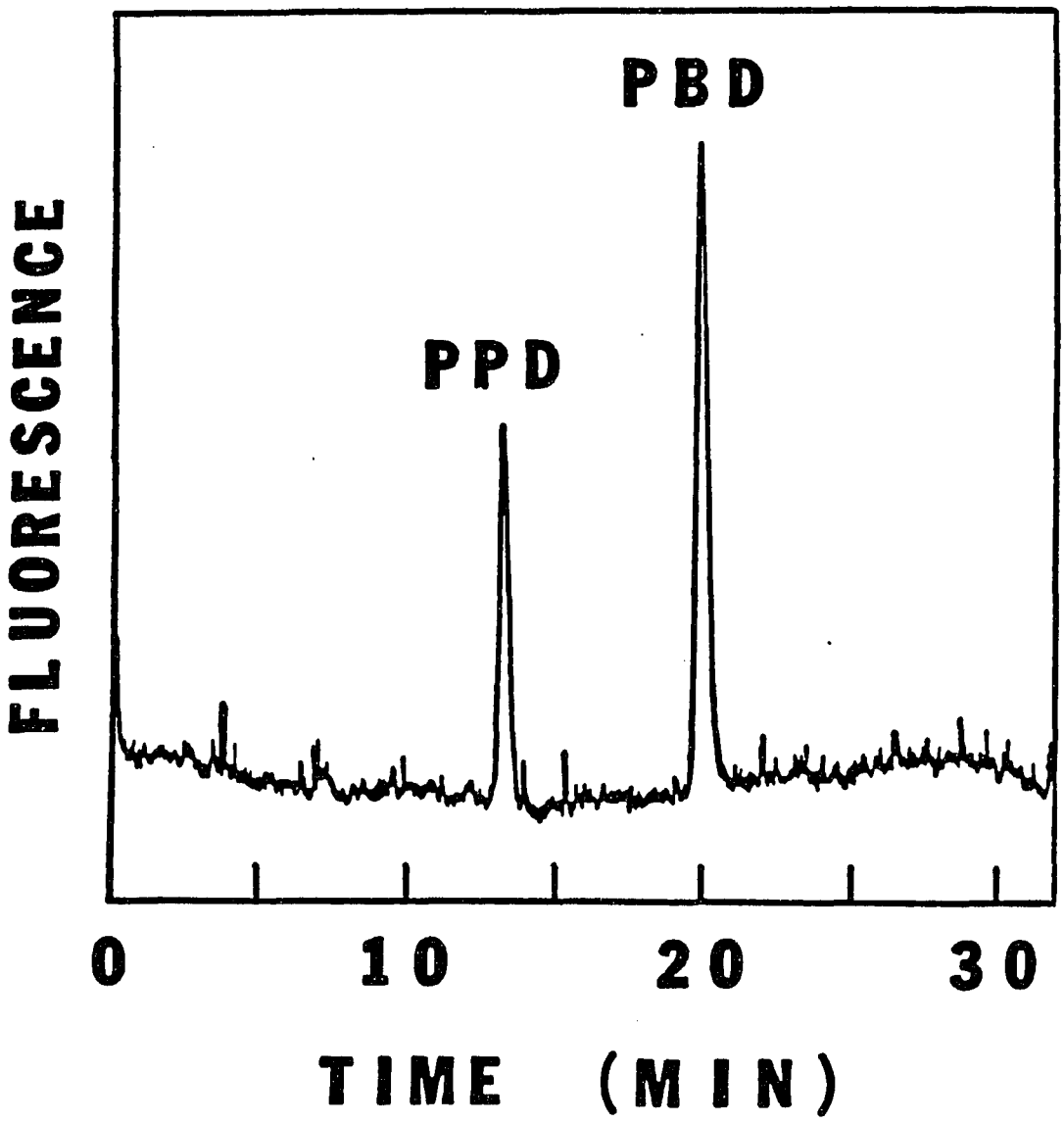
PBD
PPD
FLUORESCENCE
0
10
20
30
TIME (MIN)

due to turbulent mixing after the optical region. The quartz rod can be replaced by an optical fiber (1) so that the visible fluorescence can be monitored to achieve two-dimensional detection in complex samples. Despite the filters, the background is not at exact zero. So, laser intensity fluctuations (±1%) still contribute to baseline noise. The slow drift in baseline also corresponds to a change in average laser power during observation. Spikes in the baseline correspond to an occasional dust particle crossing the laser beam which increase scattered light. The PBD peak is higher because of a better match in the absorption wavelength for this laser system. The detectability (S/N = 3) of PBD is estimated from Figure 2 to be 250 fg injected. Over the range of 1×10^{-8} M to 1×10^{-6} M injected, the signal is found to be linear after corrections for laser power variations.

The detectabilities here are more than 4 orders-of-magnitude better than those in ref (5). Since the excitation wavelengths are almost identical, the differences reflect real improvements. The use of microbore columns immediately provides a factor of 25 (ratio of i.d.) in mass detectability. The chromatographic efficiency here is substantially better, probably enhancing detection by a factor of 4. So, a gain of 300 can be attributed to the laser alone. The unstable resonator cavity of the copper vapor laser still does not provide a TEM_{00} mode like the Ar ion laser. A spot size roughly 5 times the diffraction limit can be expected, so the peak powers in Table 1 are not realized. Thus, only an enhancement of 2.4×10^3 is theoretically possible. With a less stable baseline because of larger intensity

fluctuations in the laser here, there is further degradation in S/N. So, the observed improvement of 300 is consistent with the characteristics of the laser systems.

With the improved detectabilities here, two-photon excited fluorescence is competitive with most other LC detectors in sensitivity. Normal fluorescence will still be slightly better in ideal cases where emission is far away from solvent Raman bands. The fact that there is so little background from the solvent here implies that solvent purity requirements can be relaxed. The transverse excitation geometry and small optical volume make this detector suitable for even on-column measurements in capillary LC, super-critical fluid chromatography, or capillary zone electrophoresis. The 510 nm and 578 nm laser lines effectively excite bands around 255 nm and 289 nm respectively, allowing coupling with a large group of chromophores. Future work in resonance enhancement and polarization selection can make this an even more powerful technique.

References

1. Sepaniak, M. J.; Yeung, E. S. Anal. Chem. 1980, 52, 1465A-1481A.

2. Diebold, G. J.; Zare, R. N. Science 1977, 196, 1439-1441.

3. Folestad, S.; Johnson, L.; Josefsson, B.; Galle, B. Anal. Chem. 1982, 54, 925-929.

4. Hershberger, L. W.; Callis, J. B.; Christian, G. D. Anal. Chem. 1979, 51, 1444-1446.

5. Sepaniak, M. J.; Yeung, E. S. Anal. Chem. 1977, 49, 1554-1556.

6. Huff, P. B.; Tromberg, B. J.; Sepaniak, M. J. Anal. Chem. 1982, 54 946-950.

7. Huie, C. W.; Yeung, E. S. Department of Chemistry, Iowa State University.

SECTION II. ANION CHROMATOGRAPHY IN OPEN TUBULAR CAPILLARY COLUMNS WITH INDIRECT FLUOROMETRIC DETECTION

Introduction

Recently, there has been a lot of interest in the use of microcolumns in HPLC (1). The main advantages are the enhanced mass detectability and the reduction of the amounts of mobile phase and stationary phase used. The former is particularly important when the sample size is limited, such as in natal or prenatal body fluids, or in analysis at the cellular level. The latter allows designs of special separation modes, such as chiral phases or affinity phases, or the use of unique detection schemes. Very efficient separations have been obtained in microcolumns (2). It is predicted that optimum open-tubular capillary liquid chromatographic (LC) columns can generate in excess of 10^6 theoretical plates (3,4). The internal volume of such a column is around or less than 10 nL. Therefore, injection and detection volumes should be substantially reduced compared with conventional LC so that they do not degrade column efficiency. Injection of small volumes of sample can be readily achieved by split injection techniques, while detection has been a more difficult problem in open-tubular capillary LC.

Ion chromatography (IC) has become an important analytical method as a result of research efforts in the last few years (5-7). Much attention has been

given to nonsuppressed ion chromatography, because of the potential for minimizing band broadening. Most of the detectors have very similar limits of detection (LOD), which are in the nanogram range for typical ions. Since these detectors have already been utilized to their full potential, additional improvements in LOD can only come if new detection principles are introduced.

In conventional liquid chromatography (LC), the lowest LODs have been reported for the fluorescence detector (7). For ions that fluoresce, one can thus expect improved LOD in IC as well. However, the number of ions that inherently show fluorescence is very small. Recently, several indirect detection methods for LC have been demonstrated (8,9). Indirect fluorescence detection (10-12) is particularly interesting. Briefly, a fluorescing eluting ion is used in the nonsuppressed IC mode. So, there is a constant background signal generated at the detector when no analytes are present. When the analyte ion elutes, it displaces an equal amount of the eluting ion at the detector. Even though the detector does not respond to the analyte, the lower eluent concentration at the detector causes a decrease in signal. The analyte can then be monitored as a negative signal, i.e., indirectly.

There is an important feature in indirect fluorescence detection versus indirect photometry (8). As the volume of the detector decreases, such as in moving to microcolumns, the sensitivity of absorption methods will decrease to the point where they are no longer suitable for indirect detection. The background level cannot be maintained high enough to observe the negative signal. In

fluorescence, especially if lasers are used for excitation, there is adequate sensitivity even if pathlengths are small or if the concentration of the eluting ion is low. In this paper, we report the use of open-tubular-capillary column for ion chromatography. Indirect fluorescence allows detection of non-fluorescing anions at very low levels.

Experimental

Apparatus

Figure 1 shows a diagram of the chromatographic system employed in this work. A syringe pump (ISCO, Lincoln, NE, Model 2600) was used as a pump and was operated in the constant-pressure mode. A line filter SSI 05-0105 (0.5 μm, supplied by Alltech, Deerfield, IL) was connected before the injector. A Rheodyne Model 7520 (1μL, Cotati, CA) was employed as a sample injector and the split ratio was regulated by a SSI two-way valve (Alltech) and stainless-steel tubing of 2 m x 0.1 mm i.d. (Japan Spectroscopic, Tokyo, Japan). An SB-OCTYL-50 (n-octylmethylpolysiloxane, 50% n-octyl groups) open-tubular fused-silica capillary column (10 m x 50 μm i.d. and 0.5 μm thickness) was commercially available from Lee Scientific (Salt Lake City, UT). The capillary column was directly connected to the sample injector through a T-joint (0.75 mm bore; Valco, Houston, TX). A linearly polarized 325-nm UV beam of a HeCd laser (Liconix, Sunnyvale, CA, Model 4240NB) at about 7 mW is used as an excitation source.

Figure 1. Diagram of the chromatographic system. 1 = pump; 2 = injector; 3 = T-joint; 4 = two-way valve; 5 = restrictor; 6 = 1/16 in. x 1/32 in. reducing union; 7 = capillary column; 8 = sample flow cell; 9 = gravity flow system; 10 = reference flow cell; 11 = optical fibers; 12 = photomultiplier tube.

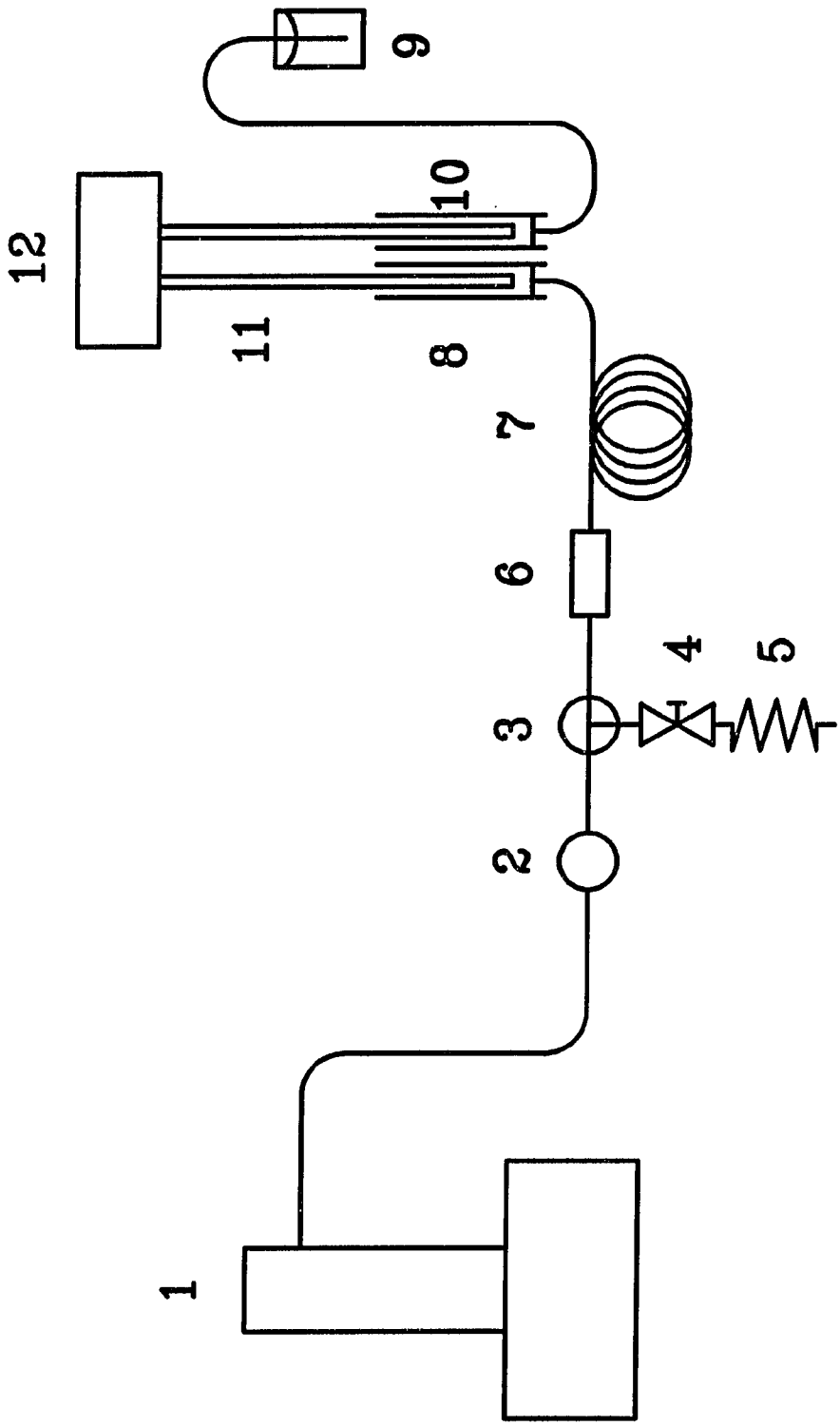
9
10
12
11
8
7
6
4
5
3
2
1

The polarization of the beam is modulated at 100 kHz by an electrooptic modulator (Lasermetric, Inc., Teaneck, NJ, Model 3030), which is driven by a high-frequency modulator driver (Conoptics, Inc., Danbury, CT, Model 25). Unipolar positive-going square waves (0 to + 1.0 V) from a wave generator (Wavetek, San Diego, CA, Model 162) are in turn applied to the modulator. A calcite beam displacer (Karl Lambrecht Corp., Chicago, IL, MBDA10) splits the polarization-modulated beam into two separate beams. The perpendicularly polarized beam continues straight through while the horizontally polarized beam goes through the calcite at 6°. The horizontally polarized beam emerges displaced 3.3 mm apart from the first, and parallel to it. The two beams are directed to the centers of the sample and reference flow cells, respectively.

Two parallel 1-mm i.d. x 2-mm o.d. quartz tubes are held 3.3 mm apart. A 50-cm focal length quartz lens is used to collimate the laser beam into the modulator. A 4.5-cm focal length quartz lens is placed before the calcite displacer in order to focus the 1.2 mm-diameter laser beam down to 54 μm at the flow cells. The fluorescence from each cell is collected by separate optical fibers similar to the arrangement in ref 13. Both fibers are directed to a single photomultiplier tube (Hamamatsu, Bridgewater, NJ, R928) after passing through three filters (Corning Glass, Corning, NY, 0-52 and 3-75 and Schott Glass, Duryea, PA, K-5). The photomultiplier tube output is directed to a lock-in amplifier with a 1-s time constant (EG&G, PAR, Princeton, NJ, Model 5202) through a 100x amplifier (Hewlett Packard, Palo Alto, CA, Model 420). Initially the fluorescence signals

from the sample and reference cells are maximized and balanced (during the two half-cycles of the modulation) by adjusting the distance of each fiber to the irradiated zones. This then provides a null output at the lock-in amplifier when eluent is present. The reference cell contains identical eluent flowing at approximately the same rate in a conventional gravity-induced flow system. A typical flow rate is 2 μL/min.

Reagents

HPLC-grade methanol was supplied by Fisher Scientific (Fair Lawn, NJ). Water employed in this work was pure water prepared with the Barnstead Nanopure II system (Barnstead, Division of Sybron, Boston, MA). Cetylpyridinium chloride monohydrate (CPC) was supplied by Aldrich (Milwaukee, WI). The other reagents used in this work were reagent grade and supplied by Fisher Scientific, unless otherwise noted. The mobile phase was degassed in an ultrasonic bath under vacuum. The reference solution for fluorometric detection was degassed the same way and then filtered with a disposable Nylon 66 filter (Alltech, 0.2 μm). The samples were dissolved in the eluent.

Preparation of the column

The quaternary ammonium salt (50 mM) was dissolved in 2% methanol. The prepared reagent solution was passed through the column for 6 h, followed by

washing with water for 30 min. After the above dynamic modification, the sodium salicylate solution used as the eluent was passed through the dynamically modified column. In order to wash out the modifying reagent from the column, methanol was passed through the column for at least 1 h.

Results and Discussion

In the indirect detection method, the dynamic reserve (which is defined as the ratio between the background signal and its noise level), the concentration of the visualization reagent, and the displacement ratio (which is defined in this work as the number of visualization ions which are transferred by one analyte ion) all play important roles in the sensitivity that can be achieved. The concentration detectability (C_{lim}) at the detector is given by these parameters as follows:

$$C_{lim} = C_m/RD \qquad (1)$$

where C_m is the concentration of the visualization reagent, R is the displacement ratio, and D is the dynamic reserve. The dynamic reserves for fluorescence and for absorption vary differently with the magnitude of the background signal, while the former maintains a 5×10^3 level until the concentration of the visualization reagent falls below 1.0 a.u. The displacement ratio for monovalent ions is expected to be unity in ion-exchange chromatography (independent of the mobile phase concentration). Ion-exchange columns having a very low capacities are

required to demonstrate the separation of ions using a mobile phase with low concentrations of visualization reagent.

To produce an open tubular capillary column that allows low concentrations of eluting ions to be used, one needs a low capacity. This can be achieved by dynamic modification. The column generation procedure is similar to earlier reports (12,14). The limited surface area of the open tube automatically lends itself to a low capacity mode. We found that common anions can be separated by elution with salicylate ions at the micromolar range. This is two to three orders of magnitude lower than those typically used for analytical scale nonsuppressed IC. According to eq (1), this is favorable for detection.

Figure 2 shows a chromatogram of anion exchange chromatography using such a dynamically modified column. The conditions there have been optimized for the detection of the two anions Cl^- and NO_3^-. Salicylate at 2.5 x 10^{-6} M is used as the eluent. At higher salicylate concentrations, the elution strength does not allow separation of the two ions. At lower salicylate concentrations the retention times become too long, and the peak heights decrease proportionately. The 50 μm i.d. of the open-tubular column is not optimal for LC. Ideally, one wants to use i.d. of the order of 1-3 μm (4). At this time, our choice is limited by the commercially availability of such columns. Another advantage is that a smaller column will improve mass detectability even further because of the reduced peak volume.

The magnitudes of the signals can be compared to those predicted from the

Figure 2. Indirect fluorescence chromatograms of anions. 1 = salicylate (system peak); 2 = chloride; 3 = nitrate. Random spikes before the salicylate peak are due to microbubbles in the effluent. Flow rate = 2 μl/min. O.5 pmol of each ion was injected.

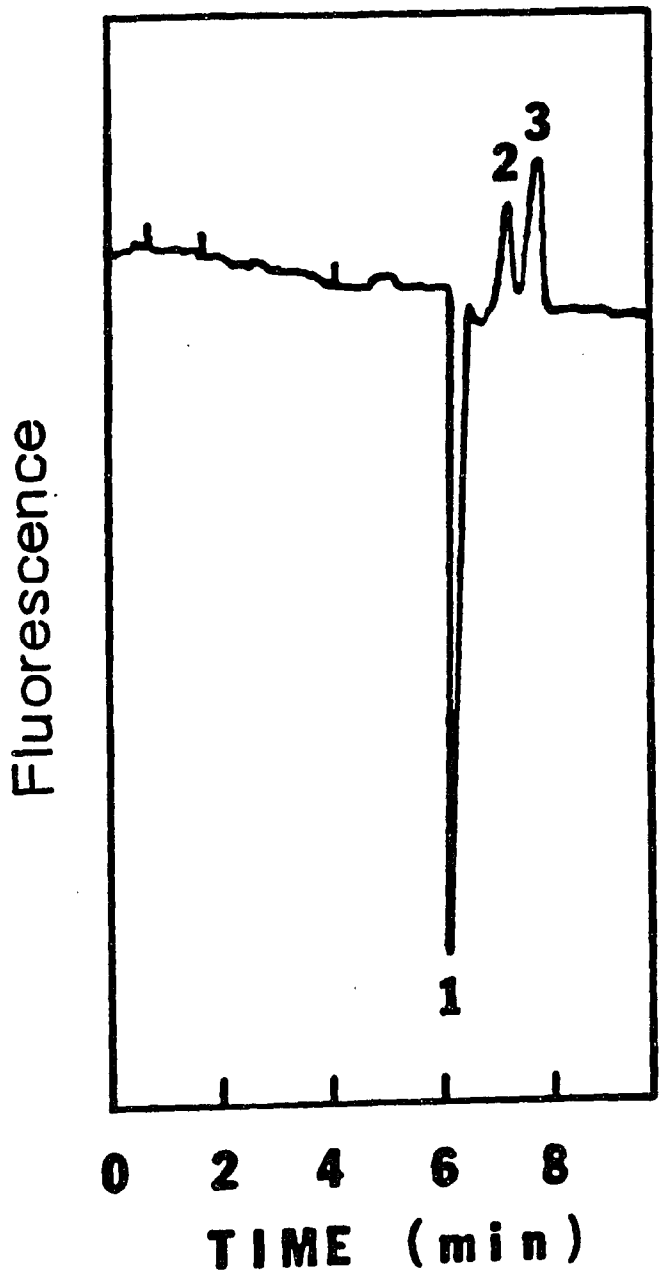
Fluorescence
1
2
3
0
2
4
6
8
TIME (min)

displacement of the eluting ions by the analyte ions on a per equivalent basis. The background fluorescence signal, as determined by irradiating only the sample flow cell, was 14.4 mV measured by the lock-in amplifier. The peak heights of chloride and nitrate in Figure 2 corresponded to 0.50 mV and 0.70 mV, respectively. So, the signals at the peaks corresponded to decreases of roughly 1/29 and 1/21 of the total fluorescence, or a displacement of 8.6×10^{-8} N and 1.2×10^{-7} N of salicylate ions, respectively. Now 5×10^{-13} mol of each of the two ions were injected, and these were diluted to peak volumes (fwhm) of 0.4 μL each. The actual concentrations of the analyte ions at the peaks are then 1.2×10^{-6} N. This is 10 times larger than the signals levels would indicate, since an ion exchange mechanism for separation and a displacement mechanism at the detector (due to electroneutrality) must be responsible for the observed chromatogram. In previous work (10), a one-to-one correspondence was observed. The present results indicate that stray light is dominating over fluorescence at this low a concentration of salicylate. If stray light can be further reduced, one would expect even better detectability for the anions. Possible contributors to stray light include Raman scattering of the solvent, fluorescent impurities in the eluent, and fluorescence from both the quartz tube and the optical fiber that is coupled to the phototube. We have independently confirmed the contribution of stray light in this arrangement by measuring the phototube current while water alone is passed through the flow cell.

The peak height of the nitrate ion is about 0.7 mV. So, the noise level in

the chromatogram corresponds to 1 pg of NO_3- injected. This is substantially better than previous results in detection in IC (6,10). This is due to the small peak volumes in open tubular capillary LC. The noise level corresponds to 4.5×10^{-8} N of ion present at the detector. This is similar to those in standard detectors for nonsuppressed IC. Because of stray light and the lower fluorescence intensity, the dynamic reserve here is lower than that in ref (10). However, the eluent concentration here is lower. According to eq (1), the two balance out and the concentration detectability did not change.

Future improvements in this system should be possible. These can include better stray light rejection, better coupling between the capillary column and the detection cell, the use of smaller i.d. capillary columns, still lower concentrations of the eluent by further reducing the capacity of the column, and a higher degree of intensity stability from the laser. Still, the present system provides one of the best mass detectabilities of non-fluorescing anions separated by IC.

References

1. Novotny, M., Ed., Microcolumn Separations; Elsevier: Amsterdam, 1985.
2. Menet, H. G.; Gareil, P. C.; Rosset, R. H. Anal. Chem. 1984, 56, 1170.
3. Knox, J. H.; Gilbert, M. T. J. Chromatogr. 1979, 186, 405.
4. Jorgenson, J. W.; Guthrie, E. J. J. Chromatogr. 1983, 255, 335.

5. Small, H. In Trace Analysis; Lawrence, J. F. Ed., Academic Press: New York, 1982; Vol. I, p 267.

6. Fritz, J. S.; Gjerde, D. T.; Pohlandt, C. Ion Chromatography; Huthig: New York, 1982.

7. Small, H. Anal. Chem. 1983, 55, 235A.

8. Small, H.; Miller, T. E. Anal. Chem. 1982, 54, 462.

9. Bobbitt, D. R.; Yeung, E. S. Anal. Chem. 1984, 56, 1577.

10. Mho, S. I.; Yeung, E. S. Anal. Chem. 1985, 57, 2253.

11. Takeuchi, T.; Yeung, E. S. J. Chromatogr. 1986, 366, 145.

12. Takeuchi, T.; Yeung, E. S. J. Chromatogr. 1986, 370, 83.

13. Sepaniak, M. J.; Yeung, E. S. J. Chromatogr. 1980, 190, 377.

14. Cassidy, R. M.; Elchuk, S. Anal. Chem. 1982, 54, 1558.

SECTION III. INDIRECT FLUOROMETRIC DETECTION IN OPEN TUBULAR CAPILLARY COLUMN CHROMATOGRAPHY

Introduction

The method of indirect detection in liquid chromatography has received a considerable amount of attention in the past few years (1-3). Essentially, a detectable species (probe) is present in the eluent and produces a constant background signal at the detector. When an analyte elutes from the column, it changes the concentration of the probe at the detector and with it the background signal; hence, the analyte is detected indirectly. Schemes for the indirect detection of electrolytes (4), non-electrolytes (5) or both (6) have been devised and used with considerable success. A variety of detectors have been employed including fluorometric (7-10), polarimetric (11) and electrochemical (12), but the majority of the work has been done with photometric detectors (4-6,13-18).

Another topic receiving considerable interest in chromatography is the use of microcolumns (19,20). The advantages to using microcolumns are their compatibility with small samples, reduced analyte dilution, reduced flow rate and high separation efficiency. Of the four types of microcolumns being used - small bore packed, packed capillary, semi-packed capillary and open-tubular capillary (OTC) - OTC columns have the attraction of being able to produce high separation efficiencies in a reasonable time with superior limits of detection

(LOD) (21). Theory suggests that the internal diameter of OTC columns needs to approach that of column packing material (1-10 μm) in order to operate at maximum efficiency (22,23). Although once difficult to prepare, procedures using silicone gums have simplified OTC column preparation somewhat (24,25).

The union of microcolumns with indirect detectors will allow sensitive detection of those analytes which yield poor absorption, fluorescence or electrochemical response. Analytes detected indirectly using microcolumn separations include anions (7,10,13), alcohols (9,14), hydrocarbons (15) and ethylene glycol oligomers (16). In the examples cited, the photometric detector is the most popular. Because a large, stable background signal is essential for any indirect detection method, restrictions on path length (b), probe molar absorptivity (ϵ) and probe concentration (C_m) must be adhered to. For example, since absorption detectors typically have noise around 0.0001 absorbance units (au), to maintain a stability of only 1 part in 1000, the background must be at least 0.1 au. For columns with diameters of 10-100 μm, this fact imposes even stricter constraints on the probe ϵ and C_m. Indirect fluorometric detection should not suffer from these limitations to the same degree indirect photometric detection does. When excitation is provided by a laser, reduced b, ϵ or C_m can largely be compensated for by increasing the power of the incident radiation to yield ample photons at the detector such that the system remains above the shot-noise limit; i.e., background stability is independent of ϵ, b and C_m.

In this work, polymer-coated OTC columns of 13-15-μm i.d. are used

separately for the separation of electrolytes and non-electrolytes. By treating the polymer surface with a quaternary ammonium ion, the capillary can effectively function as an ion-exchange column. The untreated polymer surface allows the capillary to function as a reversed-phase column. Indirect fluorometric detection allows extremely low levels of both types of analytes to be detected.

Experimental

Reagents

Electrolytes Sodium salicylate, sodium acetate, and HPLC-grade methanol were supplied by Fisher Scientific Co. (Fairlawn, NJ). Sodium nitrite was supplied by Mallenckrodt, Inc. (St. Louis, MO). The eluent was prepared by dissolving sodium salicylate in water and degassing the solution in an ultrasonic bath under vacuum. Samples were dissolved in eluent.

Non-electrolyte work The alkanols were supplied by Aldrich Chemical Co., Inc. (Milwaukee, WI), Sigma Chemical Co. (St. Louis, MO) or Eastman Kodak Co. (Rochester, NY). Solutions containing the probe 2,7 dichlorofluorescein (2,7 DCF, Eastman) were prepared from a 1 mM acetic acid buffer in 0-10% acetonitrile (HPLC grade, Eastman). The pH of the final solution was adjusted to a value between 3.0 and 5.0. The eluent was degassed by sparging with N_2 gas. Alkanol samples were prepared by mixing them in an acetonitrile/water solvent that was of the same ratio used in the eluent.

In both the electrolyte and non-electrolyte work, the water used was purified using a Barnstead Nanopure II system (Barnstead, Division of Sybron, Boston, MA). All chemicals were reagent grade and used as supplied unless specified.

Column preparation

The columns were prepared using a procedure adapted from Farbrot et al. (24). A fused silica capillary column (Polymicro Technologies Inc., Phoenix, AZ; 50-120 cm x 150 μm o.d.) of 13-15 μm i.d. was purged with helium for 30 min. The column was then filled with a solution of 1-2% (w/v) PS-255 or PS-265 (Petrarch Systems Inc., Bristol, PA) in pentane in which the cross-linking agent dicumyl peroxide (Pfaltz and Bauer, Inc., Waterbury, CT) was present at an amount of 1% (w/w) of the polymer. Following removal of the column from the filling device, the ends were cleaved and left open. The column was then immersed in a water bath with its ends exposed to air or placed in a GC oven and the solvent evaporated using temperatures of either 35^{o}C or 40^{o}C. After evaporation was complete, the column was again flushed with helium for 30 min. The ends were sealed using sodium silicate, and cross-linking was carried out using a temperature program of 15^{o}C/min to 175^{o}C, then 175^{o}C for three minutes. After cross-linking was complete, the polyimide coating was burned off one end of the column to facilitate on-column detection.

Chromatographic system

The chromatographic system employed in this work is identical to that described in ref (10) with the exception that a microsyringe pump (ISCO, Lincoln, NE; Model μLC-500) was used in the constant-flow mode to propel the eluent through the column. The injector (Cotati, CA; Model 7520) rotor volume was 0.2 μL for the electrolyte work and 0.5 μL in the non-electrolyte work. When being used, the ion-exchange column was kept in a water bath held at ambient temperature.

Dynamic modification of the column

The procedure used to dynamically modify the capillary column is similar to earlier descriptions (7,10,26). Here, the column was equilibrated with a solution of 30 mM cetyltrimethylammonium bromide (Aldrich) in 5/95 methanol/water. Cetyltrimethylammonium bromide could be removed by washing the column with 50/50 methanol/water, thereby returning it to a reversed-phase column.

Detector

In the electrolyte work, 330-nm radiation leaving an argon-ion laser (Spectra-Physics, Mt. View, CA; Model 2035) passes through a laser intensity stabilizer (Cambridge Research and Instrumentation, Cambridge, MA; Model LS100, UV optics installed) where it is stabilized to a power of ca. 4 mW. Upon

exiting the stabilizer, the radiation is focused onto the column via a 1-cm focal length fused-silica lens. The column normal is at Brewster's angle to the incident radiation. Collection of fluorescence is perpendicular to the plane of incidence and is effected by a 20x microscope objective. The illuminated region is magnified by approximately 60x and imaged onto a spatial filter. Fluorescence from the internal diameter of the column passes through the spatial filter, through a cut-off filter (Schott Glass, Duryea, PA; UV-360) and falls onto the cathode of a photomultiplier tube (Hamamatsu, Bridgewater, NJ; R928).

The system used for the indirect detection of non-electrolytes is essentially the same as above but with the following exceptions: excitation is provided by the 488-nm line of an argon-ion laser (Laser Ionics, Inc., Orlando, FL, Model 554A). After passing through the stabilizer, the radiation is split and ca. 2 mW is focused onto the capillary using a 0.9-cm focal length lens; background radiation was rejected via an OG-515 cut-off filter (Schott).

Data were recorded using a strip chart recorder (Houston Instruments, Austin, TX; Model B5117-5I) or subjected to analog-to-digital conversion (Data Translation, Inc., Marlborough, MA; Model DT2827, 2 Hz) and stored using a personal computer (IBM PC-AT). Data recorded on strip chart could be digitized by a frame grabber system (Data Translation, Inc., Auxiliary Frame Processor; Model DT2858). Digitized data were later smoothed using a moving-window average.

Results and Discussion

Electrolytes

The limiting concentration (C_{lim}) of an analyte that can be detected by indirect fluorometry or photometry is generally described by the following:

$$C_{\text{lim}} = \frac{C_m}{DR} \qquad (1)$$

where C_m is the concentration of the probe, D is the dynamic reserve (ratio of the background signal to noise on the background) and R is the displacement ratio (moles of probe displaced by moles of analyte). Indirect detection in ion chromatography is possible because as the analyte elutes, it displaces an equivalent amount of the probe ion. In this case, R is generally regarded as unity as long as the analyte and probe ions are of equal valence.

To achieve elution and detection of low concentrations of anions in single column ion-exchange chromatography, anion-exchange columns of low capacity are required. One way to effectively produce a low capacity anion-exchange column is by the method of dynamic modification (7,10,26). Column capacity can be varied by changing modifier concentration or organic content of the modifying solution. Previously, Takeuchi and Yeung (7) modified microbore silica-gel columns with quaternary ammonium salts to separate several common inorganic anions with sub-nanogram LOD using a laser-based double-beam indirect fluorometric

detector. Later, using a similar modification and detection scheme, a reversed-phase OTC column was used for the separation of similar anions with picogram LOD (10).

The double-beam design in indirect fluorometric detection has been shown to maintain a dynamic reserve of 5×10^3 until the probe concentration falls below 10^{-7} M (8). The dynamic reserve for indirect photometry is in excess of 10^4 but becomes proportional to probe concentration when absorption falls below 1 a.u. When capillary columns are used, the lower limit to probe C_m or ϵ is increased due to reduced path length. If C_m is raised to compensate for b, we see from eq (1) that this will result in decreased detectability.

The high dynamic reserve reported in ref (7) is due to the use of the double-beam design in conjunction with high frequency modulation and lock-in detection. This detection scheme is not particularly well suited for use with capillary columns as discussed in (10). Laser flicker noise, which can be as high as 1% of the total power, can be effectively reduced to levels below 0.02% by use of a laser intensity stabilizer. This approach has been used to produce stable fluorescence backgrounds for indirect fluorometric detection in capillary zone electrophoresis (27-28).

The chromatogram in Figure 1 shows the separation of acetate from nitrite using a dynamically modified OTC column of 15-μm i.d. Once the column had been modified, it could be used for several days without degradation in its performance. Capacity factors for the anions are similar to those reported for a

Figure 1. Anion chromatogram of A, salicylate (system peak); B, acetate; and C, nitrite. The amount of acetate and nitrite injected is 7 fmol each. Flow rate: 35 nL/min; eluent: 2×10^{-6} M sodium salicylate;column: 120 cm long, 15 μm i.d., 2% PS-264.

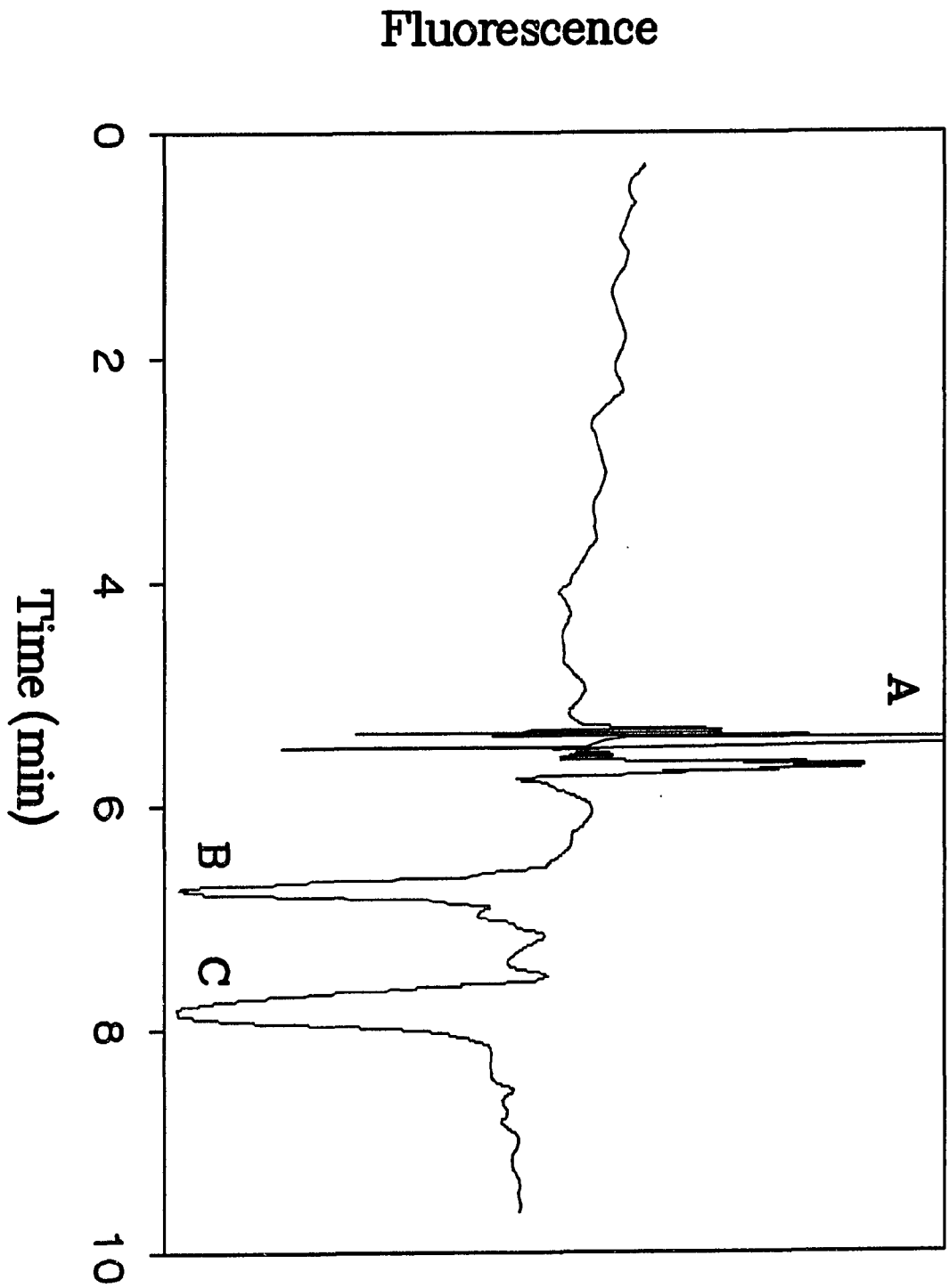
Fluorescence
Time (min)
0
2
4
6
8
10
A
B
C

dynamically modified C_8 OTC column of 50-μm i.d. (10). The displacement ratio for both anions was calculated using peak height and peak volumes and found to be 1/18 for acetate and 1/12 for nitrite. Equation (1) suggests lowering of C_m to decrease C_{lim}, but further reduction of C_m results in a corresponding reduction in D. Displacement ratios less than 1 have been observed before for separations using salicylate concentrations of less than 10^{-5} M (7,10). These low displacement ratios can be attributed to interactions other than ion-exchange occurring at the column surface when low capacity columns and low probe concentrations are used.

The baseline in Figure 1 represents a 0.93 μA current from the PMT and is stable to 1 part in 10^3. This is a direct consequence of the intensity stabilized beam and the use of a 30 point moving-window average on the digitized data. The use of the microscope objective in conjunction with spatial and cut-off filters keep stray radiation levels to below 20% of the total signal when low concentrations of fluorophore are used. This is important since the displacement ratio is calculated from only that fraction of signal due to probe fluorescence. These improvements in design from ref (10) keep the baseline noise at a level of 0.93 nA, which corresponds to 15 fg of NO_2^- injected. This is a factor of approximately 70 less than that reported in (10). The majority of this improved mass detectability can be attributed to the reduced column dimensions. The remaining improvement is due to an increase in dynamic reserve and differences in displacement ratio. The concentration detectability for NO_2^-, which was

calculated to be 2.4 x 10^{-8} N, is slightly better than that reported in (10) due to the increase in dynamic reserve for this work. In separate experiments using 10-μm capillaries, we have achieved baseline noise levels equivalent to 10 fg or 0.2 fmol of NO_3^- injected.

Non-electrolytes

As opposed to equivalent displacement of the probe ion for analyte ion in ion-exchange chromatography, indirect detection of non-electrolytes in reversed-phase chromatography relies on the analyte perturbing the partitioning dynamics of the probe which has been equilibrated between the mobile and stationary phase. In so doing, the eluting zone of the analyte contains either an excess or a deficit of the probe as compared to the unperturbed probe concentration. In this case, R is usually much less than 1.

Most separations involving indirect photometric or fluorometric detection of non-electrolytes employ an ultraviolet absorbing, non-ionic probe (5,9,14-16). Separations using a probe which absorbs in the visible have been reported and are based on a type of complexation between the analyte and probe (17,18). A simple argon-ion laser capable of emitting at 488.0 nm is a popular, relatively low cost, reliable laser with excellent beam characteristics. Fluorescent molecules capable of absorbing at this wavelength tend to be large, ionizable species which do not chromatograph well in the reversed-phase mode. Ion suppression, as its name implies, is a technique which can improve the chromatographic behavior of

ionizable compounds by suppressing their ionization with the use of a buffer to control pH (29). By maintaining the pH of a 2,7 DCF solution between 3.0 and 5.0, we found that the dye could be used as a probe for indirect detection of non-electrolytes. Although 2,7 DCF has reduced fluorescence in this pH range, fluorescence was easily visible when micromolar solutions were excited using a 2 mW unfocused beam of 488.0-nm radiation.

The chromatogram in Figure 2 shows the separation of various alcohols using an OTC column of 13 μm i.d. For the laser power and photomultiplier tube voltage being used, this concentration of 2,7 DCF allowed the system to remain above the shot noise limit. Unlike ion-chromatography, lowering of C_m does not result in better detectability for non-electrolytes (9). The peak area of the positive peaks does not equal the peak area of the negative peaks. This could be the result of the ionizable nature of the probe but has been observed for neutral probes on occasion (14). The hour-to-hour reproducibility of the system was good and could be maintained for several days by allowing the pump to run continuously at a reduced flow rate. However, if the column was washed with a methanol/water solvent and later re-equilibrated with the eluent containing the probe, the retention of the alcohols would remain essentially the same but the system peak retention would be unpredictable. This suggests that the retention of 2,7 DCF is, in part, due to sites different from those responsible for alcohol retention.

The displacement ratios for each of the alcohols in Figure 2 were calculated

Figure 2. Chromatogram of A, solvent disturbance due to excess acetonitrile in sample solution; B, 2-heptanol; C, 1-heptanol; D, 2-octanol; E, 1-octanol; F, 1-nonanol; and G, 2,7-DCF (system peak). All alcohols are at 0.01% (v/v) except 1-nonanol which is at 0.005%. Eluent: 2×10^{-6} M 2,7-DCF in 5% acetonitrile, 1×10^{-3} M acetic acid at pH = 4.0; flow rate: 23 nL/min; injection vol.: 230 pL; column: 50 cm long, 13 μm i.d., 1% PS-255.

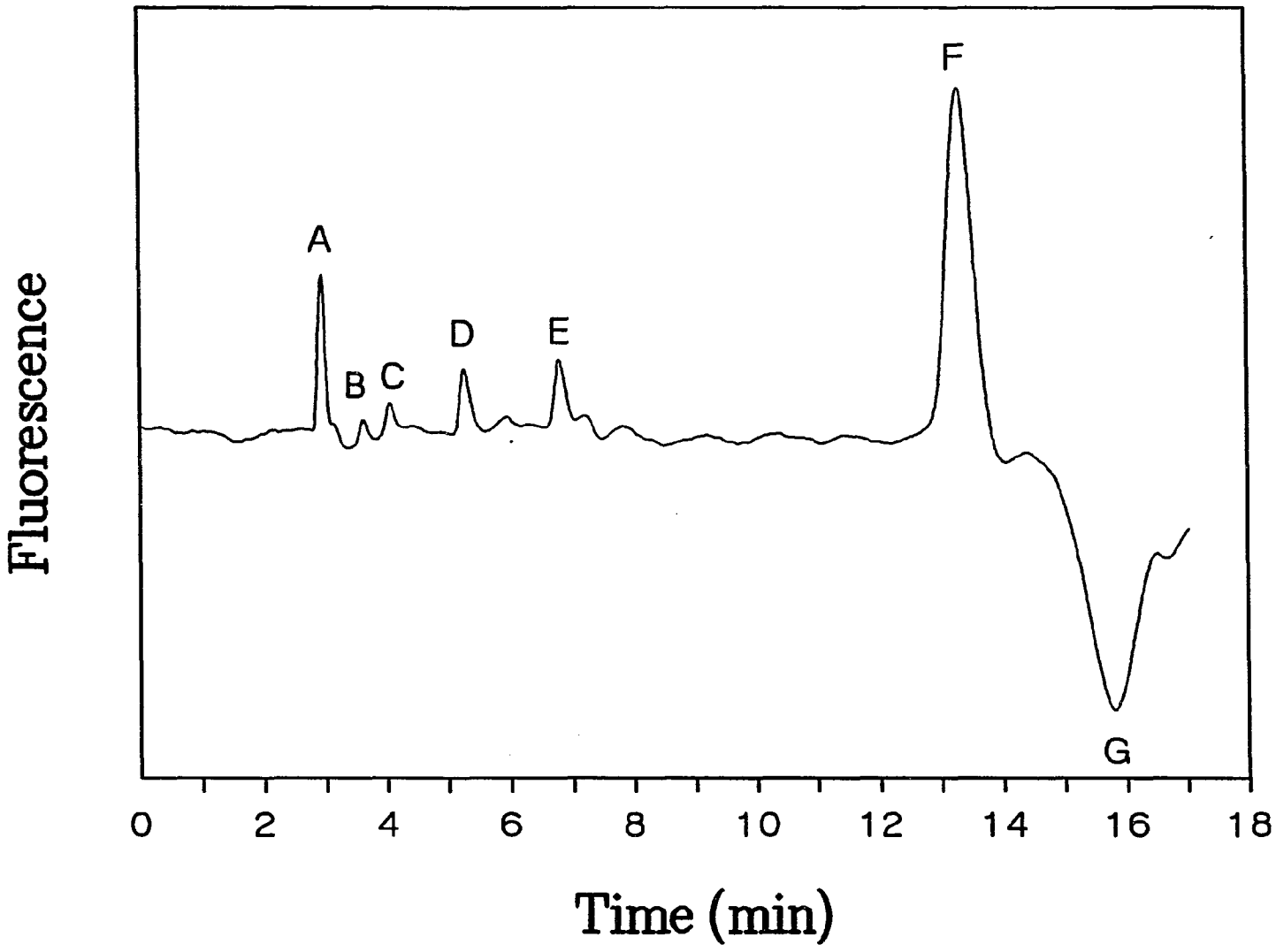
Fluorescence
A
B
C
D
E
F
G
0
2
4
6
8
10
12
14
16
18
Time (min)

and are as follows: 2-heptanol, 1/3000; 1-heptanol, 1/2400; 2-octanol, 1/850; 1-octanol, 1/870; and 1-nonanol, 1/27. As with other non-electrolyte indirect detection systems, those analytes eluting closer to the system peak produce larger displacement of the probe (9). These ratios are larger than those reported in ref. (9) but comparable to those in ref. (14).

The dynamic reserve in Figure 5 is calculated to be 1500. As before, this stability is attributed to the use of a laser intensity stabilizer and a moving-window average (10 point). The limit of detection (S/N = 2) for the early eluting alcohols is a few picograms and 72 fg or 0.5 fmol for 1-nonanol injected. This figure for 1-nonanol is about 4 orders of magnitude less than that reported for 1-nonanol in (14), which used packed capillaries (340-μm i.d.) and indirect photometric detection. Again, the majority of this improvement is due to the reduction of column dimensions, specifically i.d. Naturally, indirect photometry is not compatible with these column dimensions.

It is interesting to note that when the baseline concentration detectability for 1-nonanol, 3.6×10^{-8} M, is compared to the baseline concentration detectability of NO_2^-, 2.4×10^{-8} M, we see that the two are nearly equal. This is the result of the displacement ratio for NO_2^- being unusually small for ion-exchange chromatography and the displacement ratio for 1-nonanol being unusually large for reversed-phase chromatography.

Conclusion

The use of silicone gums affords the simplified production of OTC columns. These columns may be dynamically modified to function in the ion-exchange mode or used as they are in the reversed-phase mode. Indirect fluorometric detection of analytes in either mode using OTC columns allows for extremely low mass detectability.

References

1. Schill, G.; Crommen, J. Trend Anal. Chem. 1987, 6, 111.
2. Ishii, D.; Takeuchi, T. J. Liq. Chromatogr. 1988, 11, 1865.
3. Yeung, E. S. Accounts Chem. Res. 1989, 22, 125.
4. Small, H.; Miller, T. E. Anal. Chem. 1982, 54, 462.
5. Parkin, J. E. J. Chromatogr. 1984, 287, 457.
6. Hackzell, L.; Schill, G. Chromatographia 1982, 15, 437.
7. Takeuchi, T.; Yeung, E. S. J. Chromatogr. 1986, 370, 83.
8. Mho, S-I.; Yeung, E. S. Anal. Chem. 1985, 57, 2253.
9. Takeuchi, T.; Yeung, E. S. J. Chromatogr. 1986, 366, 145.
10. Pfeffer, W. D.; Takeuchi, T.; Yeung, E. S. Chromatographia 1987, 24, 123.
11. Bobbitt, D. R.; Yeung, E. S. Anal. Chem. 1984, 56, 1577.
12. Ye, J.; Baldwin, R. P.; Ravichandran, K. Anal. Chem. 1986, 58, 2337.

13. Takeuchi, T.; Suzuki, E.; Ishii, D. J. Chromatogr. 1988, 447, 221.

14. Takeuchi, T.; Ishii, D. J. Chromatogr. 1987, 393, 419.

15. Takeuchi, T.; Ishii, D. J. Chromatogr. 1987, 396, 149.

16. Takeuchi, T.; Ishii, D. J. Chromatogr. 1987, 403, 324.

17. Gnanasambandan, T.; Freiser, H. Anal. Chem. 1982, 54, 1282.

18. Gnanasambandan, T.; Freiser, H. Anal. Chem. 1982, 54, 2379.

19. Microcolumn High-Performance Liquid Chromatography, Kucera, P., Ed.; Elsevier: Amsterdam, 1984.

20. Microbore Column Chromatography: A Unified Approach to Chromatography, Yang, F. J., Ed.; Marcel Dekker: New York, 1989.

21. Novonty, M. Anal. Chem. 1988, 60, 500A.

22. Knox, J. H.; Gilbert, M. T. J. Chromatogr. 1979, 186, 405.

23. Jorgenson, J. W.; Guthrie, E. J. J. Chromatogr. 1983, 255, 355.

24. Farbrot, A.; Folestad, S.; Larsson, M. J. High Resolut. Chromatogr. Chromatogr. Commun. 1986, 9, 117.

25. Dluzneski, P. R.; Jorgenson, J. W. J. High Resolut. Chromatogr. Chromatogr. Commun. 1988, 11, 332.

26. Cassidy, R. M.; Elchuk, S. Anal. Chem. 1982, 54, 1558.

27. Kuhr, W. G.; Yeung, E. S. Anal. Chem. 1988, 60, 1832.

28. Kuhr, W. G.; Yeung, E. S. Anal. Chem. 1988, 60, 2642.

29. Bidlingmeyer, B. A. J. Chromatogr. Sci. 1980, 18, 525.

SECTION IV. OPEN-TUBULAR LIQUID CHROMATOGRAPHY WITH SURFACTANT-ENHANCED ELECTROOSMOTIC FLOW

Introduction

Open tubular columns (OTC) have enjoyed increasing use in liquid chromatography (LC) over the past few years (1-4). The rewards for using OTC include high efficiency, high resolution, low sample consumption, low eluent consumption and high mass sensitivity all within a reasonable analysis time. Although significant, these rewards are kept in check bythe drawbacks which stem from the construction, detection and injection principles associated with OTC use.

From chromatographic theory, the i.d. of an OTC must be on the order of the diameter of column packing material, with the ideal diameter being near 2 μm (5,6). These small diameters pose a severe challenge in the application of a reversed-phase surface. Two methods exist for obtaining such a surface in an OTC. The first (5) is generally associated with the use of glass capillaries. Here, a stationary phase, typically octadecylsilane (ODS), is chemically bonded to the walls of a glass capillary after a chemical etching step. Fused silica, due to its superior optical quality, is often the material of choice for OTCs today. The disadvantages are that only poor etching techniques exist for it (2) and that it is difficult to establish a high density of stationary phase on its surface (3). In the second method, a polymeric stationary phase is coated on the walls of the fused

silica and later cross-linked to provide a non-extractable, reversed-phase surface (2,3). In either case, construction of these columns and subsequent detection of the analytes will be greatly simplified if 10-μm rather than 2-μm capillaries can be used without sacrificing efficiency.

The introduction of a sample into an OTC is often the limiting factor in terms of separation efficiency and resolution since injection volumes must also be less than a nL when 10-μm i.d. or smaller OTCs are used. Injection methods such as split injection (7), microsyringe injection (8) and stopped-flow injection (9) have been developed to meet these low volume requirements. However, each of these techniques can be characterized as one or more of the following: connection cumbersome, multivalve intensive or eluent and sample wasteful. Increased applications of OTCs in areas such as biomedical, biochemical and single cell analysis, which are often limited by sample size and concentration, seem likely. A simplified injection technique compatible with dilute and limited volume samples would only benefit the future of OTCs in these areas, especially if it can be done at low pressures.

Propulsion of a liquid through an OTC is usually effected by the application of high pressure to one end of the tube. The flow which results from the pressure gradient along the tube is characterized by a parabolic profile. In the theory of band broadening for this type of flow profile, the resistance to mass transfer coefficients are given by the Golay equation (10). Another method of liquid propulsion is known as electroosmosis, and is commonly employed for separations

based on capillary zone electrophoresis (CZE) and micellar electrokinetic chromatography (MECC). The flow originates from the electrical double layer of the column liquid-solid interface and is due to ions in the diffuse region migrating toward the oppositely charged electrode when a potential difference is applied along the column axis (11).

The most celebrated advantage to using electroosmotic flow for LC in OTCs is the reduction in the resistance to mass transfer term in the mobile phase due to the nearly flat flow profile which exists for systems having a double layer (δ) much smaller than the column diameter (12). Since the profile is nearly flat rather than parabolic, the golay equation is no longer descriptive of mass transfer. Although the exact expression for mass transfer is intricate due to the complex velocity profile, Martin et al. (13,14) have developed approximations which allow for system characterization. In so doing, they have shown (13) that the contribution to band broadening by resistance to mass transfer is small but increases with increasing retention; however, this contribution is less than in conventional (parabolic flow) chromatography for each value of retention.

Several other advantages of electroosmotic flow become apparent when it is used in conjunction with OTCs. First, since the instrumentation is essentially that of a CZE system, one can readily change from one separation mode to the other by changing the column. Second, since high pressure is not used, the need for special capillary adapters and fittings is lost. Finally, valveless injections, either by hydrodynamic or electrokinetic means, become possible such as in CZE and

MECC. This will allow for dilute and limited volume solutions to be sampled easily and effectively.

Electroosmotic flow has been used for LC in conjunction with both packed (15,16) and OTCs (17). OTC has the advantage that on-column injection and on-column detection are possible so that the inlet and outlet plumbing can be simplified.

Jorgenson and Lukacs (15), using a 65-cm column (0.17 mm i.d.) packed with 10 μm ODS packing obtained plate numbers around 31,000 for a peak eluting at 30 min. They noted that although their column was 'poorly packed' according to current theories, they expected and obtained decent performance since electroosmotic flow is predicted to be uniform and independent of channel irregularities. Knox and Grant (16), using 5-μm particles achieved a plate number of 69,000 for peaks eluting around 30 min with a column (50 μm i.d.) of similar length to that in (15). In the OTC work by Tsuda (17), a 42 cm x 30 μm i.d. soda-lime glass column having an ODS stationary phase chemically bonded to the surface produced a plate number of 10,500 in about 20 min. Clearly, "electrochromatography" has not reached the performance level predicted based on the flat flow profiles.

In the examples cited above, a substantial electroosmotic flow has to be present. The exact velocities are difficult to determine since no capacity coefficients are given. This is as expected since either the packing material (15,16) or column wall (17) would have been negatively charged due to ionization

of silanol groups. This charge is essential in the development of electroosmotic flow. On the other hand, exposed silanol groups imply incomplete surface coverage by the stationary phase, which in turn can degrade the separation efficiency.

In this paper, we report the use of electroosmotic flow in small-diameter capillaries for OTCLC. When polymer-coated, fused silica columns, prepared in a manner similar to that in (3), are used in conjunction with electroosmotic flow, low velocities are obtained and electrochromatography becomes impractical. However, surface active reagents, specifically surfactants, have been used to control electroosmotic flow in CZE (18,19). So, in this study, a surfactant is incorporated into the chromatographic eluent at concentrations well below its critical micelle concentration (CMC). This eluent, when used in a polymer-coated, reversed-phase OTC, allows a substantial electroosmotic flow to be developed such that highly efficient and fast separations of neutral compounds can be performed. In addition, direct gravity injection allows nanomolar analytes in subnanoliter sample volumes to be detected using a laser based, on-column fluorescence detector.

Experimental Section

The fused silica capillaries (Polymicro Technologies Inc., Phoenix, AZ; 50-115 cm x 150-μm o.d.) were of 10-μm i.d. These capillaries were coated with a polymer solution of 0.9% (w/v) PS-264 (Petrarch Systems Inc., Bristol, PA) using the procedure outlined in (4). In addition to burning off the polyimide coating to allow for on-column detection, the coating at the injection end of the capillary was also removed to keep analytes from possibly absorbing to it during an injection.

Citric acid (Fisher Scientific, Fair Lawn, New Jersey) and phosphoric acid (Fisher) buffers containing cetyltrimethylammonium bromide (CTAB; Aldrich Chemical Co., Milwaukee, WI) were dissolved using various percentages of HPLC grade acetonitrile (Fisher) in water. The analytes anthracene (J. T. Baker Chemical Co., Phillipsburg, New Jersey) fluoranthene, pyrene (Eastman Kodak Co., Rochester, New York), 9-methylanthracene, 2-methylanthracene (Aldrich), 1-naphthol and 2-naphthol (Fluka, Switzerland) were prepared in the running buffer prior to their injection.

The chromatographic system used in this experiment is similar to the CZE system described in (20). Vials containing the buffer at both ends of the column were fitted with special caps to reduce the evaporation of acetonitrile. The electric field which drives the electroosmotic flow is supplied by a low cost, 0-30 kV, negative polarity high voltage supply (Glassman High Voltage Inc., Whitehouse Station, NJ; Model MJ30N0400-11).

Gravity injection of the analytes into the column is accomplished by raising the injection end (cathode) of the capillary 10-15 cm above the output end of the column for a period of 5-60 sec. Injection volumes were calculated with the aid of Poiseuille's law. This method is legitimate since the actual hydrostatic flow has been found to agree with that of the calculated flow to within 30% (21).

The detector used in this work is essentially as described in (4) with the following exceptions: excitation is provided by the combination of the 350 and 360 nm lines of the argon laser; stray light rejection is accomplished by passing the collected radiation through two Corning (Corning, NY) 3-74s and one 4-96 color filter, respectively.

Flow rates were calculated with the aid of injecting a buffer containing a slight excess of acetonitrile with respect to the running buffer. This excess caused a baseline disturbance due to a refractive index change and was used as a marker for t_o.

The chromatographic data were subjected to analog-to-digital conversion (Data Translation, Inc., Marlborough, MA; Model DT 2827, 1-25 Hz) and stored using a personal computer (IBM PC-AT).

Results and Discussion

When an electric field, E, is applied across the axis of a tube containing a liquid, an effective electroosmotic flow having a linear velocity, U, develops and is related to E by the following (18):

$$U = \frac{keE}{|Z|\eta C^{\alpha}} \qquad (1)$$

Here, k, e, n, Z, C and α are a proportionality constant, the charge per unit surface area on the wall, viscosity of the liquid, the number of valence electrons, the concentration of electrolyte and a constant, respectively.

With positive flow defined as the movement of liquid to the more positive electrode, we see from eq (1) that flow in a fused silica capillary, which has fixed negative charges on its surface, will be in the negative direction. For a typical system having a buffer concentration of 10 mM at pH 6.0, the electroosmotic mobility would be on the order of -4×10^{-4} cm^2 V^{-1} s^{-1} (19).

Using a 1 mM solution of citric acid at pH = 6.5, the electroosmotic mobility in a capillary having a cross-linked, polyvinylsiloxane surface was experimentally determined to be -0.3×10^{-4} cm^2 V^{-1} s^{-1}. This is due to the fairly complete coverage by the stationary phase, greatly reducing the exposed silanol groups (22). Under these conditions, a chromatographic system using a 50 cm OTC with 30 kV placed across its axis, would take greater than 40 minutes to elute a compound having a capacity coefficient (k) of zero -- a long period of time

even for the simplest of separations. In addition, based on theoretical discussions by Martin et al. (14), the optimum flow rate (plate height being at its minimum) is larger for electroosmotic flow than for the corresponding optimum velocity for parabolic flow, especially when k is small. Therefore, if appreciable velocities cannot be achieved, the use of electroosmotic flow for LC in these columns is not practical.

The charge on surface can also be affected through the addition of a surface active reagent to the buffer. Both Tsuda (18) and Huang et al.(19) have used the surfactant CTAB in their CZE buffers to manipulate the electroosmotic flow in bare fused silica capillaries. In both cases, the increase in concentration of surfactant in the buffer resulted in first a reduction in the magnitude of U, to finally a reversal in the direction of U. This reversal occurred at a concentration of approximately 3.5×10^{-4} M CTAB in both reports.

For a capillary having a hydrophobic surface such as that provided by the cross-linked polymer PS-264, one would expect the interaction of the hydrophobic portion of a surfactant to be substantial. Figure 1 shows the effect of CTAB on the electroosmotic mobility. Even at the lowest concentration (1 μM), the direction of the flow has been reversed with respect to a system having no CTAB in the buffer. Note that these concentrations are substantially lower than those in bare silica capillaries (18,19). CTAB adsorbs (partitions) efficiently onto the hydrophobic stationary phase here, compared to the inefficient adsorption onto bare silica. Figure 1 also depicts saturation around 10-μm, while in ref 18 and 19

Figure 1. Dependence of electroosmotic mobility on the concentration of CTAB in a pH = 3.5, 10 mM phosphoric acid buffer containing 10% acetonitrile.

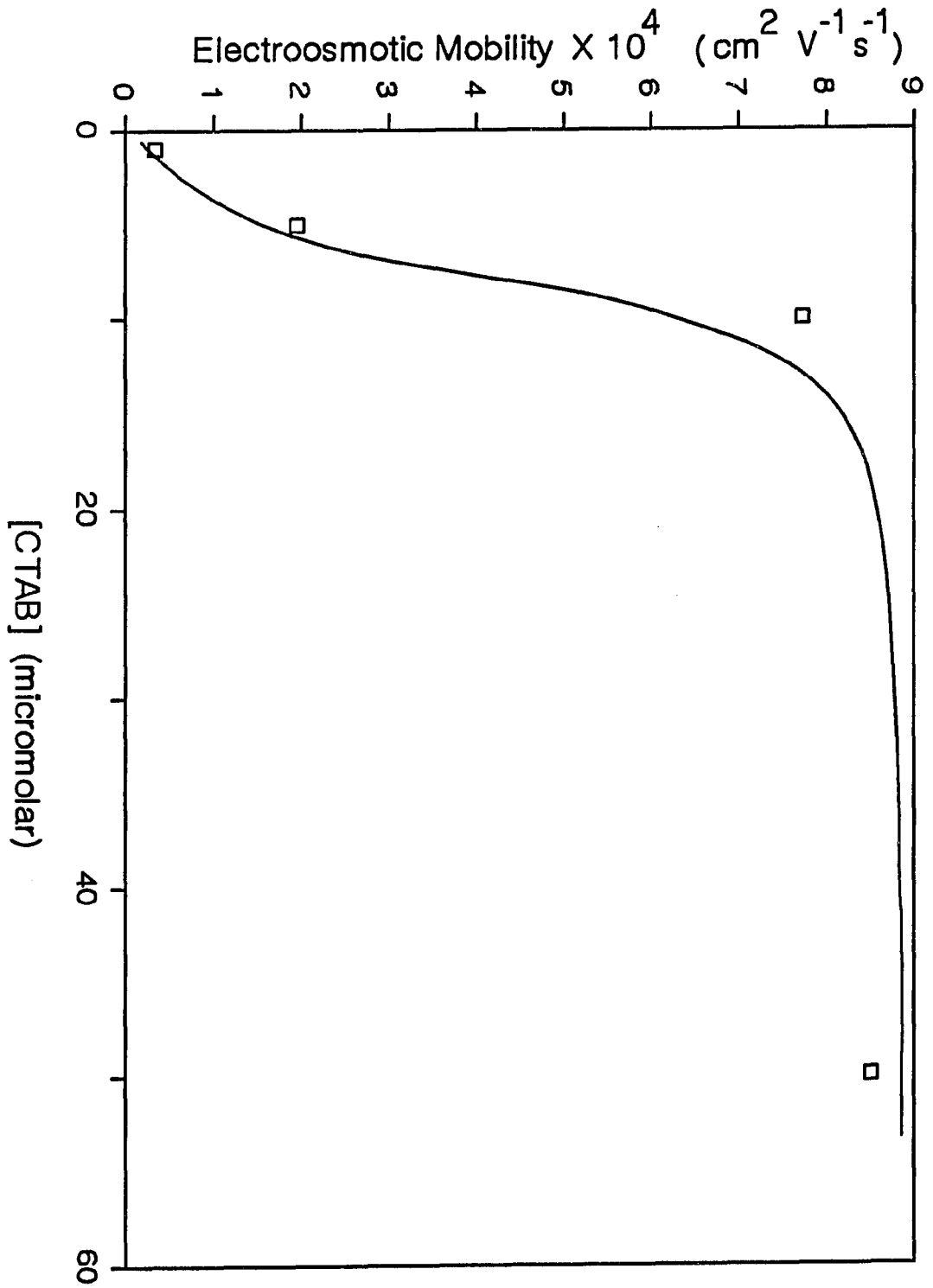
Electroosmotic Mobility X 10^4 (cm^2 V^-1 s^-1)
0
1
2
3
4
5
6
7
8
9
[CTAB] (micromolar)
0
20
40
60

a linear increase is found up to 1 mM CTAB. This is because the surfactant on the stationary phase prevents further adsorption due to charge repulsion when the coverage is high enough. For the condition of 10 μM CTAB in Figure 1 and considering the hypothetical situation presented earlier, a compound with k = 0 would be eluted in 1.6 minutes.

By increasing the amount of acetonitrile in the buffer, the viscosity of the buffer, dielectric constant of the buffer, the interaction of the buffer with the polymer and the interaction of CTAB with the polymer can all be expected to change. Figure 2 shows the effect of increasing acetonitrile content on the electroosmotic mobility. The approximate linear relationship in this range is fortuitous. There is more than an order of magnitude change in flow compared to the 20% or so effect observed for acetonitrile in bare silica capillaries (23). Here, acetonitrile affects the partitioning of CTAB between the mobile and stationary phase. This is quite different from the mechanism in ref 23. Although the value of 0.29×10^{-4} cm^2 V^{-1} s^{-1} for the 40% acetonitrile condition will result in long elution times in LC with respect to the example above, this can be effectively dealt with by increasing the concentration of CTAB to 100 μM, which then results in an electroosmotic mobility of 2.4×10^{-4} cm^2 V^{-1} s^{-1}. This type of concentration dependence is indicative of true partitioning of CTAB between the mobile phase and the stationary phases.

Even at concentrations of 100 μM, CTAB is well below its CMC in water (940 μM) (24). In fact, at 40% acetonitrile, one expects that the CMC in water

Figure 2. Dependence of electroosmotic mobility on the percent acetonitrile in a pH = 3.5, 10 mM phosphoric acid buffer containing 10 μM CTAB.

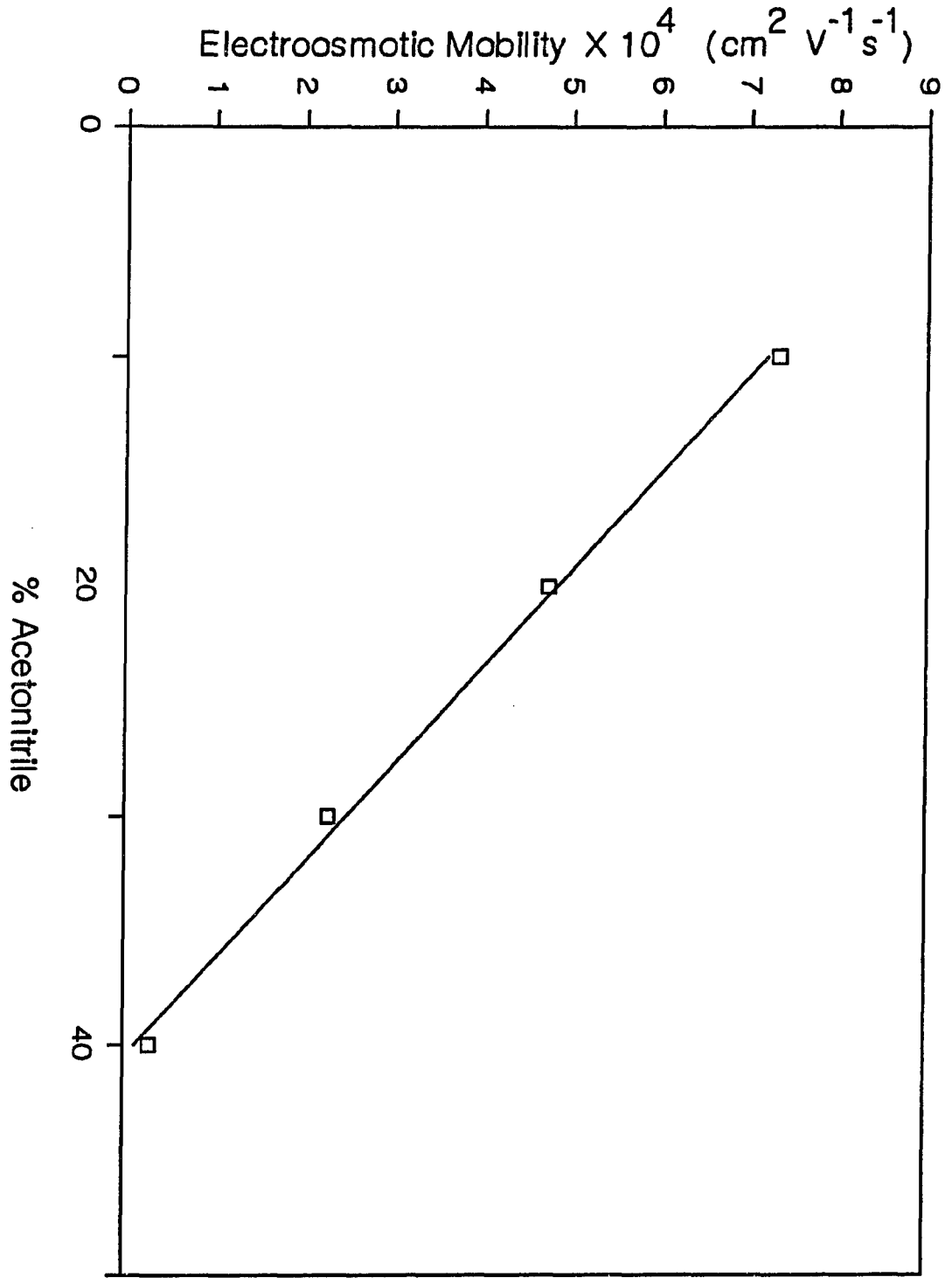
Electroosmotic Mobility X 10^4 (cm^2 V^-1 s^-1)
0
1
2
3
4
5
6
7
8
9
0
20
40
% Acetonitrile

for CTAB is much higher, considering hydrophobicity. The concentration is purposely kept below the CMC so as not to confuse the separation scheme with those based on either micellar chromatography or MECC. We ran control experiments using the same eluents and the same sample mixtures as below, and were not able to achieve any separation in bare silica capillaries, i.e., without the stationary phase. The separation mechanism here thus clearly different from those systems with an organic modifier and a large (10 mM) concentration of an organic ion (25). In ref 25, there is sufficient adsorption of the organic ions onto the neutral analytes to allow the latter to be separated by capillary zone electrophoresis. With respect to MECC, the presence of a reversed-coating here can also facilitate separation of both charged and neutral analytes (26), but does not suffer from the limited retention window and limited analyte solubilization which is characteristic of MECC (25) or polymeric ion exchange separations (28). It is important to note that in MECC, the different analytes must partition differently into the micelles for the separation to occur. For the very nonpolar analytes used here, the solubility in water is almost negligible. The analytes will exist exclusively in the micelles ($k = \infty$) and move down the column without being separated from one another. In fact, these analytes are often used as markers to measure the mobility of the micelles. The stationary phase here is critical to these separations.

The efficiency and resolving power of a chromatographic system based on electroosmotic flow using these polymer-coated columns is shown in Figure 3 for

Figure 3. Chromatogram obtained from a 70 pL injection of the following: A) 19 fg anthracene; B) 11 fg fluoranthene; C) 86 fg pyrene; D) 4 fg 9-methylanthracene; and E) 21 fg 2-methylanthracene. Buffer: pH = 3.5, 1mM citric acid buffer containing 100 μM CTAB and 40% acetonitrile. Column dimensions: 111 cm x 10-μm i.d. with 99 cm distance from point of injection to detection. Separation voltage: -30 kV. Flow rate: 3.1 nL/min.

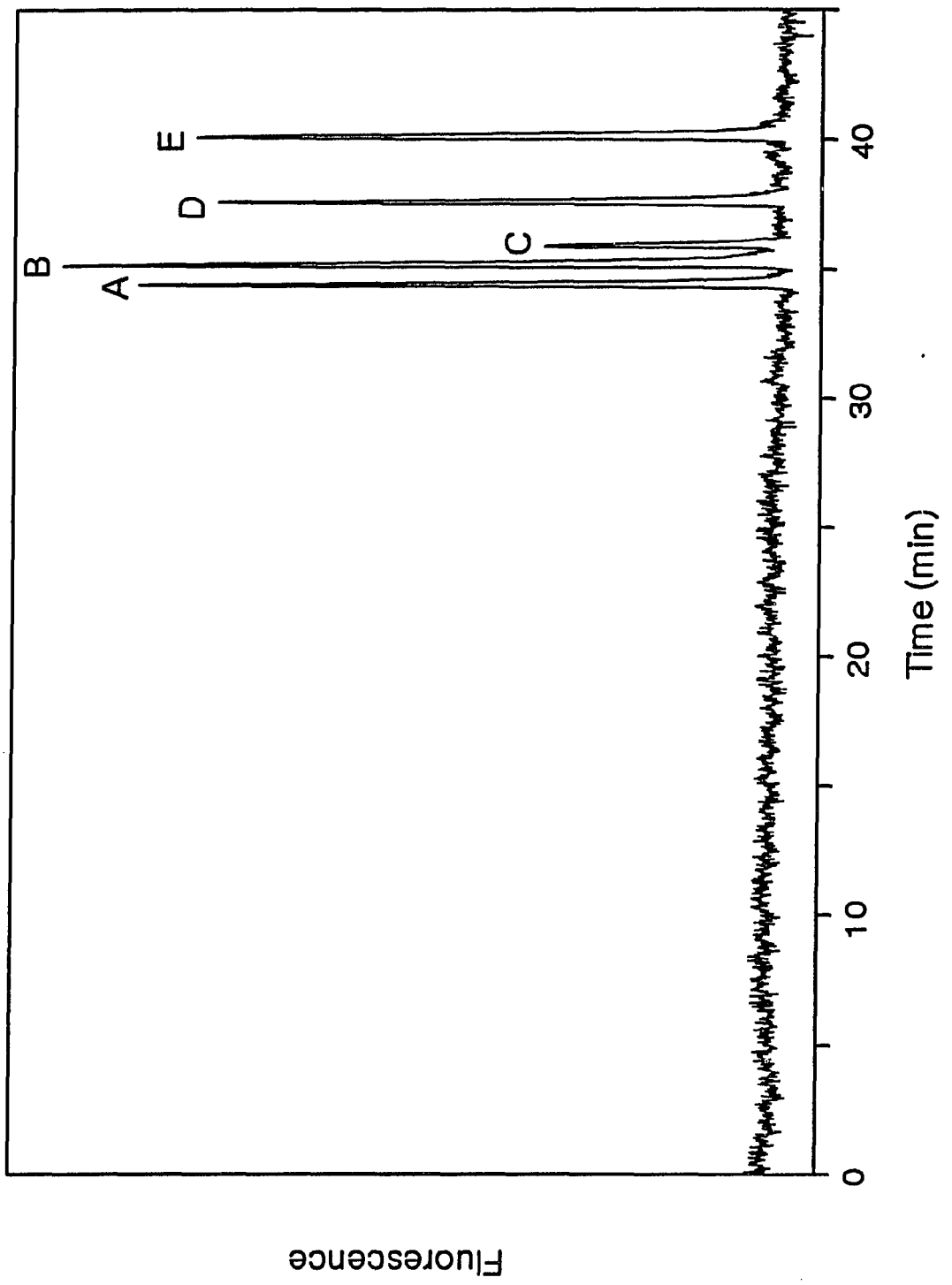
A
B
C
D
E
0
10
20
30
40
Time (min)
Fluorescence

a group of neutral compounds. Anthracene, the positional isomers 2-methylanthracene and 9-methylanthracene and the geometrical isomers fluoranthene and pyrene are all resolved from one another with $R \geq 1$. The average plate number is in excess of 250,000 (triangular approximation) with that of anthracene being 290,000. Based on the retention of anthracene ($k = 0.34$), a calculated plate height of 3.4 μm is obtained. Assuming δ to be 10 nm and the diffusion coefficient (D_m) to be 1×10^{-5} cm^2 s^{-1}, the theoretically predicted plate height, as calculated by the approximation in (14), is also 3.4 μm. Further, keeping all experimental conditions the same except for column i.d., it would take a column having a 4.4-μm i.d. to realize the same plate height under pressurized flow conditions. Therefore, the use of electroosmotic flow relaxes the requirement of using extremely narrow capillaries to obtain efficient separations. This fact will benefit on-column detection schemes since larger i.d. columns are generally easier to work with.

Although the detector was not optimized for any one of the analytes, good concentration and mass limits of detection (LOD; S/N = 3) were observed. This is highlighted by the analyte 9-methylanthracene, which after an injection from a 500 nM solution, gave a concentration LOD of 1.4 nM and a mass LOD of 150 attograms or 0.75 attomoles. In this particular case, the raw data was subjected to a 15-point Golay smooth.

The flow rate in Figure 3 (0.065 cm/sec) was limited by the power supply and the degree of insulation, which allowed us to place, at maximum, -30 kV

across the column. In order to obtain a faster flow rate, the value of E was increased by using a shorter column. Figure 4 shows a separation of 2-naphthol (k = 0.043) from 1-naphthol (k = 0.058) in less than 4 min using such a column. The S/N is poorer in Figure 4 compared to Figure 3 because the naphthols are less efficient fluorophores. The plate number for 2-naphthol was calculated to be 230,000. This is as expected since the contribution to band broadening by resistance to mass transfer should be low for analytes with small values of k (13).

To further characterize the role of the mobile phase on the separation, we obtained chromatograms for anthracene and 9-methylanthracene (peaks A and D in Figure 3) over a range of CTAB concentrations. The acetonitrile content of the mobile phase was lowered to 30% to favor the formation of Micelles at high CTAB concentrations. In contrast to Figure 1, the electroosmotic mobility increases rapidly until [CTAB] reaches 1 mM (to 6.2 x 10^{-4} cm^2 V^{-1} s^{-1}). However, the mobility drops off to 5.3 x 10^{-4} cm^2 V^{-1} s^{-1} when [CTAB] is at 50 mM. This is due to changes in both the viscosity and the electrolyte concentration, as prescribed by eq (1).

The flow rate can of course be increased by increasing the applied potential. For these analytes, we found that the k values decreased by less than 5% between flow rate of 0.09 cm/s and 0.21 cm/s. The number of theoretical plates, however, decreased by 30% over the same range. These observations further confirm that the separation mode is quite different from that in capillary electrophoresis, where increasing the flow rate (field strength) generally leads to sharper peaks.

Figure 4. Chromatogram obtained from a 5 pL injection of A) 72 fg 2-naphthol and B) 720 fg 1-naphthol. Buffer: pH = 3.5, 1 mM citric acid buffer containing 100μm CTAB and 25% acetonitrile. Column dimensions: 64 cm x 10-μm i.d. with 54 cm distance from point of injection to detection. Separation voltage: -30 kV. Flow rate: 12 nL/min.

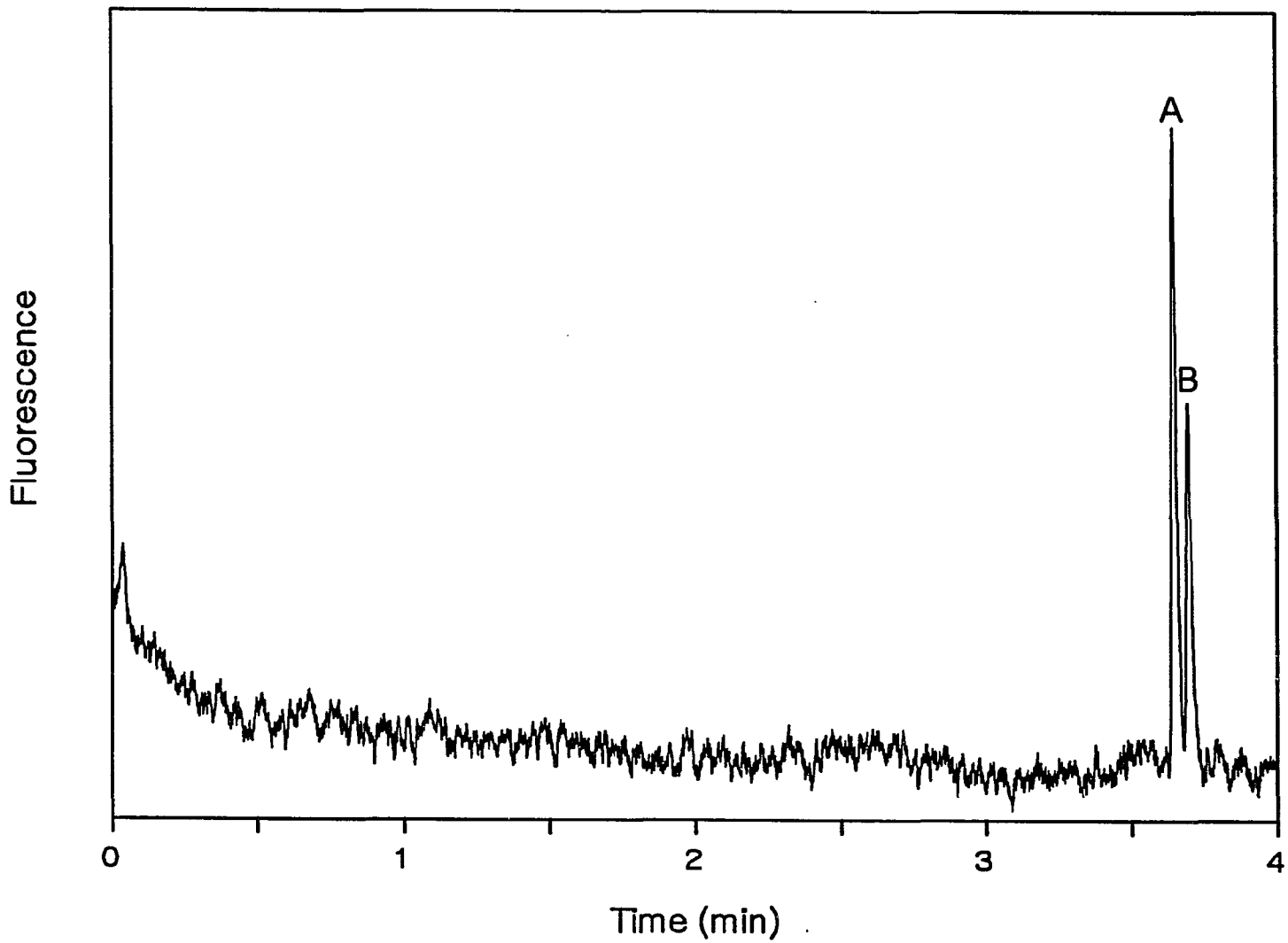
Fluorescence
A
B
0
1
2
3
4
Time (min)

Figure 5(a) shows the variations in k as a function of [CTAB]. A small change is evident between 0.01 to 1mM, mainly reflecting the contribution of the increased flow rate. A large decrease in k is found going from 1 mM to 10 mM, even though the flow rate hardly changed. This is expected as the nonpolar analytes become increasingly soluble in the organic-rich mobile phase as surfactant is added. The increased solubility is however not due to charging of the analytes by association with the surfactant at these concentrations, since we were not able to separate these analytes by zone electrophoresis in bare silica tubes at identical surfactant concentrations. This trend reverses between 10 mM and 50 mM CTAB, providing strong evidence that micelles are formed in the mobile phase, retarding the analytes as they partition into these slower moving entities.

The separation efficiency can be judged from the plot of N vs [CTAB] in Figure 5(b). There is no significant change below 10 mM. Note that these plate numbers are much smaller than those in Figure 3 and 4, reflecting the effect of substantially larger k values (13,14) that accompany a decrease in solvent polarity. When [CTAB] reaches 50 mM, a large increase in separation efficiency is observed. This can be explained by the formation of micelles. Partitioning is now mostly between the stationary phase and the micelles rather than the water/organic medium. k now has a different meaning than those displayed in Figure 5(a), which were determined relative to an nonretained marker in the water/organic phase. This then is a hybrid of micellar LC with electroosmotic pumping. Naturally, micelles are not required for the efficient separation of this

Figure 5. Effect of CTAB concentration (M) on column performance. □ anthracene, + 9-methylanthracene. (a) capacity coefficient, k (b) theoretical plates, N, and (c) resolution, R, for the two analytes. Conditions are identical to those in Figure 4, except that the mobile phase contains 30% acetonitrile.

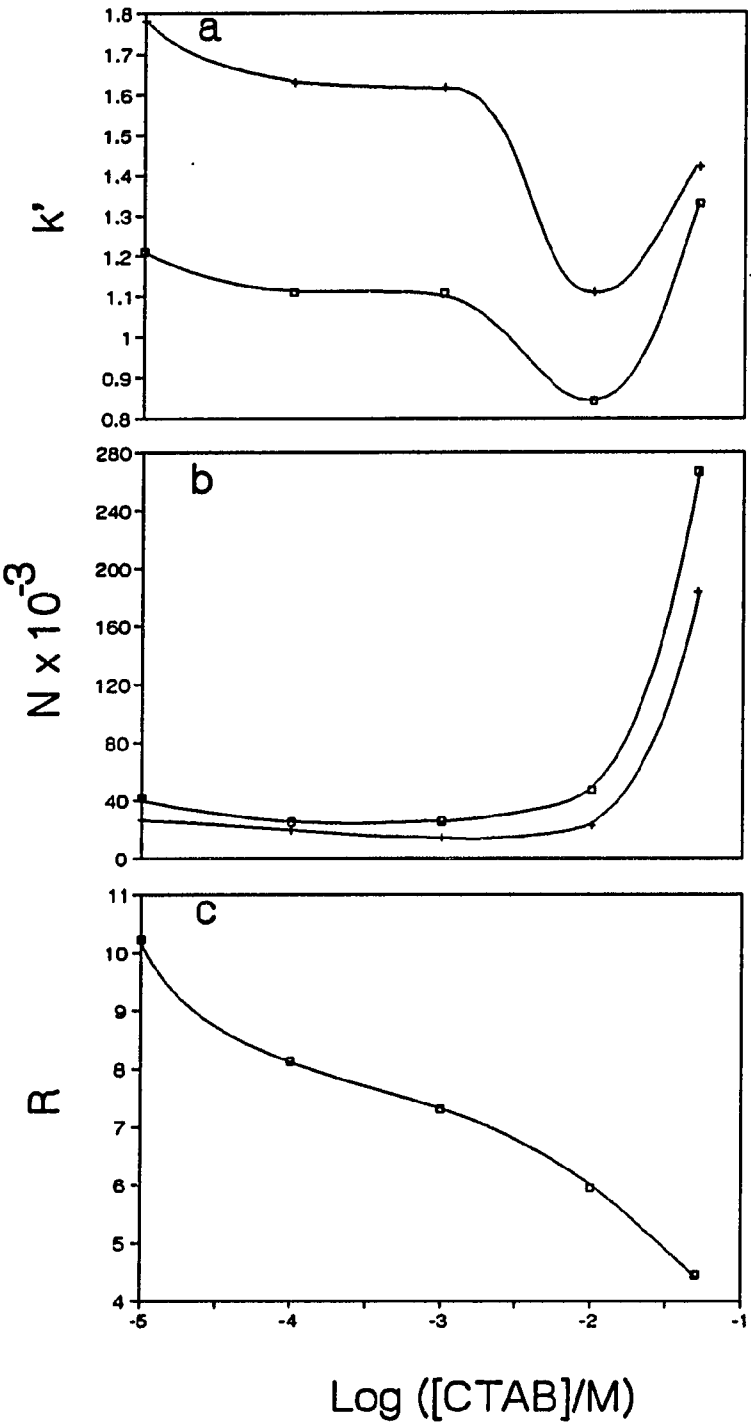
a
b
c
k'
N x 10^-3
R
Log ([CTAB]/M)
1.8
1.7
1.6
1.5
1.4
1.3
1.2
1.1
1
0.9
0.8
280
240
200
160
120
80
40
0
11
10
9
8
7
6
5
4
-5
-4
-3
-2
-1

set of neutral compounds, as shown in Figure 3. In fact, Figure 5(c) shows that the resolution, R, between the two peaks actually decreases as [CTAB] increases. That is, partition into the micelles is not as selective as partition into the water/organic phase for these analytes and this stationary phase. However, this shows that it is possible through the use micelles to overcome the low plate numbers that are inherent to strongly retained analytes in electrochromatography (13,14).

The separations in Figures 3 and 4 are superior to those performed on similar columns, but under pressurized flow conditions. For example, the plate number (260,000) for 2-methylanthracene (k = 0.58, t = 40 min) is similar to the plate number (about 300,000) for fluorescein isothiocyanate tagged methylamine (k = 0.82, t = 95 min) for which Dluzneski and Jorgenson (2) obtained using a 3 meter column with an i.d. of 5 μm (half the column diameter used in this work). In addition, the plate number of 2-naphthol (230,000, t = 3.7 min) is about 4 times the plate number (60,00, t= 4.1 min) of 9-fluorenyl-methanol, a compound barely retained, which Farbrot et al. (3) obtained on a 43 cm x 12 μm i.d. column.

Conclusion

In conclusion, we have shown that although the electroosmotic flow velocity, using conventional buffers, column lengths and electric fields, is too slow to be useful, this technique becomes a viable alternative for pumping liquid in LC when

low concentrations of a surfactant are incorporated into the buffer. This addition appears in no way detrimental to the resolution or efficiency in the separations performed here. Moreover, it has been shown, in both theory and practice, that similar results could only be realized with columns having much smaller internal diameters than those used in this work when pressurized flow conditions are imposed.

The separation mode can readily be converted into a variation of micellar LC, offering additional analyte selectivity. By saturating the stationary phase with a surfactant (the plateau region of Figure 1), one should be able to maintain a constant electroosmotic flow, free from the effects of charged sample constituents adsorbing to the column surface. The high efficiency, high mass sensitivity, neutral and charged analyte compatibility and injection simplicity make this system ideally suited for such areas as biochemical, biomedical and single cell analysis where samples are often small, dilute and consist of both charged and neutral analytes.

References

1. Kennedy, R. T.; Oates, M. D.; Cooper, B. R.; Nickerson, B.; Jorgenson, J. W. Science 1989, 246, 57-63.

2. Dluzneski, P. R.; Jorgenson, J. W. J. High Resolut. Chromatogr. Chromatogr. Commun. 1988, 11, 332-336.

3. Farbrot, A.; Folestad, S.; Larsson, M. J. High Resolut. Chromatogr. Chromatogr. Commun. 1986, 9, 117-119.

4. Pfeffer, W. D.; Yeung, E. S. J. Chromatogr. in press, 1990.

5. Jorgenson, J. W.; Guthrie, E. J. J. Chromatogr. 1983, 255, 335-348.

6. Novonty, M. Anal. Chem. 1988, 60, 500A-510A.

7. Yang, F. J. J. Chromatogr. 1982, 236, 265-277.

8. Kennedy, R. T.; Jorgenson, J. W. Anal. Chem. 1988, 60, 1521-1524.

9. Manz, A.; Simon, W. J. Chromatogr. 1987, 387, 187-196.

10. Golay, M. J. E. In Gas Chromatography; Desty, D. H., Ed.; Buttersworths: London, 1958, p 36.

11. Voyutsky S., Colloid Chemistry; Mir Publishers: Moscow, 1978, Chapter 7.

12. Pretorius, V.; Hopkins, B. J.; Schieke, J. D. J. Chromatogr. 1974, 99, 23-30.

13. Martin, M.; Guiochon, G. Anal. Chem. 1984, 56, 614-620.

14. Martin, M.; Guiochon, G.; Walbroehl, Y.; Jorgenson, J. W. Anal. Chem. 1985, 57, 209-216.

15. Jorgenson, J. W.; Lukacs, K. D. J. Chromatogr. 1981, 218, 209-216.

16. Knox, J. H.; Grant, I. H. Chromatographia 1987, 24, 135-143.

17. Tsuda, T.; Nomura, K.; Nakagawa, G. J. Chromatogr. 1982, 248, 241-247.

18. Tsuda, T. J. High Resolut. Chromatogr. Chromatogr. Commun. 1987, 10, 622-624.

19. Huang, X.; Luckey, J. A.; Gordon, M. J.; Zare, R. N. Anal. Chem. 1989, 61, 766-770.

20. Kuhr, W. G.; Yeung, E. S. Anal. Chem. 1988, 60, 1832-1834.

21. Gross, L.; Yeung, E. S. Anal. Chem. in press.

22. Hjerten, S. J. Chromatogr. 1985, 347, 191-198.

23. Rosen, M. J. Surfactants and Interfacial Phenomena; Wiley-Interscience:

New York, 1978; Chapter 3.

24. Pfeffer, W. D. and E. S. Yeung, unpublished results, Department of Chemistry, Iowa State Universtiy.

25. Gorse, J.; Balchunas, A. T.; Swaile, D. F.; Sepaniak, M. J. J. High Resolut. Chromatogr. Chromatogr. Commun. 1988, 11, 544-559.

SECTION V. ELECTROOSMOTICALLY DRIVEN ELECTROCHROMATOGRAPHY OF ANIONS HAVING SIMILAR ELECTROPHORETIC MOBILITIES BY ION PAIRING

Introduction

Recently, Everaerts et al. discussed the concept of electrophoresis versus electrochromatography (1). They argue that for capillary zone electrophoresis (CZE), a pure electrophoretic separation can only be accomplished in capillaries of 200 μm i.d. or greater. Separations in capillaries of smaller i.d., especially those with i.d. < 50 μm and having electroosmotic flow (EO) as the major mode of solute transport, tend to exhibit behavior that is a hybrid between "purely" electrophoretic and "purely" chromatographic (1). Nevertheless, in a typical CZE separation of ionic solutes, the separation will be predominately based on the differential migration of the solutes. Highly efficient separations can be achieved in capillaries without the need for wall adsorption, which is essential for the complementary technique, open-tubular capillary liquid chromatography (OTCLC). In fact, for certain solutes, adsorption to the wall is viewed as disastrous to efficiency and avoided if possible (2,3). However, narrow capillaries (i.d. < 200 μm) are desirable because they increase the surface-area-to-volume ratio, which results in efficient heat dissipation.

In the typical CZE separation, the resolution between two solutes will be

dependent on their electrophoretic mobility differences as well as the EO flow. Increases in resolution are commonly achieved by changing the pH of the buffer, which can alter the degree of charge on the solutes, thereby altering their mobilities. At the same time, EO flow can be reduced, eliminated or reversed through buffer additives so that differences in mobility are better exhibited.

Achieving adequate resolution for ionic solutes whose mobilities are nearly identical and whose degrees of charge remain constant over a wide pH range, such as isomeric strong acids or bases, is an exceptionally difficult task. Increasing resolution based on varying pH or EO flow can be ineffective. In these instances, other methods to improve resolution must be adopted. These include the addition of an organic modifier to the buffer (4) and the use of electrokinetic chromatography (5,6).

Our approach to this problem is to take the mixed-mode behavior discussed earlier to an extreme by giving CZE separation a strong chromatographic component. Realizing that isomeric strong acids and bases are easily separated using reversed-phase ion-pair liquid chromatography, we decided to combine the high degree of analyte discrimination associated with the ion-pair technique with the ease and efficiency of a CZE separation. This is accomplished by replacing the CZE column with a reversed-phase OTCLC column of narrow i.d. (~10 μm) and by including an ion-pairing agent into the buffer. Because narrow i.d. columns are used, and because the flow profile is flat (electroosmosis) rather than parabolic, the mass transfer contribution to zone broadening is minimized for partitioning

solutes (7). The ion-pairing agent is used to control the affinity of the anions for the stationary phase. We demonstrate the resulting technique, which can be called ion-pair electrochromatography, by separating a series of anions whose mobilities at the working pH are nearly identical.

Experimental

The buffer used throughout this experiment was 10 mM phosphate. The 0.1% hydroxypropylcellulose (HPC; Aldrich Chemical Co., Milwaukee, WI) solution was prepared from buffer and the final pH adjusted to 7.0. Ion-pairing solutions were prepared by diluting 40.0% (w/w) tetrabutylammonium hydroxide (TBA; Aldrich) with the buffer and adjusting the final pH to 7.0. The anions, 4-amino-1-naphthalenesulfonic acid (4A1N), 2-amino-1-naphthalenesulfonic acid (2A1N), 5-amino-2-naphthalenesulfonic acid (5A2N), 8-amino-2-naphthalenesulfonic acid (8A2N; all from Aldrich), and 1-naphthol-4-sulfonic acid (1H4N; Eastman Kodak Co., Rochester, NY) were prepared in running buffer prior to their injection.

The fused silica capillaries (Polymicro Technologies Inc., Phoenix, AZ) were 50 cm in length and nominally 10-μm in i.d. These capillaries were used as supplied or coated, and the coating later crosslinked, with either 0.9% (w/v) PS-264 (Petrarch Systems, Inc., Bristol PA) or 10.0% (w/w) OV-17v (Alltech Associates, Inc., Deerfield, IL) as described in ref. 8 or 9, respectively. The polyimide

coating was burned off at one tip of the capillary to prevent analytes from possibly adsorbing to it during an injection. It was also burned off at 40 cm from this tip to facilitate on-column detection.

The CZE/electrochromatography system is similar to one described previously (10), except a stationary phase is used in some instances. The electric field is supplied by either a positive or negative high-voltage supply (0-30 kV, Glassman High Voltage Inc., Whitehouse Station, NJ; Model MJ30P0400-11 or MJ30N0400-11).

Chromatography was performed by disconnecting the CZE column from the high voltage isolation unit and attaching it to a solvent reservoir (Valco Instruments Co. Inc., Houston, TX; Part No. ZU4L) which had a head pressure supplied by a regulated high-pressure He tank.

Sample introduction for all three types of separations was accomplished by using hydrodynamic injection. Chromatographic solvent velocity and electroosmotic flow velocity were calculated from the baseline disturbance that resulted from the injection of running buffer containing approximately 10% acetonitrile. Detection of the anions in all instances is accomplished by using a laser-based fluorescence detector that has been described previously (7).

All data were collected on either a strip chart recorder or subjected to analog to digital conversion (Data Translation, Inc., Marlborough, MA; Model DT2827, 5-10 Hz) and later stored on a personal computer (IBM PC-AT).

Discussion

When an anion in a buffer-filled capillary is subjected to an electric field, E, the anion will migrate with a velocity, v, described by

$$v = v_{ep} + v_{eo} = (\mu_{ep} + \mu_{eo})E \qquad (1)$$

where v_{ep}, v_{eo}, μ_{ep} and μ_{eo} represent the electrophoretic velocity component, the electroosmotic velocity component, the electrophoretic mobility of the anion and the coefficient for electroosmotic flow, respectively. When two anions, 1 and 2, are subjected to these conditions, they will separate with a resolution, R, defined by

$$R = \frac{1}{4\sqrt{2}}(\mu_{ep_1} - \mu_{ep_2})\sqrt{\frac{EL}{D(\overline{\mu}_{ep} - \mu_{eo})}} \qquad (2)$$

where $\overline{\mu}_{ep}$ is their average mobility, D is their diffusion coefficient, and L is the length of the column (11).

In a typical CZE separation of anions, μ_{ep} and μ_{eo} are of opposite sign; therefore, by reducing μ_{eo} in eq (2), the resolution between the two anions will be increased. In practice, this can be accomplished through the use of certain buffer additives, such as HPC. Figure 1A represents an attempted separation of two anions using a buffer containing HPC. Although the EO flow has been nearly

Figure 1. (A) Elution profile of a CZE separation with reduced EO flow for 5A2N and 1H4N. Buffer conditions: 10 mM phosphate, 0.1% HPC, pH 7.0. The separating column is a 50 cm x 10 μm i.d. uncoated capillary having a 40 cm separation distance. Separation voltage is -21 kV. (B) Elution profile for an electrochromatographic separation of the same two anions. Buffer: 10 mM phosphate, pH 7.0. The column is a capillary coated with PS-264 and is 50 cm x 10 μm i.d. with a separating distance of 40 cm. Separation voltage is -21 kV. (C) Electrochromatographic elution profile for the same two anions using a column coated with OV-17v. Buffer, column dimensions and separating voltage are as described for Figure 1B. eliminated, the resolution between the two anions is still close to zero.

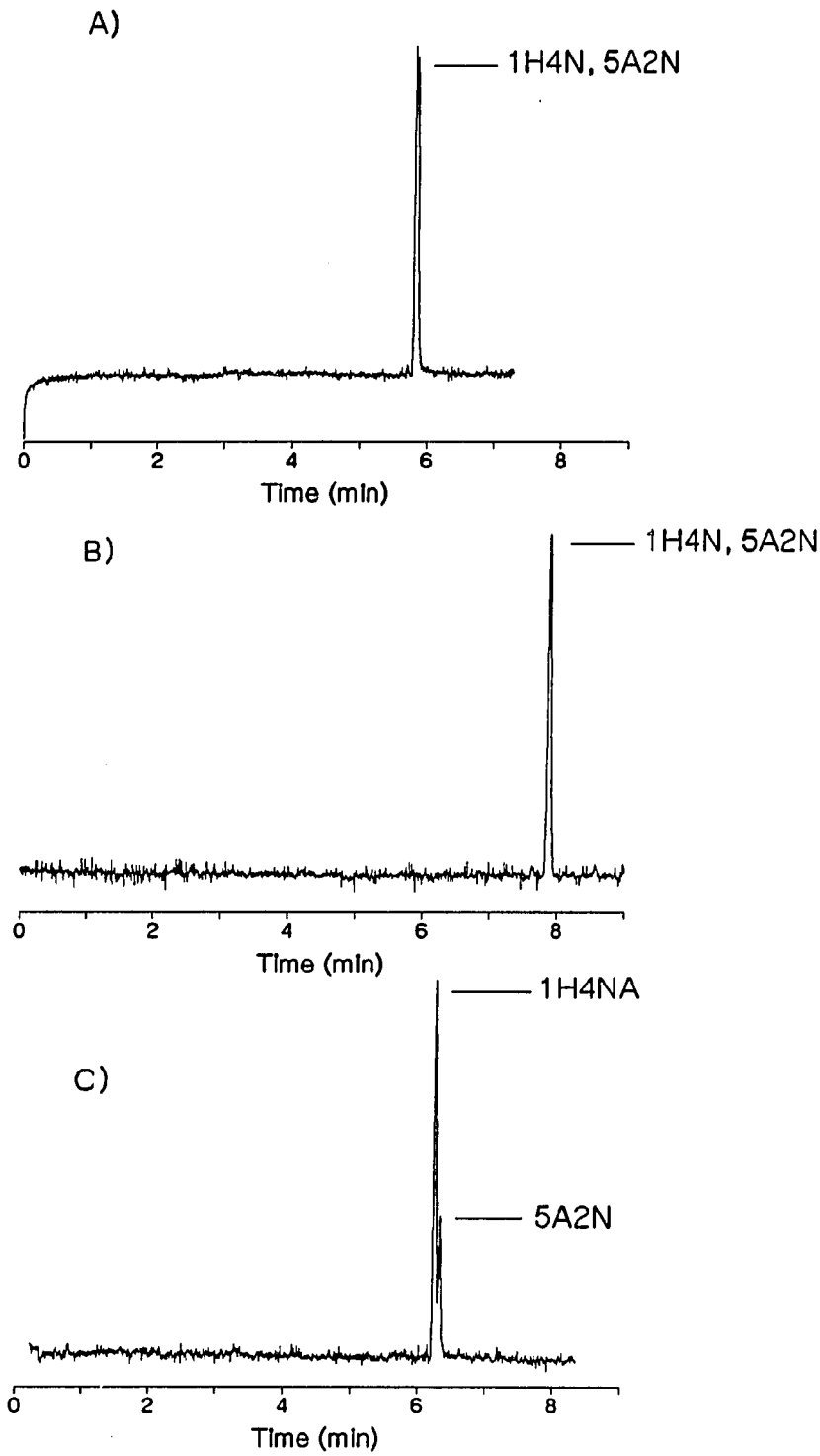
A)
1H4N, 5A2N
0
2
4
6
8
Time (min)
B)
1H4N, 5A2N
0
2
4
6
8
Time (min)
1H4NA
C)
5A2N
0
2
4
6
8
Time (min)

eliminated, the resolution between the two anions is still close to zero.

If these two anions were subjected to a separation using capillaries similar to those used in OTCLC, two results can be expected. First, due to the stationary phase shielding the silanol groups, the EO flow will be drastically reduced; therefore, migration of the anions will be based on their mobility alone ($v \approx v_{ep}$). Second, if the anions have enough hydrophobic character, there is the possibility of the solutes partitioning onto the stationary phase. In such a case, an anion will travel with a velocity, v', which is related to v by

$$v' = \frac{v}{(1 + k)} \tag{3}$$

where k is the capacity coefficient of the anion. In the situation where two anions have similar mobilities but different capacity coefficients, they will elute with a velocity difference, $\Delta v'$, defined by

$$\Delta v' = \frac{v(k_2 - k_1)}{(1 + k_2)(1 + k_1)} \tag{4}$$

Since $\Delta v'$ is proportional to the difference in the capacity coefficients, if a large enough difference exists, complete separation can be expected.

Using this rationale, we attempted to separate the two anions discussed earlier using a column coated with polymer, PS-264. From Figure 1B, it can be seen that the electroosmotic flow has been nearly eliminated, but as before, the resolution for the anions is again near zero. An attempt to separate the two

chromatographically in a pressure-driven system yielded the same results in that the anions were barely retained, if at all, and were inseparable under conditions similar to those in Figure 1B.

We observe that since the individual capacity coefficients are small, increasing k for each anion may increase their difference, and hence, $\Delta v'$. The retention of a solute may be increased by modifying the stationary phase or the mobile phase. In the case of the stationary phase, an OTCLC column can be made more retentive by increasing the film thickness of the stationary phase. Because the column used in Figure 1B is representative of the most retentive column we are able to produce repeatedly using the method in ref. 8, we adopted a procedure developed by Dluzenski and Jorgenson (9). They describe a procedure for coating columns of similar i.d. using the polymer, OV-17v. After preparing a column from conditions which produced the thickest polymer film in ref. 9, we again attempted to separate the two anions. It can be seen from Figure 1C, although incomplete, the beginning of a separation is present.

This approach has several drawbacks. The first is that changing columns to improve a separation is tedious and time consuming. The second, as Figure 1C demonstrates, is that this technique will fail for many polar, ionic solutes. A similar problem existed in liquid chromatography, but the technique of ion-pairing provided a useful solution. Therefore, to increase the retention of these anions through mobile phase modification, the principles of ion-pair chromatography were adopted.

It is well known in ion-pair chromatography that the addition of a salt, which contains a large organic cation, to the eluent will increase the affinity of an anion for the stationary phase. Although several models exist for reverse-phase ion-pair chromatography (12,13), many experimental results involving a bonded stationary phase have been described by the dynamic ion-exchange model (14-18). An important requirement for the dynamic ion-exchange model is that the ion-pairing agent, in our case a cation, C^+, be partitioned onto the stationary phase. This can be described through the equilibrium

$$C_m^+ \underset{}{\overset{K_1}{\rightleftharpoons}} C_s^+ \qquad (5)$$

where the subscripts m and s denote the mobile phase and the stationary phase, respectively. The anion, A^-, is partitioned onto the column through the equilibrium

$$A_m^- + C_s^+ \overset{K_2}{\rightleftharpoons} (A^-C^+)_s \qquad (6)$$

We have observed previously (7) that when a cationic surfactant is incorporated into an electrochromatographic system using a column similar to that in Figure 1B, the EO flow is in the direction of the anode, and its velocity is dependent on the surfactant concentration. This is due to the surfactant partitioning itself between the mobile and stationary phases, which then modifies the charge on the surface. The EO velocity is directly proportional to this surface

charge. Because of the equilibrium that exists, this charge, and hence, EO velocity, are dependent on the cation concentration. For this same reason, it is evident from Figure 2 that the cation, TBA, which is a common ion-pairing agent, also partitions itself onto such a stationary phase. Based on this, we assume that the dynamic ion-exchange model is the dominant retention mechanism. However, since it is unlikely that only one retention mechanism exists, we also take into account the formation of ion pairs.

For the model of ion-pair formation, the anion and the cation form an ion-pair through

$$A^-_m + C^+_m \underset{}{\overset{K_3}{\rightleftharpoons}} (A^-C^+)_m \qquad (7)$$

and this pair partitions onto the stationary phase through

$$(A^-C^+)_m \underset{}{\overset{K_4}{\rightleftharpoons}} (A^-C^+)_s \qquad (8)$$

In the absence of ion-pair formation, ν' and $\Delta\nu'$ are described by eqns (3) and (4), with ν now being the sum of ν_{ep} and ν_{eo}. However, in the presence of ion-pair formation, the ion pair will have zero charge; therefore, it will be transported by EO flow alone. This makes ν' and $\Delta\nu'$ more complicated. In this case, ν' becomes

$$\nu' = \frac{F\nu}{1 + k} + \frac{(1 - F)\nu_{eo}}{1+k'} \qquad (9)$$

Figure 2. Dependence of the coefficient for electroosmotic flow (μ_{eo}) on the concentration of TBA in a buffer of 10 mM phosphate, pH 7.0. Column and voltage conditions are as described in Figure 1B.

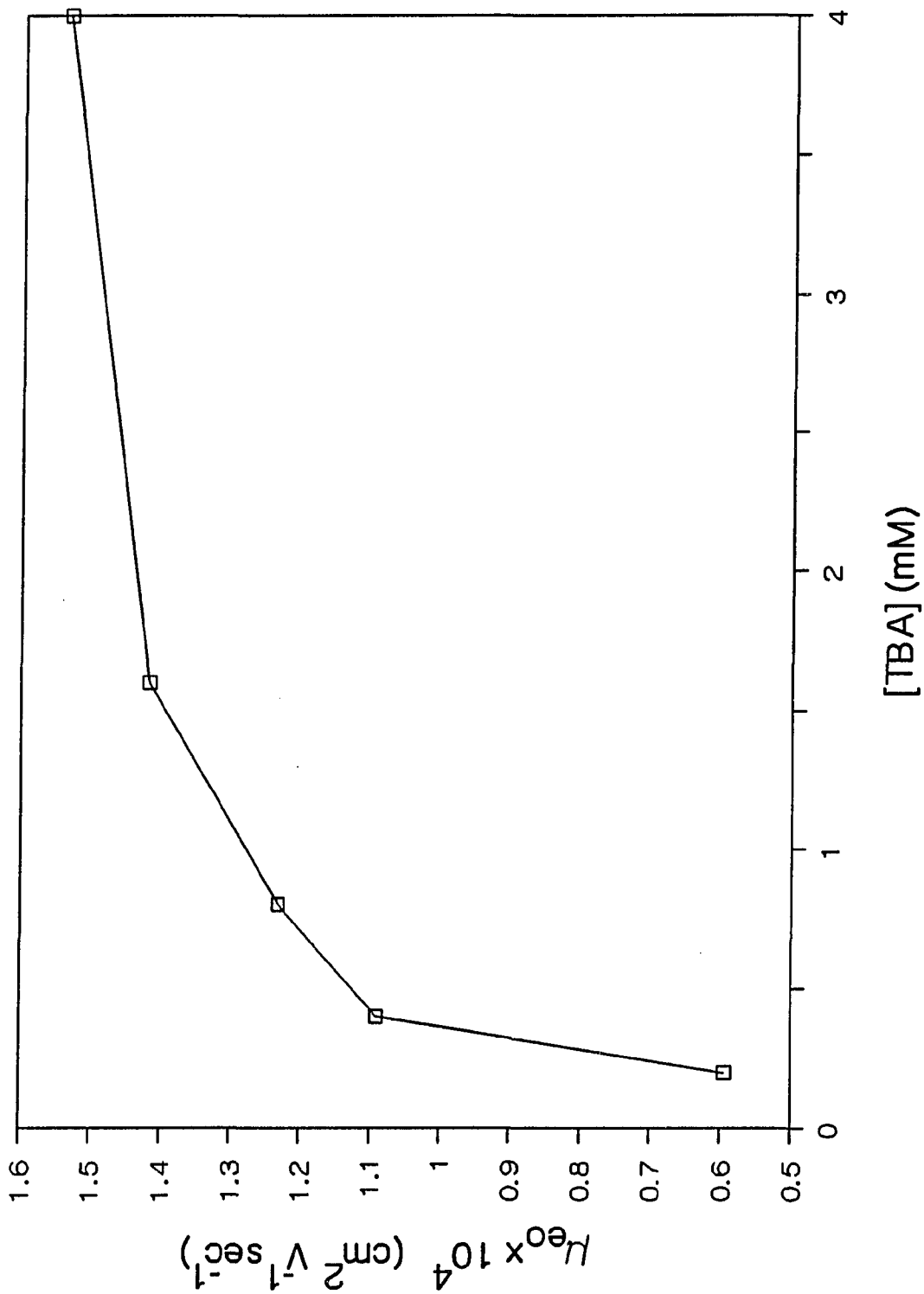
$\mu_{eo} \times 10^4$ (cm^2 V^{-1} sec^{-1})
1.6
1.5
1.4
1.3
1.2
1.1
1
0.9
0.8
0.7
0.6
0.5
0
1
2
3
4
[TBA] (mM)

and $\Delta v'$ becomes

$$\Delta v' = v\left[\frac{F_1 - F_2 + F_1k_2 - F_2k_1}{(1 + k_2)(1 + k_1)}\right] \qquad (10)$$

$$+ v_{eo}\left[\frac{F_2 - F_1 + (1 - F_1)k_2' - (1 - F_2)k_1'}{(1 + k_2')(1 + k_1')}\right]$$

where F is the fraction of free anion, k is the capacity coefficient for free ion, and k' is the capacity coefficient of the ion pair. F can be determined from:

$$F = \frac{[A_m^-]}{[A_m^-] + [A^-C_m^+] + [A^-C_s^+]} = \frac{1}{1 + K_3(1 + K_4)[C_m^+]} \qquad (11)$$

We can illustrate the effect of the ion-pairing agent on $\Delta v'$ using these equations for the case where the dynamic ion-exchange model is dominant ($K_1K_2 >> K_3K_4$). At low concentrations of ion-pairing agent, F will be near unity and the second part of eq (10) can be neglected. In addition, if $F_1 \approx F_2$, eq (10) can be approximated by eq (4). With $k \propto K_1K_2[C_m^+]$ (19) and $\Delta v' \propto (k_1 - k_2)$, increasing retention via the ion-pairing agent will increase $\Delta v'$.

To demonstrate this, five anions were subjected to the same separation as in Figure 1A. From the electropherogram in Figure 3, it is observed that 4 out of the 5 anions are unresolved because of similar mobilities. Next, the column was replaced with one identical to it, and equilibrated with a buffer containing 1.25

Figure 3. CZE elution profile for five anions, four of which have similar electrophoretic mobilities. Column, buffer and voltage conditions are as described for Figure 1A.

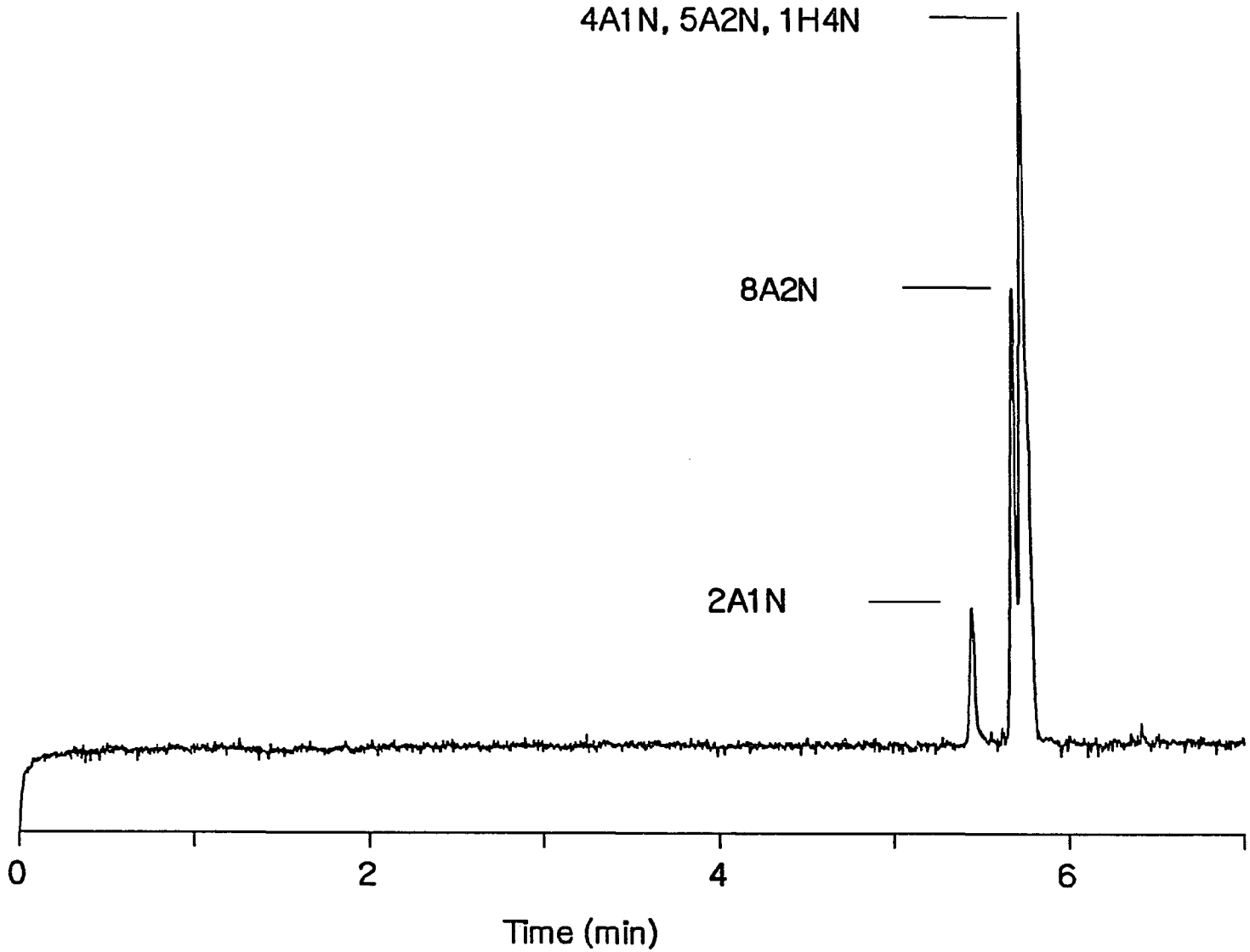
4A1N, 5A2N, 1H4N
8A2N
2A1N
0
2
4
6
Time (min)

mM TBA. Separating the same five anions under conditions resulted in no elution of any anion. To explain this, consider that when large, linear organic cations are incorporated into CZE buffers, the direction and magnitude of the EO flow becomes dependent on the concentration of the cation. This has been discussed earlier (20,21), but the effect in those reports is much less than that when a stationary phase is used (7). In the case above, it was concluded that due to the bulky nature of TBA, the amount adsorbed on the wall was ineffective at reducing the EO flow, which was later determined to be in the direction of the cathode (away from the detector). Attempting the same separation again, but with the polarity of the electric field reversed, resulted in the electropherogram shown in Figure 4. Although the four anions with similar mobility are poorly resolved, the fact that 1H4N is separated from 5A2N is of interest. Under similar conditions (5 mM phosphate buffer, pH 7.0; +27 kV separating voltage), but with no TBA in the buffer, these two anions do not separate. Since dynamic ion-exchange is unlikely due to the poor column adsorption of TBA (stationary phase absent), this may be the result of ion-pair formation in the mobile phase.

The discussion above brings up a related point. The cations of such salts as cetyltrimethylammonium bromide and tetradecyltrimethylammonium bromide adsorb onto uncoated, capillary walls (20,21). Therefore, CZE separations which have these or similar salts in the buffer may experience an ion-pairing effect. If such a separation is performed in a capillary with an i.d. >> 10 μm and if the ion-pairing effect is significant, the bands may exhibit solute zone broadening due

Figure 4. CZE elution profile for the five anions using a 10 mM phosphate buffer, pH 7.0, containing 1.25 mM TBA. Column parameters are the same as in Figure 1A. Separating voltage is +21 kV.

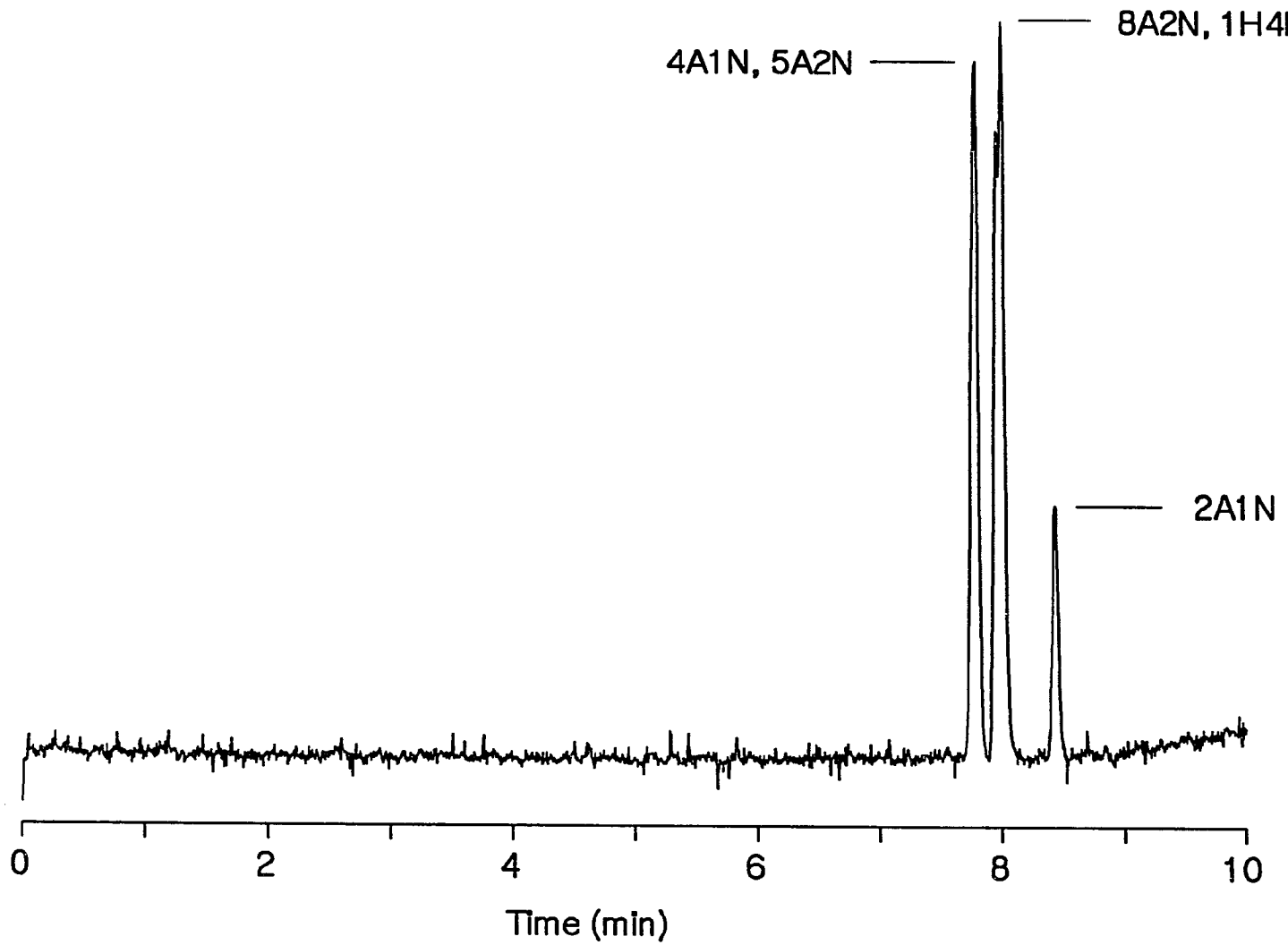
4A1N, 5A2N
8A2N, 1H4N
2A1N
0
2
4
6
8
10
Time (min)

to poor mass transfer.

To switch from capillary zone electrophoresis to electrochromatography, the CZE column was replaced with an OTCLC column similar to that used in Figure 1B and equilibrated with a buffer containing 1.25 mM TBA. Subjecting the same five anions to a separation under these conditions resulted in the electrochromatogram shown in Figure 5. Although the TBA concentration in Figure 5 was 1.25 mM, the four anions of similar mobility can be separated completely using TBA even at 600 μM. At that concentration, however, the 2A1N peak is fused with the 1H4N peak. Notice that the 2A1N, which was first to elute in Figure 3, is now second from last. This is due to the amino group being adjacent to the sulfonic group for 2A1N, which results in a large k value when compared to its isomers (22). When TBA is at 7.5 mM, 2A1N becomes the last component to elute. Although not indicated in Figure 5, all components elute with $v' > v_{eo}$; however, when TBA is at 7.5 mM, only 2A1N elutes with $v' < v_{eo}$. This illustrates the control of retention through $[C_m^+]$.

In order to compare this technique with that of ion-pair chromatography, the 5 anions were subjected to a pressure-driven chromatographic separation using the exact same column and conditions as listed in Figure 5. The result of this is shown in the chromatogram in Figure 6. For the four anions of similar mobility, the dominant separating factor present in Figure 5 is their differences in column affinity, which is also the major separating factor in Figure 6; hence, the similarities in elution order and relative peak positions. As for the anions with

Figure 5. Electrochromatographic separation of the five anions. Column conditions are as described in Figure 1B. Buffer conditions are the same as in Figure 4. Separating voltage is -21 kV.

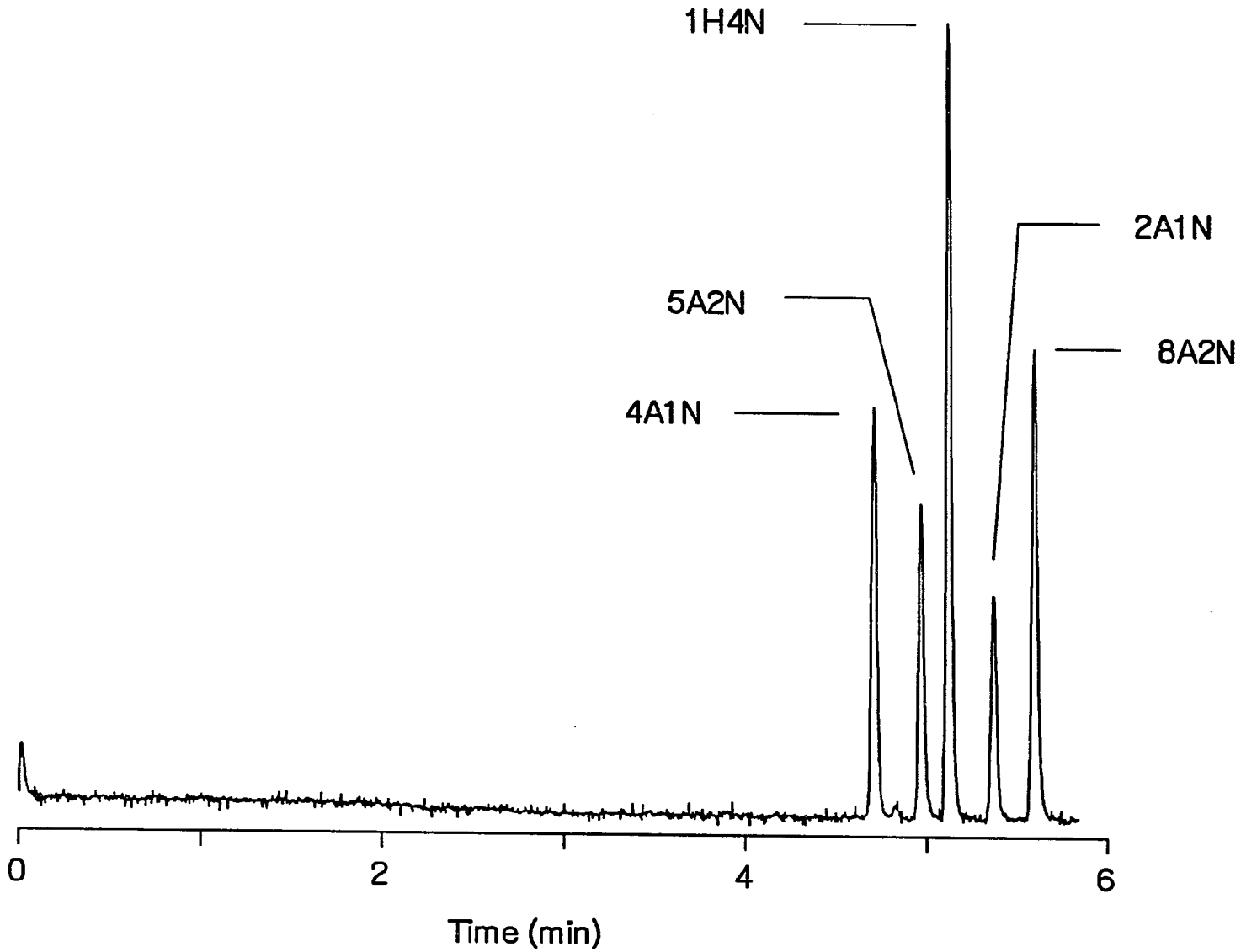
1H4N
2A1N
5A2N
8A2N
4A1N
0
2
4
6
Time (min)

Figure 6. Pressure-driven chromatographic separation of the five anions using exactly the same buffer and column as in Figure 5.

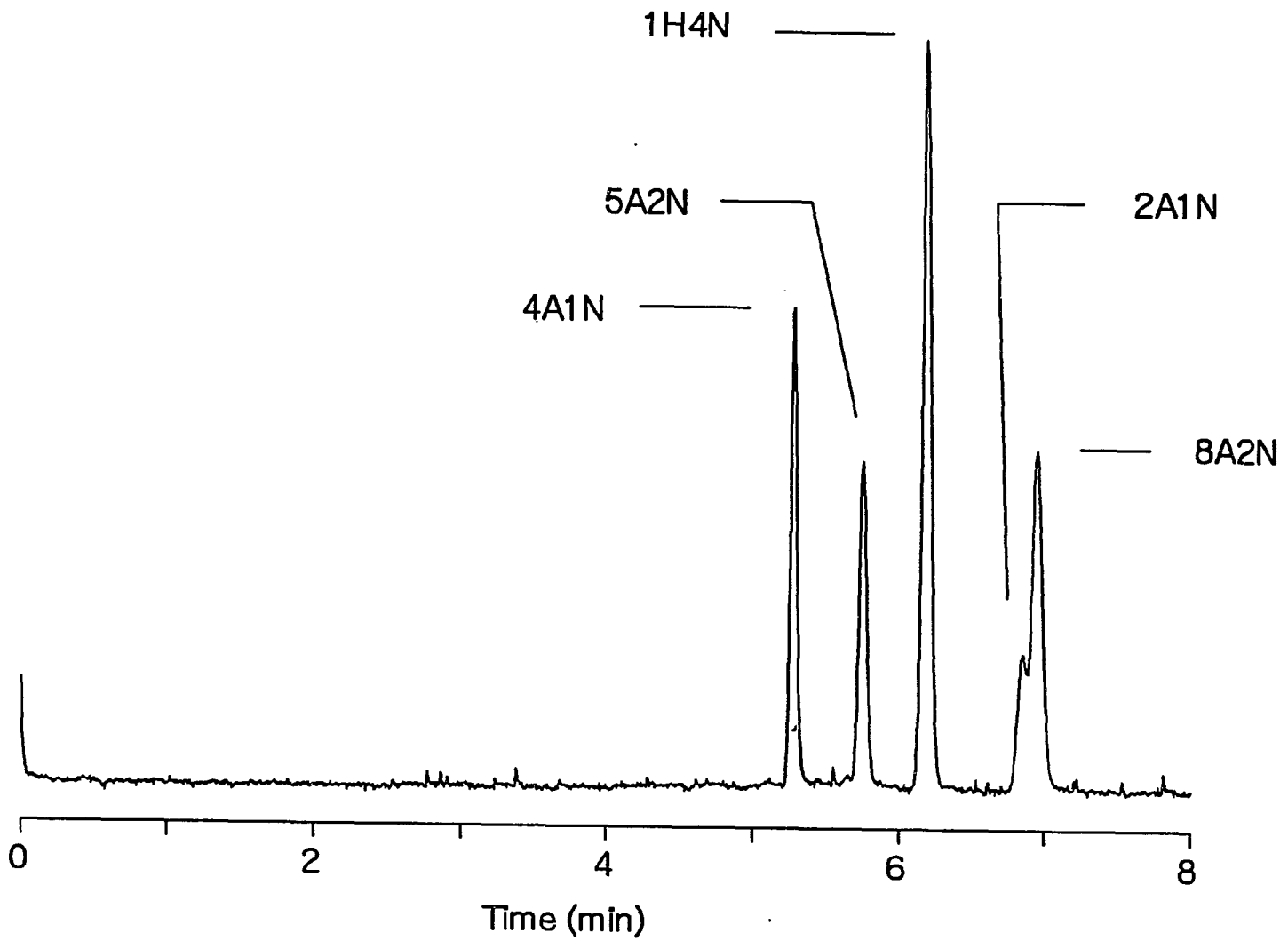
1H4N
5A2N
2A1N
4A1N
8A2N
0
2
4
6
8
Time (min)

different mobilities, elution order and relative peak position will be a function of both mobility and column affinity, both of which are present only in the electrochromatographic technique. This explains the difference in peak position in Figs. 5 and 6 for the 2A1N peak relative to its neighbors.

The capacity coefficients for the anions in Figure 6 are as follows: 4A1N, k = 0.047; 5A2N, k = 0.140; 1H4N, k = 0.228; 2A1N, k = 0.361; and 8A2N, k = 0.380. The fact that these capacity coefficients are relatively small ($k < 1$) was anticipated because of the high separation efficiency observed in Figure 5. The smallest number of theoretical plates, N, in Figure 5 is for the 4A1N peak, with N = 140,000. Comparing this N with those calculated for Figure 6 reveals that this N is nearly twice that for the 4A1N peak, and three times that for the 1H4N peak (smallest N). This is the result of the flat flow profile of electroosmotic flow which contributes less to mass-transfer broadening than the parabolic flow profile in pressure-driven systems (7,23-25). Comparing the N value of 145,000 plates for the 2A1N peak in Figure 5 to that in Figs. 3 or 4 reveals that they are nearly identical. Although no capacity coefficients were obtained, when TBA is at 7.5 mM, 2A1N is eluted with N = 50,000. Therefore, it can be seen that this technique will produce efficient separations only when k is kept small.

Resolution for each of the anion pairs in Figure 5 was calculated and found to be > 1 in all instances. As predicted, resolution can easily be controlled through the concentration of TBA, as shown in Figure 7. The negative numbers in Figure 7 results from the fact that the anion, 2A1N, changes elution order with

Figure 7. Dependence of resolution on TBA concentration for ion-pairing electrochromatography. All conditions are as described in Figure 5.

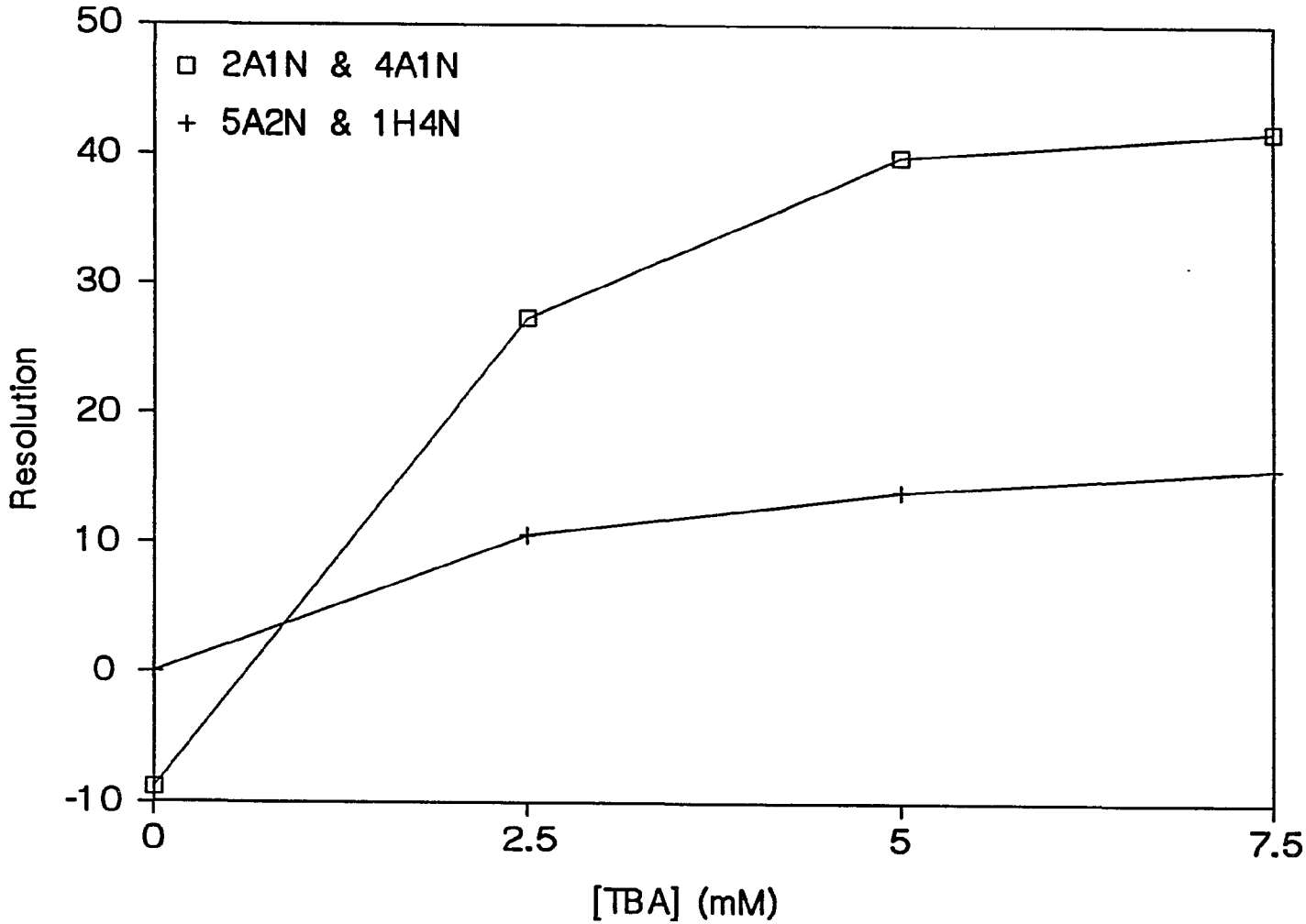
50
40
30
20
10
0
-10
Resolution
2A1N & 4A1N
5A2N & 1H4N
0
2.5
5
7.5
[TBA] (mM)

4A1N as the concentration of TBA is increased; i.e., R actually becomes zero at some point in this range. The leveling off of the curves at high TBA concentration can be attributed to increased mass transfer broadening due to increased retention.

Conclusion

We have shown that anions which do not separate based on mobility differences in CZE can be made to separate electrochromatographically. The anions, which need no native affinity for the stationary phase, can be made to partition onto the column via an ion-pairing agent added to the buffer. In so doing, the anions now separate based on affinity differences for the column. Because mass transfer broadening is minimized by using columns of narrow i.d., by keeping the capacity coefficients small, and by the flat flow profile which exists for electroosmotic flow, the efficiency of the resulting separation rivals that of a CZE separation. In addition, since there exists a similarity between ion-pair electrochromatography and ion-pair chromatography, foundations for separation of ionic solutes whose mobilities are similar can be derived from the vast amount of ion-pair chromatography literature. Finally, this technique is expected to be more sensitive than CZE to adjustments of such buffer parameters as pH, ionic strength, percent organic modifier, etc., since not only will the electrophoretic component of the separation be affected, but the chromatographic component of

the separation will be affected as well.

References

1. Everaerts, F. M.; Van de Goor, A. A. A. M.; Verheggen, Th. P. E. M.; Beckers, J. L. J. High Resolut. Chromatogr. Chromatogr. Commun. 1989, 12, 28.

2. Hjertén, S. J. Chromatogr. 1985, 347, 191.

3. Bruin, G. J. M.; Chang, J. P.; Kuhlman, R. H.; Zegers, K.; Kraak, J. C.; Poppe, H.; J. Chromatogr. 1989, 471, 429.

4. Fujiwara, S.; Honda, S. Anal. Chem. 1987, 59, 487.

5. Gassman, E.; Kuo, J. E.; Zare, R. N. Science 1985, 230, 813.

6. Terabe, S.; Isemura, T. Anal. Chem. 1990, 62, 652.

7. Pfeffer, W. D.; Yeung, E. S. Anal. Chem. 1990, 62, 2178.

8. Pfeffer, W. D.; Yeung, E. S. J. Chromatogr. 1990, 506, 401.

9. Dluzenski, P. R.; Jorgenson, J. W. J. High Resolut. Chromatogr. Chromatogr. Commun. 1988, 11, 332.

10. Kuhr, W. G.; Yeung, E. S. Anal. Chem. 1988, 60, 1832.

11. Jorgenson, J.; Lukacs, K. D. Anal. Chem. 1981, 53, 1298.

12. Bidlingmeyer, B. A. J. Chromatogr. Sci. 1980, 18 525.

13. Colin, H.; Guichon, G. J. J. Chromatogr. 1977, 141, 289.

14. Zein, A.; Baerns, M. J. Chromatogr. Sci. 1989, 27, 249.

15. Del Rey, M. E.; Vera-Avila, L. E. J. Liq. Chromatogr. 1988, 11, 2885.

16. Van De Venne, J. L. M.; Hendrix, J. L. H. M.; Deelder, R. S. J. Chromatogr. 1978, 167, 1.

17. Kissinger, P. T. Anal. Chem. 1977, 49, 883.

18. Hoffman, N. E.; Liao, J. C. Anal. Chem. 1977, 49, 2231.

19. Melander, W. R.; Horvathin, C. In Ion-Pair Chromatography; Hearn, M. T. W., Ed.; Marcel Dekker; New York, 1985; Chapter 2.

20. Tsuda, T. J. High Resolut. Chromatogr. Chromatogr. Commun. 1987, 10, 662.

21. Huang, X.; Luckey, J. L.; Gordon, M. J.; Zare, R. N. Anal. Chem. 1989, 61 766.

22. Prandi, C.; Venturini, T. J. Chromatogr. Sci. 1981, 19, 308.

23. O'Farrell, P. H. Science 1987, 227, 1587.

24. Tsuda, T. Anal. Chem. 1987, 59, 521.

25. Tsuda, T. Anal. Chem. 1988, 60, 1677.

GENERAL SUMMARY

In this work, we have demonstrated that by using a laser as the light source, many hurdles to detection in microcolumn LC can be overcome. The use of a laser two-photon excited fluorescence detector used with a slurry-packed microbore column allows for both highly sensitive and selective detection. At the opposite end of the scale, the use of a laser-based indirect fluorometric detector in conjunction with open-tubular capillary columns allows for extremely low mass limits of detection for non-fluorescing electrolytes and nonelectrolytes.

Unfortunately, because of cost and complexity, the use of the laser is limited mainly to research laboratories. However, this is changing rapidly. HeCd lasers have been available in a "turn key" style for some time, and the argon ion laser has been compacted into a small, air cooled unit. Both are available for under $10,000. The most significant future developments may be in the maturing diode laser technology. By 1992, the United States and Japan hope to produce 1 W continuous wave lasers for under $10.00. Diode lasers capable of emitting visible radiation (~650 nm) already exist for under $300. Those capable of emitting in the blue are expected in roughly 10 years. Meanwhile, radiation at 410 nm has been demonstrated by frequency doubling diode lasers (104).

In the area of microcolumn separations, we have demonstrated the usefulness of electroosmotic flow for separations in open-tubular capillary columns. By exploiting this flow, rapid and efficient separations of neutral

analytes was demonstrated. In addition to this, we have shown that by applying the principle of ion-pairing LC, analytes inseparable by capillary zone electrophoresis can be effectively separated by electroosmotically driven electrochromatography. In so doing, the instrumental simplicity of CZE, specifically in the area of sample injection and eluent propulsion, is brought to OTCLC.

LITERATURE CITED

1. Golay, M. J. E. In Gas Chromatography; Coates, V. J.; Noebels, H. J.; Fargerson, I. S., Eds.; Lansing Symposium 1957; Academic Press: New York, 1958; p. 1.
2. Giddings, J. C. Anal. Chem. 1964, 36, 1890.
3. Golay, M. J. E. Chromatographia 1973, 6, 242.
4. Hovarth, C. B.; Dreiss, B. A.; Lipsky, S. R. Anal. Chem. 1967, 39, 1422.
5. Scott, R. P. W.; Kucera, P. J. Chromatogr. 1976, 125, 251.
6. Scott, R. P. W.; Kucera, P. J. Chromatogr. 1979, 185, 27.
7. Takeuchi, T.; Ishii, D. J. Chromatogr. 1980, 190, 150.
8. Tsuda, T.; Novotny, M. Anal. Chem. 1978, 50, 632.
9. Tsuda, T.; Novotny, M. Anal. Chem. 1978, 50, 271.
10. Hirata, Y.; Novotny, M.; Tsuda, T.; Ishii, D. Anal. Chem. 1979, 51, 1807.
11. Knox, J. H.; Gilbert, M. T. J. Chromatogr. 1979, 186, 405.
12. Bristow, P. A.; Knox, J. H. Chromatographia 1977, 10, 279.
13. Knox, J. H. J. Chromatogr. Sci. 1980, 18, 453.
14. Novotny, M. Anal. Chem. 1988, 68, 500A.
15. Scott, R. P. W.; Kucera, P. J. Chromatogr. 1979, 169, 51.
16. Karlsson, K. E.; Novotny, M. Anal. Chem. 1988, 60, 1662.
17. McGuffin, V. L.; Novotny, M. J. Chromatogr. 1983, 255, 381.
18. Jorgenson, J. W.; Guthrie, E. J. J. Chromatogr. 1983, 255, 335.
19. Tsuda, T.; Tsuboi, K.; Nakagawa, G. J. Chromatogr. 1981, 214, 283.
20. Ishii, D.; Takeuchi, T. J. Chromatogr. Sci. 1984, 22, 400.

21. Farbot, H.; Folestad, S.; Larsson, M. J. High Resolut. Chromatogr. Chromatogr. Commun. 1986, 9, 117.

22. Dluzneski, P. R.; Jorgenson, J. W. J. High Resolut. Chromatogr. Chromatogr. Commun. 1988, 11, 332.

23. Guiochon, G. Anal. Chem. 1981, 53, 1318.

24. Golay, M. J. E. In Gas Chromatography; Desty, D. H. Ed.; Butterworths: London, 1958, p. 36.

25. Novotny, M. In Microcolumn High Performance Liquid Chromatography; Kucera, P., Ed.; Elsevier: Amsterdam, 1984; Chapter 7.

26. Martin, M.; Eon, C.; Guichon, G. J. Chromatogr. 1975, 108, 229.

27. Yang, F. J. J. Chromatogr. 1982, 236, 265.

28. Kennedy, R. T.; Jorgenson, J. W. Anal. Chem. 1988, 60, 1521.

29. Manz, A.; Simon, W. J. Chromatogr. 1987, 387, 187.

30. Pfeffer, W. D.; Yeung, E. S. J. Chromatogr., in press, 1991.

31. Berry, V.; Lawson, K. J. Liq. Chromatogr. 1987, 10, 3257.

32. Mysels, K. J. Introduction to Colloid Chemistry; Interscience: New York, 1959; Chapters 15-16.

33. Stevens, T. S.; Cortes, H. J. Anal. Chem. 1983, 55, 1365.

34. Pretorious, V.; Hopkins, B. J.; Schieke, J. D. J. Chromatogr. 1974, 99, 23.

35. Jorgenson, J. W.; Lukacs, K. D. J. Chromatogr. 1981, 218, 209.

36. Otsuka, K.; Terebe, S.; Ando, T. J. Chromatogr. 1985, 332, 219.

37. Rice, C. L.; Whitehead, R. J. Phys. Chem. 1965, 69, 4017.

38. Tsuda, T.; Nomura, K.; Nakagawa, G. J. Chromatogr. 1983, 264, 385.

39. Cantwell, F. F.; Puon, S. Anal. Chem. 1979, 51, 623.

40. Otsuka, S.; Listowsky, I. Anal. Biochem. 1980, 102, 419.

41. Tsuda, T.; Nomura, K.; Nakagawa, G. J. Chromatogr. 1982, 248, 241.

42. Antrim, R. F.; Scherrer, R. A.; Yacynych, A. M.; Anal. Chim. Acta. 1984, 164, 283.

43. O'Farrell, P. H. Science, 1985, 227, 1586.

44. Tsuda, T. Anal. Chem. 1987, 59, 523.

45. Knox, J. H.; Grant, I. H. Chromatographia 1987, 24, 135.

46. Tsuda, T. Anal. Chem. 1988, 60, 1677.

47. Muramatsu, Y.; Tsuda, T. J. Chromatogr. 1990, 515, 645.

48. Pfeffer, W. D.; Yeung, E. S. Anal. Chem. 1990, 62, 2178.

49. Martin, M.; Guiochon, G. Anal. Chem. 1984, 56, 614.

50. Martin, M.; Guiochon, G.; Walbroehl, Y.; Jorgenson, J. Anal. Chem. 1985, 57, 559.

51. Folestad, S.; Galle, B.; Josefsson, B. J. Chromatogr. Sci. 1985, 23 273.

52. Yeung, E. S.; Sepaniak, M. J. Anal. Chem. 1980, 52, 1465A.

53. Yeung, E. S. In Microculumn Separations: Columns, Instrumentation and Ancillary Techniques; Novotny, M. V.; Ishii, D., Eds.; Elsevier: Amsterdam, 1985, p. 135.

54. Dovichi, N. J.; Zarrin, F.; Nolan, T. G.; Bornhop, D. J. Spectrochimica Acta 1988, 43B, 639.

55. Sagliano, N.; Hartwick, R. A. J. Chromatogr. Sci. 1986, 24, 506.

56. Belenkii, B. G. J. Chromatogr. 1988, 434, 337.

57. Yeung, E. S. In Advances in Chromatography; Giddings, J. C.; Grushka, E.; Cazes, J.; Brown, P. R., Eds.; Marcel Dekker, Inc.: New York, 1984; 23, Chapter 1.

58. Hecht, E. In Optics; Addison-Wesley Publishing Co.: Reading, Massachusetts, 1987; Chapter 8.

59. Ingle, J. D.; Crouch, S. R. Spectrochemical Analysis; Prentice Hall: Englewood Cliffs, New Jersey, 1988, Chapter 16.

60. Synovec, R. E.; Yeung, E. S. Anal. Chem. 1985, 57, 2606.

61. Synovec, R. E.; Yeung, E. S. J. Chromatogr. 1986, 368, 85.

62. Christensen, P. L.; Yeung, E. S. Anal. Chem. 1989, 61, 1344.

63. Winefordner, J. D.; Schulman, S. G.; O'Haver, T-C., Luminescence Spectrometry in Analytical Chemistry; John Wiley and Sons, Inc.: New York, 1972.

64. Schulman, S.G. Fluorescence and Phosphorescence Spectroscopy Physiochemical Principles and Practice; Pergamon Press: New York, 1977.

65. McClain, W. M. Acc. Chem. Res. 1974, 7, 129.

66. Sepaniak, M. J. Ph. D. Dissertation, Iowa State University, Ames, IA., 1980, pp. 31-33.

67. Sepaniak, M. J.; Yeung, E. S. Anal. Chem. 1977, 49, 1554.

68. Sepaniak, M. J.; Yeung, E. S. J. Chromatogr. 1981, 95, 211.

69. Wirth, M. J.; Lytle, F. E. Anal. Chem. 1977, 49, 2054.

70. Gluckman, J.; Shelly, D.; Novotny, M. J. Chromatogr. 1984, 317, 443.

71. Karlsson, K. E.; Wiesler, D. Alasandro, M.; Novotny, M. Anal. Chem. 1985, 57, 229.

72. Andreolini, F.; Beale, S. C.; Novotny, M. J. High Resolut. Chromatogr. Chromatogr. Commun. 1988, 11, 20.

73. Beale, S. C.; Sarage, J. C.; Wiesler, D.; Wieststock, S.; Novotny, M. Anal. Chem. 1988, 60, 1765.

74. Lingeman, H; Underberg, W. J.; Takadate, A.; Hulshoff, A. J. J. Liq. Chromatogr. 1985, 8, 792.

75. Small, H.; Miller, T. E. Anal. Chem. 1982, 54, 462.

76. Stanahan, J. J.; Deming, S. N. Anal. Chem. 1982, 54, 1540.

77. Denkert, M.; Hackzell, L.; Schill, G.; Sjögren, L. J. Chromatogr. 1981, 218 31.

78. Parkin, J. E.; Lau, H. T. J. Chromatogr. 1984, 314, 488.

79. Yeung, E. S. Acc. Chem. Res. 1989, 22, 125.

80. Schill, G.; Crommen, J. Trends in Anal. Chem. 1987, 6, 111.

81. Schill, G.; Arvidsson, E. J. Chromatogr. 1989, 492, 299.

82. Ishii, D; Takeuchi, T. J. Liq. Chromatogr. 1988, 11, 1865.

83. Crommen, J.; Schill, G.; Westerlund, D.; Hackzell, L. Chromatographia 1987, 24, 252.

84. Crommen, J.; Schill, G.; Herné, P. Chromatographia 1988, 25, 397.

85. Bobbitt, D. R.; Yeung E. S. Anal. Chem. 1984, 56, 1577.

86. Bobbitt, D. R.; Yeung, E. S. Anal. Chem. 1985, 57, 271.

87. Ye, J.; Baldwin, R. P.; Ravichandran, K. Anal. Chem. 1986, 58, 2337.

88. Mho, S-I.; Yeung, E. S. Anal. Chem. 1985, 57, 2253.

89. Takeuchi, T.; Yeung, E. S. J. Chromatogr. 1986, 366, 145.

90. Takeuchi, T.; Yeung, E. S. J. Chromatogr. 1986, 370, 83.

91. Takeuchi, T.; Suzuki, E.; Ishii, D. J. Chromatogr. 1988, 447, 221.

92. Takeuchi, T.; Ishii, D. J. Chromatogr. 1988, 447, 221.

93. Takeuchi, T.; Ishii, D. J. Chromatogr. 1987, 396, 149.

94. Takeuchi, T.; Hashimoto, Y.; Ishii, D. J. Chromatogr. 1987, 403, 324.

95. Pfeffer, W. D.; Takeuchi, T.; Yeung, E. S. Chromatographia 1987, 24, 123.

96. Pfeffer, W. D.; Yeung, E. S. J. Chromatogr. 1990, 506, 401.

97. Yang, F. J. J. High Resolut. Chromatogr. Chromatogr. Commun. 1981, 4, 83.

98. Guthrie, E. J.; Jorgenson, J. W. Anal. Chem. 1984, 56, 483.

99. Takeuchi, T.; Yeung, E. S. J. Chromatogr. 1987, 389, 3.

100. Hersberger, L. W.; Callis, J. B.; Christian, G. D. Anal. Chem. 1979, 51, 1444.

101. Dovichi, N. J.; Martin, J. C.; Jett, J. H.; Trkula, M.; Keller, R. A. Anal. Chem. 1984, 56, 348.

102. Van Vliet, H. P. M.; Poppe, H. J. Chromatogr. 1985, 346, 149.

103. Sepaniak, M. J.; Yeung, E. S. J. Chromatogr. 1980, 190, 377.

104. Laser Spectroscopy: Assessment of Research Needs for Laser Technologies Applied to Advanced Methods; U.S. Department of Energy. U.S. Government Printing Office: Washington, D.C., 1990; DE-AC01-88ER30131.

ACKNOWLEDGEMENTS

Looking at my cluttered desk while I prepare this portion of my thesis, I'm reminded of my start here at Iowa State. My desk was a mess then, too.

This work was performed at Ames Laboratory under contract no. W-7405-eng-82 with the U. S. Department of Energy. The United States government has assigned the DOE Report number IS-T 1501 to this thesis.

I believe that writing the acknowledgements should be the most enjoyable part of preparing a thesis simply because you get to thank those who have helped you along the way. However, I find it one of the most difficult sections to prepare because there are so many people to thank. For example, I could thank the manufacturers at Subaru for building my fine, 1978, 4 WD wagon. It started on the coldest days of winter and ran for two years (50,000 miles) without a tune up. Appreciation in a case such as this, though, would be to the extreme. Therefore, I'll try to acknowledge those who were immediately involved in helping me obtain this degree.

First and most importantly, none of this would have been possible if not for Dr. Yeung. After interning with him seven years ago, I knew there was no other research group for me. Without that experience, I shudder to think of the decision I might have made concerning graduate school. I cannot thank him enough for his guidance and leadership. Finally, his laissez faire policy toward one's graduate career truly makes that person the master of his own destiny here,

and I thank him for that, also.

I would like to thank Dr. Leo Ochrymowycz (Dr O) at the University of Wisconsin at Eau Claire, who, incidently, received his doctorate from Iowa State. Without his guidance and counsel as an undergraduate, I probably would have ended up working quality control at the Leinenkugals brewery in Chippewa Falls, Wisconsin. I also thank him for motivating me to seek an internship with Dr. Yeung. He always had a minute to spare, and I thank him for that, too.

I thank Dr. Robert Eierman, also at the University of Wisconsin at Eau Claire. His suggestions and insight on graduate school have been invaluable. Being fresh out of graduate school himself when I first met him, I could trust his advice. He's an excellent teacher and a better friend. I would also like to thank him for employing me while at UWEC. With respect to that, I'm sure the local drinking establishments in Eau Claire would also like to thank him.

Next, I would like to thank Mr. Dale Voskuil. It was his intervening in my high school career, that got the ball rolling for me. Because of him, I have no regrets for the road not taken. I value our friendship, and wish him continued success.

I thank the members of Dr. Yeung's group, both past and present. Their camaraderie has made my graduate school experience much more enjoyable. Without it, I'm sure I would have many jeremiads (that word is for you, Dave).

I thank all my friends back in Wisconsin, especially John (Harry), Mark, and Edie (who actually is from Illinois). They made my countless trips back home or

to wherever, times I'll never forget. If someone could bottle Wisconsin and sell it, I'm sure they would make a fortune. Wait. I think that's what the breweries are doing!

I thank Sherri, my fiance, for her love, understanding, patience and support. She sacrificed much in order to be with me, and I thank her for that, too. Finally, without her, completion of this work would have been a hollow victory.

Lastly, I dedicate this thesis to my parents, Earl and Helene Pfeffer. Their love of life is evidenced by the number of children they brought into it, and being born into the Pfeffer family is simply the best thing that will ever happen to me. In special dedication to my father, I must state that he was a man who cared more about others than he did for himself, and for that, he'll be sorely missed. Standing 6 feet 5 inches tall, he had big feet. I'll never be able to fill his shoes.